UNIVERSITÀ DEGLI STUDI DI PADOVA

DIPARTIMENTO DI INGEGNERIA INDUSTRIALE

CORSO DI LAUREA MAGISTRALE IN INGEGNERIA CHIMICA E DEI PROCESSI INDUSTRIALI

Tesi di Laurea Magistrale in

Ingegneria Chimica e dei Processi Industriali

GROWING CONDITIONS OF *Chlorella vulgaris* AND *Scenedesmus obliquus*: EXPERIMENTAL ANALYSIS AND PROCESS SIMULATION

Relatore: Prof. Alberto Bertucco
Correlatori: Dott. Franjo Cecelja,
Ing. Elena Barbera

Laureanda: Giulia Cuccato

ANNO ACCADEMICO 2013 – 2014

Riassunto

In questo elaborato si sono studiate le condizioni ottimali di crescita delle microalghe *Chlorella vulgaris* e *Scenedesmus obliquus* con lo scopo di utilizzarle nella futura progettazione di un impianto su scala industriale. La prima parte del lavoro, di carattere sperimentale, si è svolta presso la Faculty of Engineering and Physical Sciences, Chemical Engineering Sciences della University of Surrey (UK). Qui sono stati realizzati due fotobioreattori su scala di laboratorio, nei quali è stata monitorata la crescita in batch di *Chlorella vulgaris*, dal momento dell'inoculazione della microalga fino all'ottavo giorno di crescita. L'analisi sperimentale si è avvalsa di tecniche quali la conta cellulare con microscopio, la misura del peso secco, del valore di assorbanza e della densità cellulare. Lo studio si è concentrato su due variabili fondamentali per la crescita: l'apporto di carbonio e l'esposizione alla luce.

Sono stati forniti ai sistemi reattivi diverse concentrazioni di carbonio: il primo reattore è stato alimentato con aria atmosferica, il secondo con aria arricchita di CO_2 al 5%. Inoltre le colture microalgali sono state esposte a diverse illuminazioni, sia per intensità che per numero di ore di esposizione. In un primo momento si è indagata la rilevanza del tempo di esposizione alla luce, quindi la crescita di biomassa è stata valutata con 24, 20, 15 e 10 ore di luce al giorno. Successivamente, cambiando il valore dell'intensità luminosa da 128 $\mu mol\ m^{-2}s^{-1}$ a 85 $\mu molm^{-2}s^{-1}$, si è valutata l'influenza della quantità di energia inviata al sistema. I risultati ottenuti sono in linea con quanto presente in letteratura. È confermata infatti la preminente importanza del carbonio e la dimostrazione che aumentando l'intensità della radiazione luminosa e il tempo di esposizione ad essa, aumenta la capacità produttiva del sistema. E' da sottolineare che nel caso di illuminazione costante (24 ore di esposizione) sono stati raggiunti i massimi valori di concentrazione cellulare (194 milioni cell/ml) e di peso secco (2,62 g/L). Tuttavia il valore della velocità specifica di crescita uguale a 0.52 d^{-1} è risultato inferiore a quelli riscontrati con fotoperiodi più brevi. Il massimo è stato ottenuto in corrispondenza di 20 ore di luce e vale 0,76 d^{-1}. La motivazione proposta per spiegare questi risultati è lo stress ossidativo, ovvero il danneggiamento cellulare che si verifica quando l'illuminazione fornita alle microalghe risulta eccessiva.

La seconda parte della tesi è stata svolta presso il Dipartimento di Ingegneria Industriale della

Università di Padova. Qui è stata ulteriormente indagata l'influenza dell'illuminazione simulando il comportamento di reattori reali con linguaggio di programmazione Matlab®, in riferimento alla microalga *Scenedesmus obliquus*. Tali simulazioni hanno permesso di esaminare il comportamento di tipologie di reattori differenti (ovvero CSTR e PFR con e senza riciclo) e l'effetto di diversi regimi di illuminazione. È stata considerata sia una sorgente di luce costante, come quella fornita da lampade artificiali, sia una sorgente di luce naturale, come quella rappresentata dal sole. Nel primo caso si è considerata un'irradianza di 150μmol/(m^2s) (PAR), nel secondo lo studio ha permesso di simulare la crescita di biomassa durante il periodo estivo.

Per le simulazioni a luce costante, le prestazioni migliori, in termini di produttività, sono quelle ottenute dal reattore CSTR per bassi tempi di permanenza (cioè minori o uguali a 1 giorno). Viceversa, quando il tempo di residenza aumenta, la situazione si inverte e la migliore produttività viene raggiunta dal reattore di tipo PFR e con rapporto di riciclo basso. Il modello CSTR risulta il più affidabile anche dal punto di vista del washout. Per il CSTR è possibile effettuare un'ulteriore considerazione riguardo alla condizione di massima produttività che, nel sistema considerato, viene raggiunta in corrispondenza di un valore di concentrazione pari a 1,4 g/L. In questo caso è stato possibile determinare il valore del tempo di residenza ottimale, che risulta uguale a 0.9697 d e quello della portata di alimentazione corrispondente (avendo fissato il volume reattivo V=120m^3) che risulta essere 123,75 m^3/d.

La seconda parte della simulazione è stata svolta con l'intensità variabile della luce durante il giorno. I dati relativi alla variazione dell'intensità luminosa e dell'angolo di incidenza della luce sono stati elaborati per la stagione estiva assumendo come rappresentativo il mese di Luglio. Attraverso questo studio è stato possibile stabilire che le prestazioni del reattore PFR migliorano con il rapporto di riciclo. Tuttavia oltre il valore di R=0.3 non si hanno differenze sostanziali. Il paragone tra i valori di concentrazioni di biomassa in uscita calcolati con il modello PFR e quello CSTR ha evidenziato un comportamento simile nei due sistemi reattivi. Appare infatti evidente che le prestazioni siano sostanzialmente analoghe nei due casi. Però come verificato con illuminazione costante, aumentando il tempo di permanenza il PFR è migliore del CSTR.

I risultati ottenuti nello studio consentono di tracciare la direzione verso cui procedere in futuro. Rimane infatti da indagare il comportamento di entrambi i modelli reattivi in condizioni di periodo invernale. Al fine di progettare un impianto su scala industriale la scelta delle migliori condizioni operative dipende molto dall'intensità luminosa, dal tempo di

residenza, ma anche dai parametri del modello, che vanno ricavati da accurate misure sperimentali ad-hoc.

Abstract

The optimal growing conditions of the microalgae *Chlorella vulgaris* and *Scenedesmus obliquus* have been analyzed here, in order to define the possible future development of a real plant. In the first part the investigation is carried out experimentally. Lab-scale photobioreactors were realized specifically to study the importance of carbon sources and illumination sources in the production of algal biomass. Two systems with different carbon supplies were analyzed under different photoperiods and light intensity. The fundamental contribution of the light has been further addressed in the second part of the present work, where models of real reactors have been implemented through Matlab® codes. Various lightening conditions have been studied, simulating artificial constant illumination or the natural one provided by the sun during the summer season. The performances of CSTR or PFR reactors were compared having that the reactive system that achieves the best performance depends on the operating conditions, such as residence time, extent of mixing and irradiation.

Acknowledgments

I would like to thank the Faculty of Engineering and Physical Sciences, Chemical Engineering Sciences, University of Surrey (UK) and in particular my supervisor, Dr. Franjo Cecelja, whose kindness, understanding, and patience, added considerably to my experience.

I would like to express my gratitude to Professor Alberto Bertucco, for the assistance provided at all levels of the research project; to Ing. Elena Barbera for the precious support and to Dott.ssa Eleonora Sforza for the encouragement and collaboration.

A very special thanks goes to my family and friends, for the support they provided me through my entire life.

Contents

INTRODUCTION.....1
CHAPTER 1 – Biodiesel from Algae: state of the art.....3
1.1 WORLD ENERGY DEMAND.....3
1.2 THE CHARACTERISTICS OF ALGAE.....4
1.3 THE ALGAE CELLULAR LIFE CYCLE.....5
1.4 CULTIVATION OF ALGAE.....6
1.5 HARVESTING THE ALGAE.....11
1.6 CONVERSION TO BIODIESEL.....11
1.7 OTHER APPLICATIONS OF ALGAE.....12
1.8 THE CRITICAL ISSUE OF OPTIMAL GROWING CONDITIONS.....13
1.9 SCOPE OF THE THESIS.....13
CHAPTER 2 – Experimental materials and methods.....15
2.1 THE EQUIPMENT.....15
2.2.1 The MCS.....15
2.2 THE MICROORGANISM.....18
2.3 THE CULTURE MEDIUM.....19
2.4 THE PROCEDURE.....20
2.4.1 Cells count.....20
2.4.2 Biomass measurement.....22
2.4.3 Absorbance measurement.....23
CHAPTER 3 – Experimental results and discussion.....25
3.1 PHOTOPERIODS OF 20 HOURS.....25
3.2 PHOTOPERIODS OF 15 HOURS.....29
3.3 PHOTOPERIODS OF 10 HOURS.....32
3.4 PHOTOPERIOD OF 24 HOURS.....36
3.5 DIFFERENT LIGHT INTENSITY.....39
3.6 COMPARISON BETWEEN PERFORMANCES OF DIFFERENT PHOTOPERIODS.....43
CHAPER 4 – Photobioreactor simulation and modelling results.....51
4.1 PHOTOBIOREACTORS SIMULATED.....51
4.1.1 CSTR.....52

4.1.2 PFR……53
4.2 CORNET-PRUVOST KINETIC MODEL.....54
4.2.1 Light distribution.....54
4.2.2 Kinetic growth.....56
4.3 MODEL PARAMETERS.....58
4.3.1 Absorption, scattering and backscattering coefficient.....59
4.3.2 Half saturation constant for photosynthesis.....59
4.3.3 Maximum energetic yield for photon conversion and Mass quantum yield for Z-scheme of photosynthesis……..…….59
4.3.4 Maintenance term…….……..60
4.3.5 Other parameters……...…….60
4.4 MAXIMUM AND REAL PRODUCTIVITY……..……..61
4.4.1 Maximum productivity……..61
4.4.2 Real productivity……62
4.5 RESULTS: CONSTANT LIGHT INTENSITY SIMULATIONS.....63
4.5.1 Steady state simulations……63
4.5.2 Dynamic simulations……73
4.6 RESULTS: VARIABLE LIGHT INTENSITY SIMULATIONS.....77
4.6.1 Summer simulations……78
CONCLUSIONS.....87
NOMENCLATURE……..……..89
BIBLIOGRAPHY.....93

Introduction

It is widely acknowledged that the energy consumption is constantly increasing (Goncalves et. al., 2013) due to population growth and the rising of developing Countries such as China, India and Brazil. Nowadays the world main energy sources are fossil fuels even though their future exploitation is unsustainable. Indeed, they are considered as depleting resources. Furthermore, in the last years the environmental issues have raised many concerns. Fossil fuels are held responsible for greenhouse gas (GHG) emissions, global warming, acidification of the seas, and loss of biodiversity (Mata et al., 2010). For all of the reasons above the sustainable production of renewable energy has become one of the most important challenges for the years to come. To try to solve the problem, many solutions have been proposed. In particular, the idea of obtaining biodiesel from microalgae has a real appeal, being the transportation and electricity sectors the major consumers of energy (Brennan and Owende, 2010). The purpose of the present work is to investigate the optimal growing conditions for the algal species *Chlorella vulgaris* and *Scenedesmus obliquus*, in order to reach the maximum productivity.

In the first chapter the world's energetic condition is discussed and the possible advantages represented by algae exposed. The state of the art is illustrated in this section and the scope of the thesis outlined.

In the second chapter the experimental setup and the methodology followed during the experiments for the evaluation of the biomass growth are described.

In the third chapter the experimental results are presented. These are organized according to the different illumination conditions and subsequently they are compared and discussed.

In the fourth chapter the modelling part of the work in presented. Initially the types of reactors simulated are described. Afterwards the Cornet-Pruvost model for the evaluation of the radiation profile inside the reactor, and of the corresponding growth rate is discussed. Furthermore the simulaion results are displayed and analyzed.

Finally the conclusions drawn from the experimental and simulation study are presented with the aim to point the way for future developments of real plants for the industrial production of biodiesel from algae.

Chapter 1

Biodiesel from Algae: state of the art

In this chapter the importance and modernity of the application of microalgae as an alternative energy source are outlined. In particular, their employment for the production of biodiesel will be analysed.

After an overview of the background of the world's current energy situation, the main types of microalgae, their cultivation, harvesting and transformation into biodiesel, will be explored.

1.1 World energy demand

Energy consumption is constantly increasing due to the growth of new developing countries (Goncalves A., et al., 2013). Fossil fuels are currently the world main energy source (Lam and Lee, 2012) with transportation and electricity sectors accounting for 88% of the world primary energy consumption (Brennan and Owende, 2010). Nevertheless, the exploitation of these types of fuels is considered unsustainable due to depleting resources and arising environmental issues. In particular they are responsible for greenhouse gas (GHG) emissions that are associated with several negative effects on the environment, such as global warming, the alteration of oceans pH levels which could lead to the acidification of the seas, and loss of biodiversity (Mata et al., 2010). Moreover, with the energy crisis that is hitting most parts of the world caused by population growth and rapid industrialisation, the sustainable production of renewable energy has become a worldwide allure and the ultimate interest of many academics, investors and entrepreneurs (Lam and Lee, 2012, Oncel, 2013). In order to diversify energy sources, many opportunities are being examined and implemented such as the use of solar energy, hydroelectric, geothermal, wind and biofuels. The latter is seen as a potential solution for the transportation sector; in fact biofuels are a non-toxic, biodegradable fuel with low GHG emissions (Lam and Lee, 2012). Biofuels can be classified into three groups: first, second and third generation. The first generation biofuels are derived from food and oil crops including rapeseed oil, sugarcane, sugar beet and maize. Their technology is well known and their market is competitive. However they are not considered as a suitable

solution because of their competition for the use of arable land with food production, and the high water and fertiliser requirement. Moreover the use of first generation biofuels has impact on the food market and represents a risk to bio-diversity (Mata et al., 2010). An alternative solution is the use of non-edible oils, derived from frying or cooking oils, greases and animal fats. Unfortunately, current availability of these resources is not sufficient to satisfy the present demand for biodiesel (Chisti, 2007). The second generation of biofuels uses agricultural and lignocellulosic residues or wastes and therefore avoids competition with food crops. However, the problem with this type of biofuel is that it requires a technology which is still not sufficiently developed to reach an industrial scale (Brennan and Owende, 2010). Finally, the third generation of biofuels aims to use microalgae. Microalgae are photosynthetic microorganisms able to synthesize and accumulate large quantities of lipids carbohydrates and proteins. These in turn can be converted into different energy sources, such as biodiesel, methane, hydrogen and ethanol among others. Their convenience is linked to the high growth rates compared to terrestrial crops and improved land use (Wiley et al., 2011). The biodiesel from this source is obtained by a catalytic process of transesterification of the lipids extracted from microalgae. This type of biodiesel has no content of sulphur and less CO_2 emissions, particulate matter, hydrocarbons and SOx.

1.2 The characteristics of Algae

Microalgae are eukaryotic or prokaryotic microorganisms that have simple cellular and reproductive structures. They are photosynthetic, thus they reproduce converting solar energy into chemical energy. There are more than 50,000 different species but only around 60% has been investigated and studied so far (Mata et al., 2010).

The idea of using microalgae as an energy source is not new; in fact the production of methane derived from algae was proposed in the 1950's and consequently the interest in this sector has further developed during the energy crisis in the 1970's (Mata et al., 2010). Moreover, between 1980 and 1996 the US Department of Energy supported the Aquatic Species Program to investigate the production of oil from microalgae (Mata et al., 2010).

It has been shown that the use of microalgae in the biofuels sector has many advantages:

- easy to cultivate and to obtain nutrients;
- the growth cycle lasts a short period of time;
- it can be adapted to live in a variety of environmental conditions;
- it is possible to find species best suited for specific environment;

- they can grow in land unsuitable for agricultural purpose;
- they have high growth rate and productivity;
- low land and fresh water requirement;
- the process can be viewed as a system to remove CO_2;
- they can purify wastewater;
- other valuable compounds can be extracted;
- algal biomass can be used for fuel, feed and food;
- the cultivation does not require herbicide or pesticide application;
- the algae industry could be a job creating engine;

Nonetheless there are some negative aspects that must be addressed and investigated in order to make microalgae a feasible energy source. One of the most pressing problems concerns the dewatering of the algae since they are characterized by a substantial amount of moisture content. Another branch that requires in-depth analysis is the screening of the numerous species in order to understand their behaviour and properties. Again it is necessary to clarify how to maximize the photosynthetic efficiency and the lipids production. Last but not least, the technology for the growth and refining sectors needs to be developed taking into account economic and energetic aspects.

1.3 The algae cellular life cycle

Microalgae need a sufficient supply of light and carbon to accomplish the photosynthesis. Their metabolism can be of different types (Mata et al., 2010):

- photoautotrophic, they only use light to reproduce themselves;
- heterotrophic, they use only organic compounds as energy source, thus they operate under dark conditions;
- mixotrophic, they use a mix of different energy sources such as light and organic carbon.

Currently the only technically and economically feasible method for large plants involves the photoautotrophic production (Brennan and Owende, 2010).

Along with light and carbon sources, algae need also nutrients to grow. Nutrients can be divided into two classes: macronutrients and micronutrients. The former one involves compounds such as nitrogen and phosphorous, that are needed in large amounts. Instead the

micronutrients are elements like manganese, iron, calcium or copper and they are usually needed in less quantity.

Furthermore microalgae need equilibrium between the physical parameters that regulate their cellular growth life cycle (Mata et al., 2010). This means that oxygen, carbon dioxide, pH, light intensity and temperature must be controlled during the cultivation of microalgae. Their growth in a batch culture follows a cyclical pattern that can be divided into five different regions, as shown in Figure 1.1: 1. Lag phase 2. Exponential growth phase (that represents the maximum growth rate) 3. Linear phase 4. Stationary phase and 5. Death phase (Mata et al., 2010).

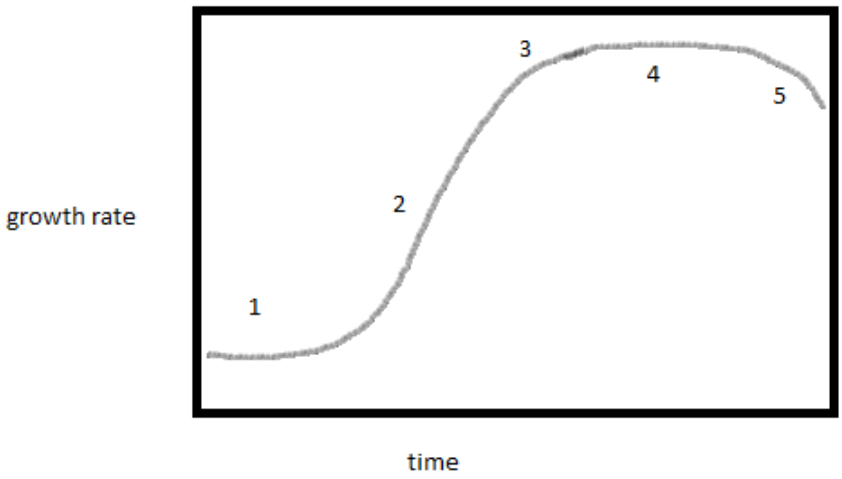

Figure1.1 *Microalgae life cycle in batch systems. (Mata et al., 2010).*

The goal is to achieve the maximum output through a productive system that operates in continuous mode. This can be obtained working always in the exponential phase of the cycle, exploiting the parameters optimization.

1.4 Cultivation of Algae

There are two basic types of culture system: open ponds and closed photobioreactors (PBRs).

The open ponds originate from natural water (like lagoons, ponds or lakes) or artificial ponds and containers, with the algae directly exposed to the environment (Mata et al., 2010). They are usually situated outdoors and rely on natural light for illumination. The open system can be classified as: (a) extensive shallow unmixed ponds; (b) circular ponds mixed with a rotating arm, (c) 'raceway' ponds, usually mixed with a paddle wheel, and (d) sloping thin-layer cascade systems (Fon Sing et al., 2013). Raceway pond is the most commonly used

design as an open culture system (Schenk et al., 2008). Open ponds are generally less expensive and more durable than closed reactors. Their maintenance and cleaning are easier since the large open access but they are also more influenced by weather conditions and require larger land area. Other negative aspects arise from their connection with the environment making them vulnerable to contaminations and loss of water via evaporation. Usually the agitation provided is inefficient and CO_2 quantity is unsatisfactory. The key limitation to productivity is light. The majority of the ponds are operated with a depth of 20-30cm, purely for hydraulic reasons. This implies that at the surface algae are exposed to very high light intensity while at the bottom they are not reached by the light. The solution is to mix the system in order to move the layers and allow the algae to receive the same quantity of light. An alternative solution is the 'cascade' system, in which the culture of algae flows over a sloping surface to the bottom where they are collected and pumped again to the top (Fon Sing et al., 2013). In Figure 1.2 an open ponds system is presented.

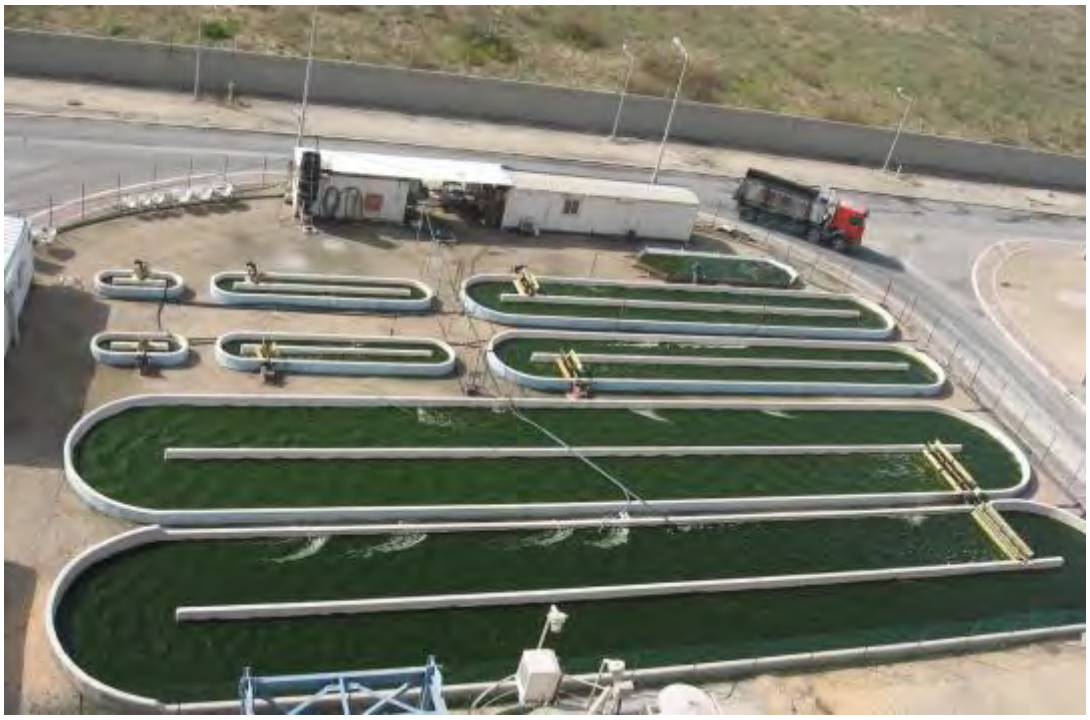

Figure1.2. *Open ponds system. (http://www.algae-energy.co.uk/).*

The PBRs are designed to avoid some of the major disadvantages of the open ponds systems. They can be classified as (a) bags or tanks, (b) towers, (c) plate reactors, or (d) tubular reactors (Fon Sing et al., 2013) and the main characteristic is that the exchange of nutrients

and contaminants between algae and the environment is controlled by the reactor's wall. The advantage of using this type of culture systems is that they allow a higher productivity in terms of biomass concentrations (Chisti, 2007). Moreover, they avoid evaporation and contamination, reduce CO_2 losses and provide more control over culture conditions and parameters (such as pH, temperature, mixing, CO_2 and O_2 quantities) (Mata et al., 2010). The circulation of the algae is realised with pumps while the temperature is controlled with heat exchangers and evaporative cooling; the periodical cleaning is achieved through an automated clean-in-place operations. The light reaches the algae through the transparent material of the wall, usually PVC or Teflon or glass. The design of these systems is of critical importance to reduce the light path in order to achieve the maximum light exposure. The oxygen generated from photosynthesis can accumulate and inhibit the cellular growth and subsequently damage them; for this reason a degassing zone is always required (Suali and Sarbatly, 2012). However there are some disadvantages connected to the use of the PBRs. There are technical difficulties including avoiding overheating, monitoring the shear stress caused on the algae by the mixing system and cleaning the bio-fouling. Furthermore, the scaling-up of equipment can be very complicated (Brennan and Owende, 2010). On top of that the energy requirement is higher compared to open systems, consequently so is the operating cost of the plant as well.

PBRs can operate both in continuous and batch mode (Mata et al., 2010). The batch system requires simpler design while the continuous set-up is convenient for the higher controllability and reliability of the experimental results, and lower production costs. However related to the residence time in the reactor, there is the risk of washout. This occurs when the algal culture is drawn out of the reactor because the residence time is too short. Moreover the long periods of growth increase the contamination risk (Mata et al, 2010).

Examples of enclosed systems are presented in Figure 1.3.

Figure1.3. *Closed systems PBRs. (http://www.bae.uky.edu/).*

A key factor to optimise the algae production is to select a suitable method for cultivation. To do this a deep knowledge of the differences between the PBRs and open ponds is required. Table 1.1 features the main differences.

To guarantee high levels of production and limit the costs associated with algal production another option has been developed: hybrid systems (Schenk et al., 2008). This particular cultivating procedure consists of a combination of the closed PBRs and the open ponds. The first stage takes place in a PBR where the absence of contaminants is monitored and the cell division is enhanced. After that the cells are transferred to the open pond, providing in such way the stress needed to increase the lipid content (Brennan and Owende, 2010). Here the cells grow and they are subsequently collected.

Anyway the technical viability of each system depends upon the intrinsic proprieties of the strain used, the land and water costs and the climatic conditions (Brennan and Owende, 2010).

Table 1.1. *Differences between open ponds and PBRs.(Ghasemi et.al, 2012).*

Factors	Open pounds	Photobioreactors
Required space	High	For PBR itself low
Water loss	Very high, may also cause salt precipitation	Low
CO_2 loss	High, depending on pond depth	Low
Oxygen concentration	Usually low enough because of continuous spontaneous outgassing	Gas exchange devices required (O_2 must be removed to prevent inhibition of photosynthesis and photo oxidative damage)
Temperature	Highly variable, some control possible by pond depth	Cooling often required (by spraying water on PBR or immersing tubes in cooling baths)
Shear	Usually low (gentle mixing)	Usually high (fast and turbulent flows required for good mixing, pumping through gas exchange devices)
Cleaning	No issue	Required (wall growth and dirt reduce light intensity), but causes abrasion, limiting PBR lifetime
Contamination risk	High (limiting the number of species that can be grown)	Medium to low
Biomass quality	Variable	Reproducible
Biomass concentration	Low, between 0.1 and 0.5 g/l	High, generally between 0.5 and 8.0 g/l
Production flexibility	Only few species possible, difficult to switch	High, switching possible
Process control and reproducibility	Limited (flow speed, mixing, temperature only by pond depth)	Possible within certain tolerances
Weather dependence	High (light intensity, temperature, rainfall)	Medium (light intensity, cooling required)
Start up	6–8 weeks	2–4 weeks
Capital costs	High ~ $100000 per ha	Very high ~ $250000 to 1000000 per ha
Operating costs	Low (paddle wheel, CO_2 addition)	Higher (CO_2 addition, oxygen removal, cooling, cleaning, maintenance)
Harvesting costs	High, species dependent	Lower due to high biomass concentration and better control over species and conditions

1.5 Harvesting the Algae

The harvesting is the algae biomass recovering for downstream processes and it requires one or more liquid-solid separation steps. The separation of the biomass from water is a critical phase that is highly expensive and energy consuming. It is considered to account for 59% of the total energy consumption in the biodiesel production (Yanfen et al., 2012). The difficulties in the separation process are linked to the small size of algal cells (3-30μm), the low specific gravity and the negative surface charges which produce stable suspensions (Fon Sing et al., 2011). Moreover since growth broths are usually dilute and the moisture content of algal cells is higher than 99%, large volumes need to be handled (Lam and Lee, 2012).

According to Brennan and Owende (2010), the algal harvesting can be divided into:

1. Bulk harvesting, which is the separation of the biomass from the bulk suspension. The technologies employed are flocculation, flotation or gravity sedimentation.
2. Thickening, which is the concentration of the slurry through techniques such as centrifugation, filtration, ultrasonic aggregation. This phase usually requires more energy than the bulk harvesting.

After dewatering the algae are ready to undergo the downstream processes.

1.6 Conversion to biodiesel

The stages that lead to the production of Biodiesel are depicted in Figure 1.4.

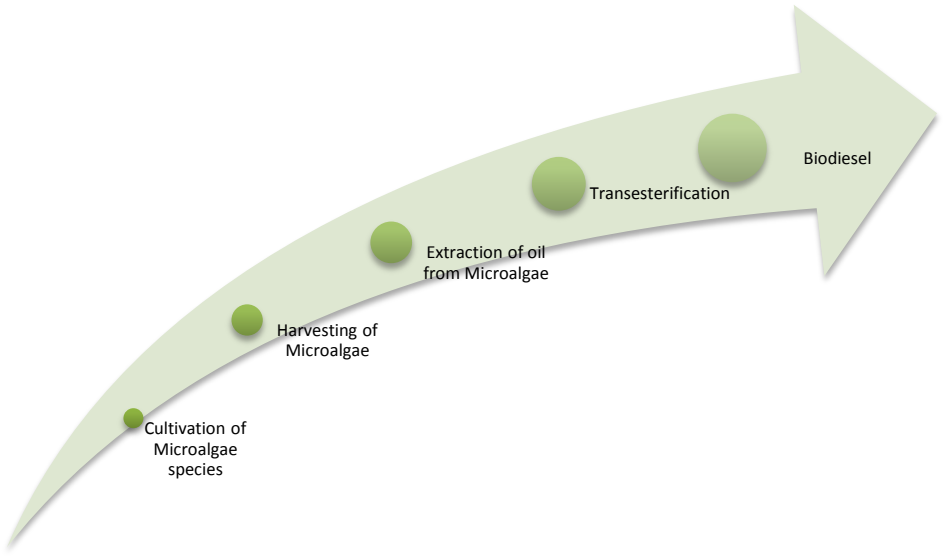

Figure1.4. *Description of biodiesel production stages. (http:// www.oilgae.com/).*

Subsequently algal oil is recovered from the disruption of the microalgae cells and consequent release of the metabolites of interest (Schenk et al., 2008). This can be achieved through different extraction methods whose efficiency is dependent upon the algae strains. The chemical methods are: solvent-extraction, that is suitable for dry biomass and supercritical fluid extraction, better with wet paste of biomass. Solvent extraction is the most common method because of its high selectivity and solubility towards lipids. The main solvents are n-hexane, methanol, ethanol and mixed methanol–chloroform. The disadvantages of these techniques are related to their toxicity towards the human health and the environment (Lam and Lee, 2012). Extraction with supercritical fluids has the advantage of using a non-toxic solvent which is highly diffusive and easily separated. Nonetheless this technology has high cost of operation and issues related to safety (Lam and Lee, 2012). The latest innovation in this sector is the use of ionic liquids (ILs) as an alternative to the classical organic solvents. Their advantages are the high solvation capacity combined with thermal stability and non-volatile character (Gonçalves et al., 2013). The disadvantage is that they are more expensive than normal solvents, and their toxicity.

The mechanical methods for microalgae oil extraction are based on pressing and crushing the biomass with different kinds of press configurations. These methods are often used in combination with chemical solvents. Another mechanical technique is the ultrasonic-assisted extraction that exploits ultrasonic waves to create a shock able to break cell walls and release their content into the solvent. This is a non-fouling process that does not induce shear stress on the biomass (Brennan and Owende, 2010).

Once the oil is extracted from the cells, the transesterification of algae lipids follows. The reaction that can take place with homogeneous or heterogeneous catalyst or in-situ has glycerol as side product. It can be described as:

$$\text{Triglyceride} + \text{methanol} = \text{Methyl Ester} + \text{Glycerol}. \quad (1.1)$$

After the separation from the other by-products, the methyl esters forming the biodiesel are collected and stored.

1.7 Other applications of Algae

Microalgae can be used as a source for different types of energy. Hydrogen can be produced through biological or photobiological process. Syn-gas, which is a mixture of CO_2 and H_2,

can obtained gasifying the algae biomass (Oncel, 2013). Along with the Syn-gas, from the biomass methane through a fermentation process can also be obtained (Chisti Y., 2007). The components extracted can be used as intermediate for bioplastics or other chemical compounds as well.

Algae are used as human food as well as animals and fish feed in many countries. Other sectors that exploit their properties are the pharmaceutical industry alongside the cosmetics industry (Mata et al., 2010). Finally algae can be used in pollution control, as they are able to capture CO_2 reducing the emissions of GHGs and there is the possibility to use wastewater as culture medium (Mata et al., 2010).

1.8 The critical issue of optimal growing conditions

One of the most addressed question related to the feasibility of exploiting microalgae to obtain biofuels is the definition of optimal conditions for the algae's growth. Understanding how to enhance their productivity means being able to design a suitable photobioreactor to produce them. Such conditions depends upon numerous factors. They refer both to physical parameters as well as medium composition and type of metabolism (Yeh and Chang, 2012). Culture conditions like irradiance, temperature, pH and dissolved oxygen concentration, have been studied extensively throughout the years and one factor appears to be of utmost importance: the light availability (Jacob-Lopes E., et al., 2009, Sforza et al., 2012, Costache et al., 2013). Light provides the energy that the algae require for their metabolism but it can also have a depressive effect. This phenomenon is called photoinibition and it occurs when the illumination is excessive. In this case the light provided causes stress and damage to the cells. Thus find the optimal light intensity and photoperiod, that are specific for each strain, allows to understand how to maximize the photosynthetic efficiency.

1.9 Scope of the thesis

This work has the aim to provide an insight of the different behaviour in two identical algae systems with CO_2 enriched air and with normal air. Different photoperiods will be investigated. The data collected through these experiments will be used to address the optimal condition of algae growth, with regards to the specific parameter of carbon source and light source. In the second part of the thesis the behaviour of real reactors will be simulated, in order to define the operating conditions that assure the best performances.

Chapter 2

Experimental materials and methods

The purpose of this chapter is to provide a description of the instrumentation used and a graphical representation of the equipment. The analytical procedures are illustrated in order to understand the methodology followed during the experimental analysis.

2.1 The equipment

The culture system used to grow the algae is an enclosed reactive system. This reactor provides a closed environment that is easier to control then open systems. Furthermore, it offers a protection against contamination from many different microorganisms such as bacteria and fungi. Another fundamental characteristic of the closed system is the high area to volume ratio. This allows the light to pass through the reactor's walls and to reach as many as possible cultivated cells.

2.1.1 The MCS

The Manufactured Culture System is the enclosed system used to grow the microalgae in the experiments performed in this thesis. The system, named with the acronym MCS, is an experimental equipment that was built specifically for the purpose. It is composed by two different culture systems positioned into one container. The two systems are cylindrical containers made of glass and they have a volumetric capacity of one litre each. The fundamental characteristic of this system is the difference in the supply of air into the two batches. The first one, positioned on the left side of the case, is connected to a tank of air enriched with CO_2 at 5%. The second batch, positioned on the right side of the case, is operated with normal air, supplied through an air pump connected to the atmosphere. The inflow is delivered to the two bottles through an air sparger and is kept constant and equal for the two systems at 20 cm^3/min. This flow is relatively high, therefore the percentage of air and CO_2 effectively used by the culture systems is much lower. However a lower value of inflow proved to be difficult to stabilize and control with the available flow meters. The agitation is guaranteed with magnetic stirrers positioned at the bottom of the containers. The mixers provide the necessary amount of turbulence to avoid the algae's deposit.

The lighting system is composed by a set of lamps attached with cable ties to the chamber's walls, on the left, right and back side. The lamps are connected to the electricity via a timing unit that allows to set the time of the switch on and switch off of the lamps. The experiments were performed with two different lightening settings. Initially all the 15 lamps, 5 on each side, were exploited. In the last experiment the light intensity was changed and only 3 lamps on each side were used. The position of the lamps gives different values of light intensity around the two cylindrical batches. These values are summarized in Table 2.1, which refers to the maximum light intensity achievable with 15 lamps switched on, and Table 2.2. which refers to the last case examined, with only 9 lamps in operations. In the first case the culture broth is provided with an average light intensity of 128 µmol/m^2s. In the second case the average light intensity delivered by the 9 lamps is 85 µmol/m^2s. The photoperiod, which is the number of hours the lightening is provided to the culture system, is decided and changed during the different cycles of experiments. A schematic representation of the MCS is illustrated in Figure 2.1. while a picture of the system is presented in Figure 2.2.

Table 2.1. *Maximum light intensity distribution.*

POSITION	**L.I. (µmol $m^{-2}s^{-1}$)**
In front of CO_2 bottle	10
To the left of CO_2 bottle	335
Behind CO_2 bottle	108
To the right of CO_2 bottle	54
In front of Solo Air bottle	7.33
To the left of Solo Air bottle	34
Behind Solo Air bottle	164
To the right of Solo Air bottle	316
In front of the two bottles, central position	7.9
Between the two bottles	46.5
Behind the two bottles, central position	105

Table 2.2. *Light intensity distribution in the last experiment.*

POSITION	L.I. (µmol $m^{-2}s^{-1}$)
In front of CO_2 bottle	0.6
To the left of CO_2 bottle	164
Behind CO_2 bottle	109
To the right of CO_2 bottle	70
In front of Solo Air bottle	0.7
To the left of Solo Air bottle	65
Behind Solo Air bottle	81
To the right of Solo Air bottle	170
In front of the two bottles, central position	0.8
Between the two bottles	24
Behind the two bottles, central position	50

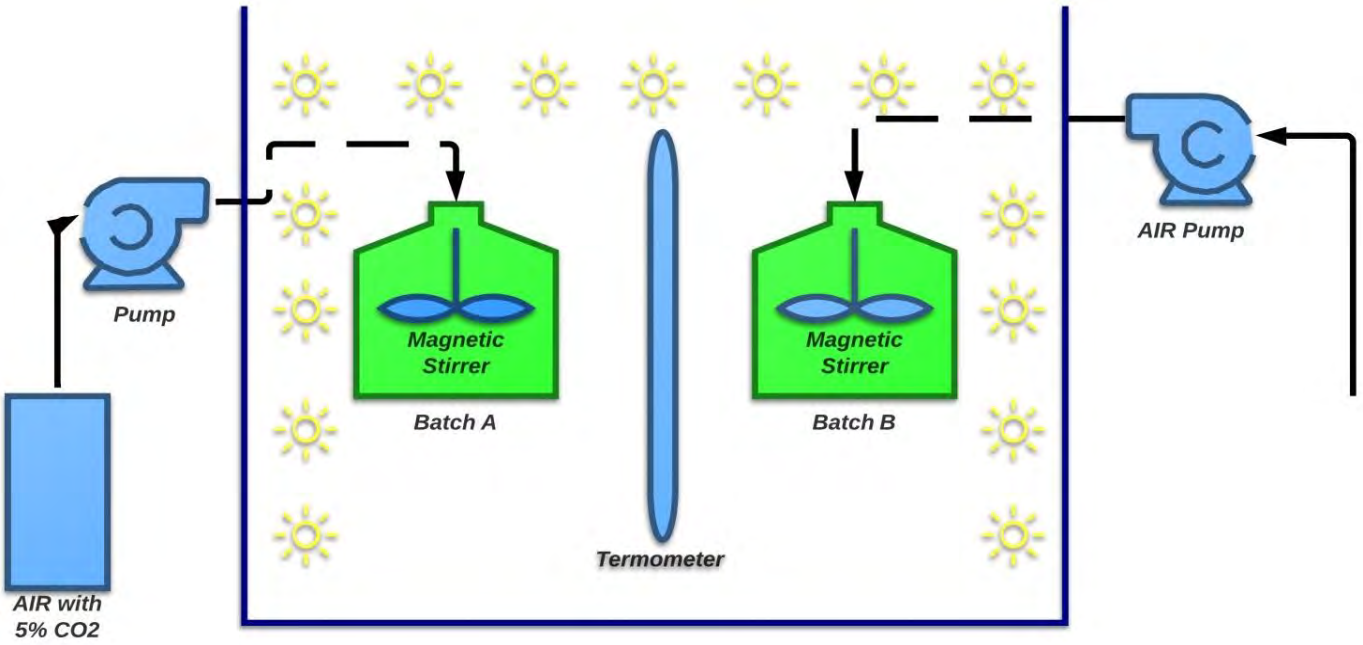

Figure 2.1. *Schematic of the MCS.*

Figure 2.2. *Picture of the MCS used during the experiments.*

Externally the unit is covered in foil to ensure the maximum employment of the lightening. Inside the unit a thermometer allows the measurement and recording of the temperature reached during the experiments. The range of temperatures goes from 23°C to 27°C.

2.2 The microorganism

The specific type of algae used in all the experiments is *Chlorella vulgaris* (strain 211/11B) obtained from Culture Collection of Algae and Protozoa (CCAP, 2012) based in Scotland. This is a freshwater-terrestrial species that has potential use in wastewater treatment (Perez-

Garcia et al., 2010) and seems to be a suitable pioneer organism for soil restoration (Lin and Wu 2014). An image of this particular strain of algae is shown in Figure 2.3

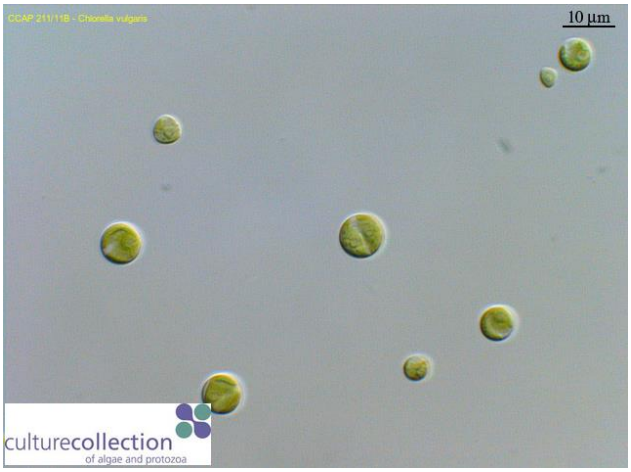

Figure 2.3. *Image of Chlorella vulgaris cells.(http://www.ccap.ac.uk/).*

2.3 The culture medium

The culture broth is prepared following CCAP recommended guidelines. For the preparation of 1 litre of medium, 932 ml of distilled water are added with 66ml of the stock solution prepared as shown in Table 2.3 and Table 2.4. After that, 1ml of each of the two vitamins, Thiaminhydrochloride and Cyanocobalamin, are added.

Table 2.3. *Macronutrients of medium composition.*

Component	Concentration (g/L)
$NaNO_3$	10
$CaCl_2.2H_2O$	10
$MgSO_4.7H_2O$	10
$K_2HPO_4.3H_2O$	10
KH_2PO_4	10
NaCl	10
Trace components (Table 2.4)	6

Table 2.4. *Nutrients of trace composition.*

Component	Concentration (g/L)
Na_2EDTA	0.75
$FeCl_3.6H_2O$	0.097
$MnCl_2.4H_2O$	0.041
$ZnCl_2$	0.005
$CoCl_2.6H_2O$	0.002
$Na2MoO_4.2H_2O$	0.004

2.4 The procedure

Samples of 10 ml are extracted from the two batches of the MCS three times a day at specific and constant hours. They are collected at 9:00 am, at 1:00 pm and at 5:00 pm each day for eight days, by a micropipette. The analyses are carried out with the aim to quantify the growth of the algal culture in terms of cells concentration and dry weight. Therefore 1ml of sample is removed for cell count purpose and 5 ml for biomass measurement purposes. The remaining 4 are kept for backup.

2.4.1 Cells count

The cells production is examined by means of manual counting. This is performed using a Neubauer haemocytometer and a CENTI Max Bino microscope with a magnification of up to 400x. The Neubauer haemocytometer is a particular slide with 2 chambers divided into 9 squares. The central square is divided into 25 smaller squares and each one of them is further divided into 16 squares. The subdivision in squares is what makes the counting procedure feasible. The haemocytometer used and its chambers are presented in Figure 2.4. Once the sample is extracted from the reactive system the haemocytometer is loaded with a micropipette set at 10µl, drawn from the centre of the well mixed sample bottle. The slide is then observed trough the microscope. After checking under low magnification any abnormal distribution, the cells in medium squares ($1mm^2$) of the central square, are counted manually.

Progressively the cells concentration in the algal solution will increase and the counting will be performed in the smallest squares ($0.04mm^2$). When the cells in the small squares exceed 50 cells on average the sample is diluted with distilled water. The standard counting procedure consists in counting any cells inside the square or touching the upper and left square lines, while the cells touching the bottom and right lines are ignored. The counting is performed for at least 10 squares to give statistical significance to the data.

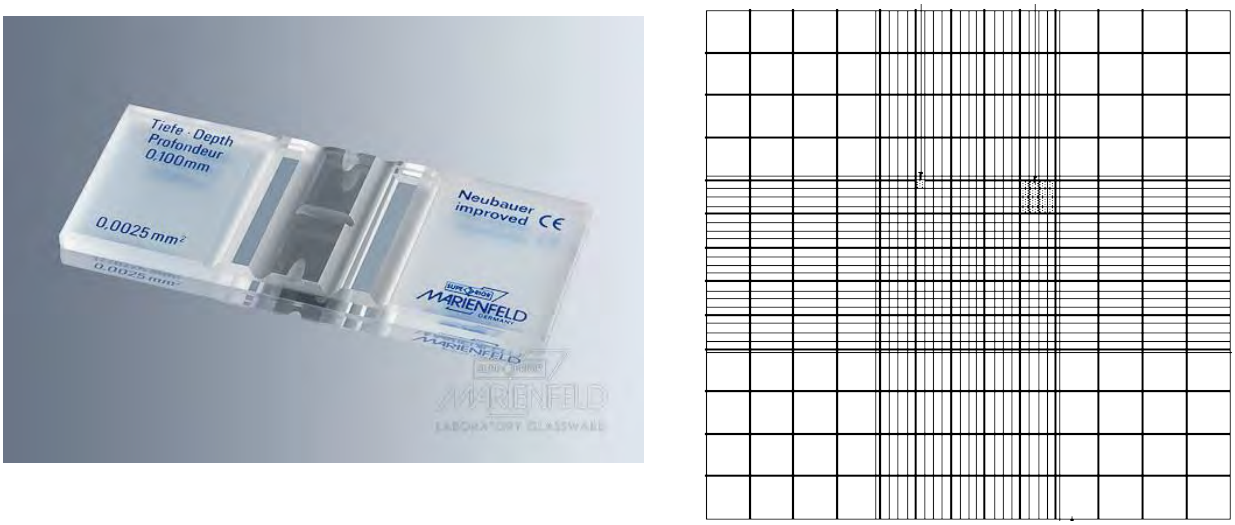

Figure 2.4. *The haemocytometer and the subdivision into chambers.(http:// www.marienfeld-superior.com/).*

From the number of cells counted, it is possible to estimate the cell concentration per millilitre. To perform the calculation Equation 2.1 and Equation 2.2 are used. Equation 2.1 is used for the cells counted in medium squares and Equation 2.2 is used for the cells counted in the small squares.

$$\text{Concentration (cells/ml)} = \frac{\text{number counted x dilution factor x } 2.5\text{x}10^5}{\text{numbers of square counted}} \quad , \qquad (2.1)$$

$$\text{Concentration (cells/ml)} = \frac{\text{number counted x dilution factor x } 4.0\text{x}10^6}{\text{numbers of square counted}} \quad . \qquad (2.2)$$

Once the concentration is calculated it is possible to gauge the trend in the growing of the algae. This is done through the definition of the term μ, which is the growth rate. It is possible to determine the growth rate with two different methods: with regards to the number of cells counted or with regards to the dry weight. The growth rate is calculated through a linearization procedure of the data in the exponential phase. Calculating the logarithm of those data a straight line is obtained. The angular coefficient represent the rapidity in the growing process of algae. The value of μ obtained with reference to the number of cells counted is the measure of the cellular duplication rate. On the other hand the growth rate calculated with regards to the dry weight is an index of the growing process in the biomass.

2.4.2 Biomass measurement

The second type of analysis performed during the experiments has the purpose to quantify the biomass growth in the algal culture. This is achieved by measuring the dry weight of samples that are collected starting from the second day of experiments. The growth during the first day it is not sufficient to estimate a difference in the biomass. The procedure requires the extraction of 5 ml of the sample from the reactive system and involves the use of a 22μm filter and a vacuum pump. The first step consists in heating the filter paper in one oven at 80°C for one hour, followed by 15 minutes in a desiccant chamber to avoid hygroscopic water absorption. After that the filter paper is weighted on a microbalance and the value is recorded. Then the filter is inserted into the vacuum system and the sample is added trough a syringe. The vacuum system has the aim of removing the water, while the biomass is retained. The next step consists in a repetition of the first one, with the filter being positioned again in the oven for one hour at 80°C and then in the desiccant chamber for 15 minutes. During this step the inter-cellular and intra-cellular water is removed. Afterwards the filter with the dried biomass is weighted again on the microbalance. Finally subtracting the value of the first weight of the filter to the second value and dividing for the volume of the sample, the dry biomass weight per millilitre is obtained by:

$$\text{Dry Biomass (g/l)} = \frac{filter\ with\ sample\ weight - filter\ initial\ weight}{volume\ of\ the\ sample} \quad . \tag{2.3}$$

The limit of the biomass analysis lies in the intrinsic precision of the microbalance. The one used during the experiments has a precision of $1*10^{-4}$g.

2.4.3 Absorbance measurement

The third analysis performed during the experiments is the measurement of the absorbance. The absorbance is also named optical density and it is identified with the acronym OD. The instrument used is the Jenway 6300 Spectrophotometer. The measure is divided into two moments. The first step consist in the analysis of the absorbance of the medium used in the batches with the algae. This stage has the purpose to calibrate the instrument thus the absorbance of the sample will not be affected by the components in the medium. The second step involves the sample removed from the reactive system. A portion of it is collected with a micropipette and inserted into a 10x10 mm plastic cuvette. Afterwards the cuvette is placed into the cell holder and the sample chamber lid is fully closed. The light bean that reaches the cuvette has a wavelength (λ) of 750 nm. This specific value of λ is due to the incapacity of the chlorophyll to absorb photons at this wavelength. This means that the only reason behind the attenuation of the light is linked to the cellular concentration. The spectrophotometer reads a range of absorbance values between 0,1 and 1. When the sample is really concentrated the value can exceed 1. In this case the sample is diluted with the medium to avoid alteration in the absorbance.

The absorbance index gives a measure of the light scattering. This phenomenon is the deviation in the trajectories of light particles, due to the presence of algal cells. Thus the absorbance index is directly related to the cellular concentration.

Chapter 3

Experimental results and discussion

During the experimental part of the work different growing conditions have been analyzed. The focus has been put on the light in particular. The two batch culture systems have been operated with four different photoperiods and, in the last experiment, with a different light intensity. Each experiment allows the comparison between the system with CO_2-enriched air and the system operating only with air. The results obtained are shown, analyzed and discussed.

3.1 Photoperiod of 20 hours

The first experiment was run with a photoperiod of 20 hours. This means that the illumination was given for 20 hours per day and the dark period was of 4 hours. The two MCSs were operated for 8 days with an average light intensity of 128 μmol $m^{-2}s^{-1}$ and an average temperature of 23°C. The two batches of 1 liter each of reactive volume were both inoculated with an initial cellular concentration of 1 million cells/ml. Throughout the experiment the cellular concentration was measured in terms of cells per milliliter, as shown in Figure 3.1, and in terms of grams of dried biomass per liter, as shown in Figure 3.2. The points in the graphs refers to the three samples collected every day during the running of the experiment, while the letter A is related to the MCS operated with air enriched with 5% CO_2 and the letter B refers to the MCS supplied with atmospheric air.

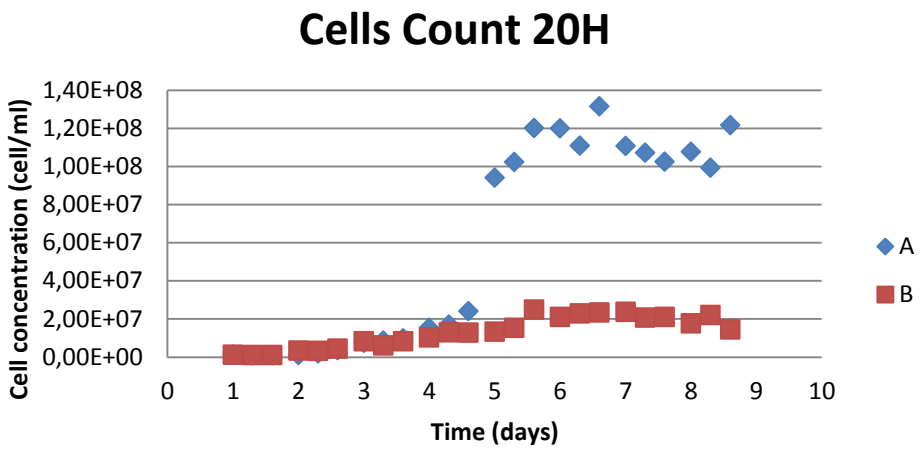

Figure 3.1. *Cellular concentration (Cells/ml) with 20 hours of photoperiod.*

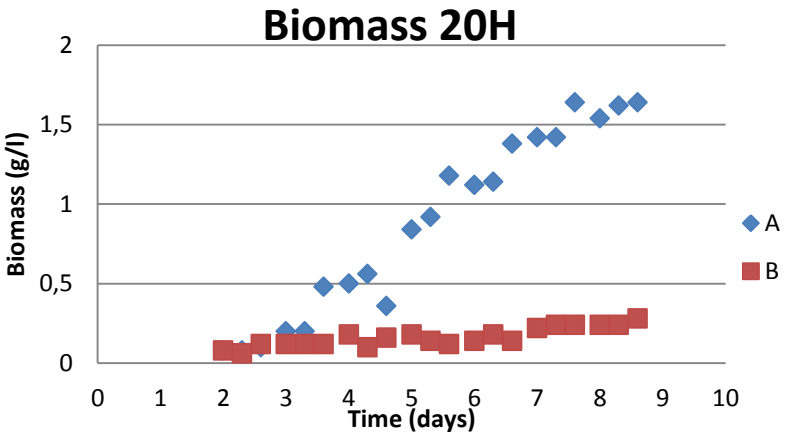

Figure 3.2. *Cellular concentration (g/l) with 20 hours of photoperiod.*

From Figure 3.1 it is clear that in the MCS-A the lag phase lasts until the 5th day, when it is observable a high rise in the number of cells per milliliter, which represent the exponential phase of the growth. It goes from a value of 24 million of cells to 94 million in one day, thus increasing of nearly 4 times. Another observation regards the last part of the curve that shows a decreasing trend. This, according to what previously stated in §1.3, represents the death phase that occurs when the nutrients are limiting the duplication capacity of cells. Figure 3.2 shows the increase in the algal biomass from the beginning of the experiment to the end. It is evident from both Figure 3.1 and Figure 3.2 that the MCS named A, supplied with air enriched with 5% CO_2, reaches higher values of cellular concentration. The difference measured is of roughly 107 million of cells/ml, or 1,36 g/l. To estimate the growth the

logarithm of the data were calculated. The graphs obtained are represented in Figure 3.3 and Figure 3.4.

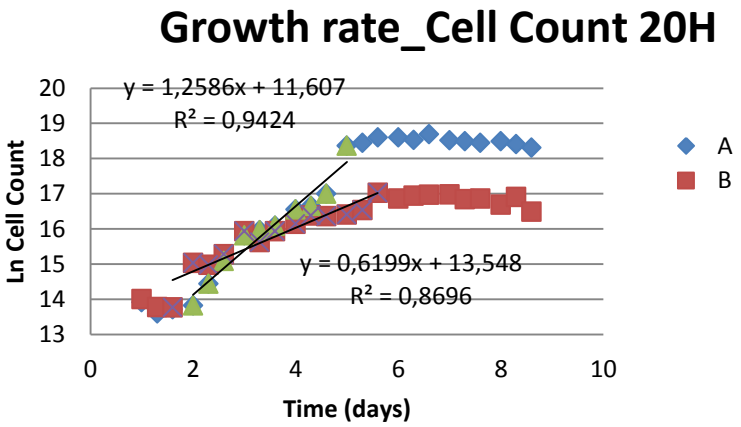

Figure 3.3. *Growth rate of Cellular concentration (Cells/ml) with 20 hours of photoperiod.*

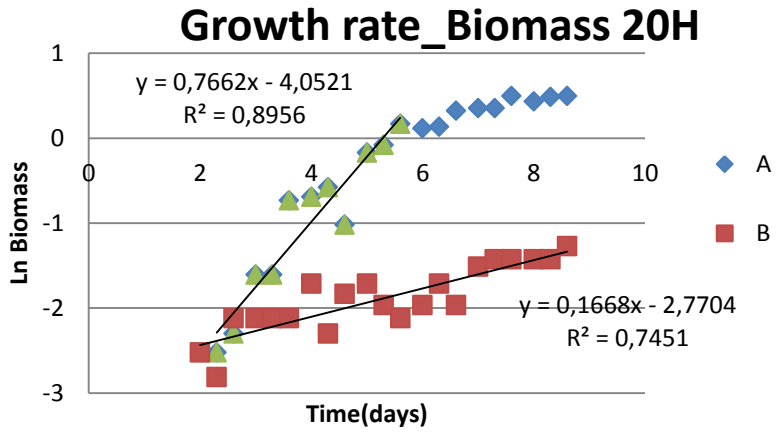

Figure 3.4. *Growth rate of Cellular concentration (g/l) with 20 hours of photoperiod.*

From Figure 3.3 and Figure 3.4 the specific growth rate (μ) of *Chlorella vulgaris* referring to 20 hours of illumination is calculated. In the first batch, MCS-A the value of μ=1,2586 [d^{-1}] was obtained on the base of cell number in the volume while μ=0,7662 [d^{-1}] expressed the mass concentration in g/l. In the MCS-B the values were respectively μ=0,6119 in cells/ml and μ=0,1668 in g/l. Therefore in terms of numbers of cells the difference in the growing rate between the two systems is nearly double, while in terms of dry weight this difference is much higher: the MCS-A is growing nearly 4,6 times more rapidly than the MCS-B (the system operated without CO_2).

Another index that clearly shows the difference in concentration between the two batches and that confirms the previous results, is the absorbance. As stated before in §2.4.3, the optical density is directly linked to cellular concentration, indeed Figure 3.5 confirms that MCS-A grow more than MCS-B.

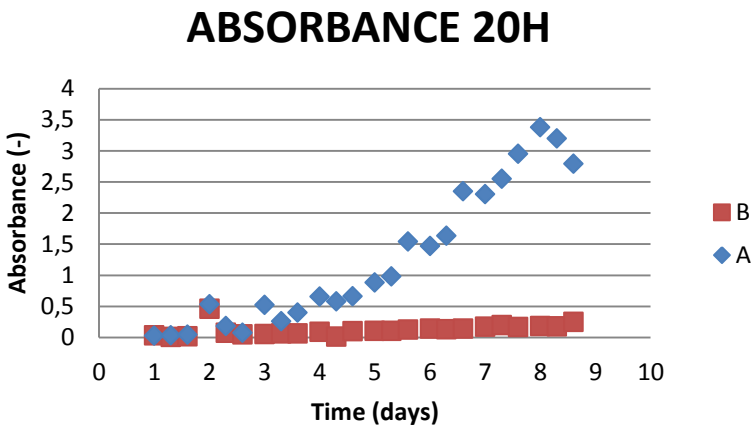

Figure 3.5. *Absorbance with 20 hours of photoperiod.*

Finally another parameter was used to address the difference in the cells dimension during the 8 days of experiment. This index is the cellular density and it is obtained dividing the value of the dry weight of one sample by the number of cells counted in that same sample. Figure 3.6 represents the evolution of cellular density throughout the experiment.

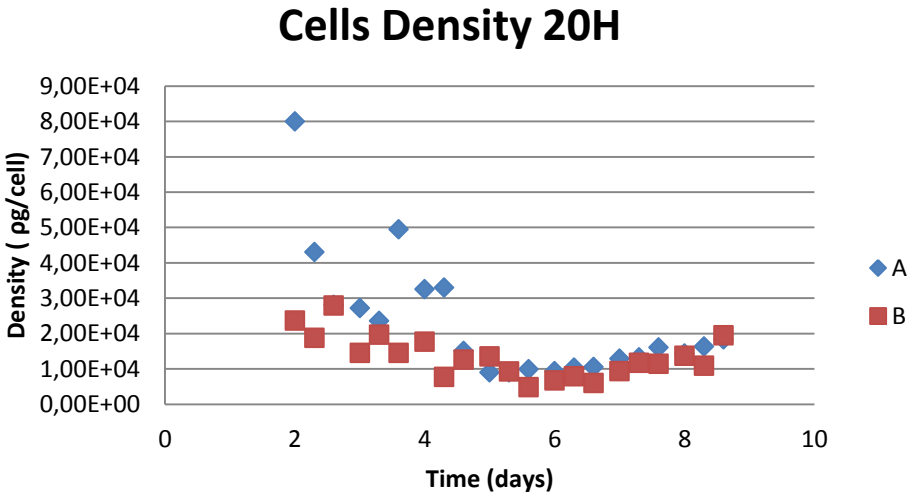

Figure 3.6. *Cells density (pg/cell) with 20 hours photoperiod.*

The trend shown in Figure 3.6 is in agreement with the previous data. The cellular density decreases for both culture systems in correspondence of the exponential growth phase. During this phase in fact, the nutrients and light are heavily exploited in the duplication process of the cells, thus growing their number.

3.2 Photoperiod of 15 hours

In the second experiment the illumination was given for 15 hours a day, the dark period being of 9 hours. The two MCSs were operated again for 8 days with the same average light intensity (128µmol $m^{-2}s^{-1}$) and average temperature (23°C). The two batches were both inoculated with an initial cellular concentration of 1 million cells/ml. Again the letter A is related to the MCS operated with air enriched with 5% CO_2 and the letter B refers to the MCS supplied with atmospheric air.

In Figure 3.7 and 3.8 the cellular concentration referring to the photoperiod of 15 hours, is showed. From Figure 3.7 is it evident that the lag phase lasts until the 5th day and the exponential one begins between that day and the 6th. This behavior is similar to the one observed in Figure 3.1 with 20 hours-photoperiod. The difference lies in the growth rate.

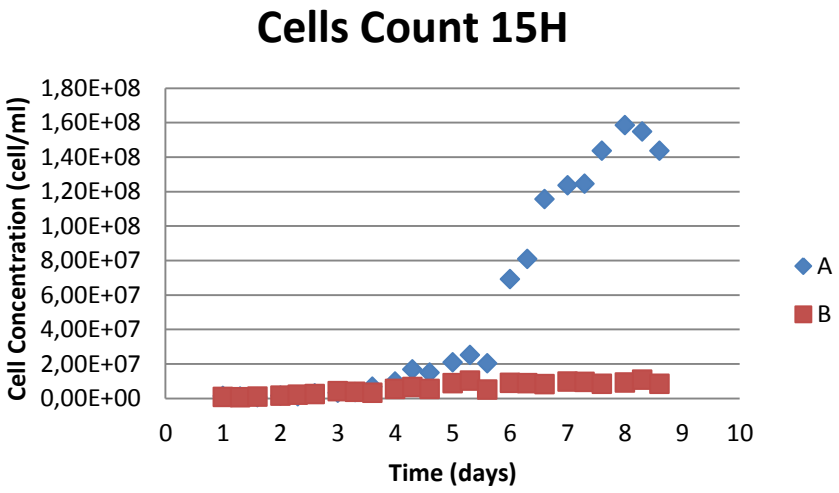

Figure 3.7. *Cellular concentration (Cells/ml) with 15 hours of photoperiod.*

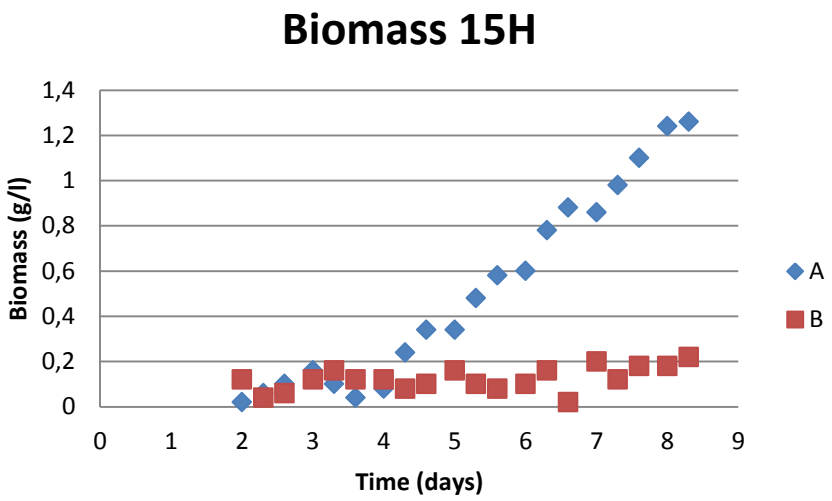

Figure 3.8. *Cellular concentration (g/l) with 15 hours of photoperiod.*

From Figures 3.7and 3.8 it clearly appears that MCS-A (operated with additional CO_2) reaches better growing performance than MCS-B (operated with atmospheric air). The different concentration between the two batches is of 148 million in terms of cell/ml and 1,04 in terms of g/l.

The growth rates calculated in this case are represented in Figures 3.9 and 3.10.

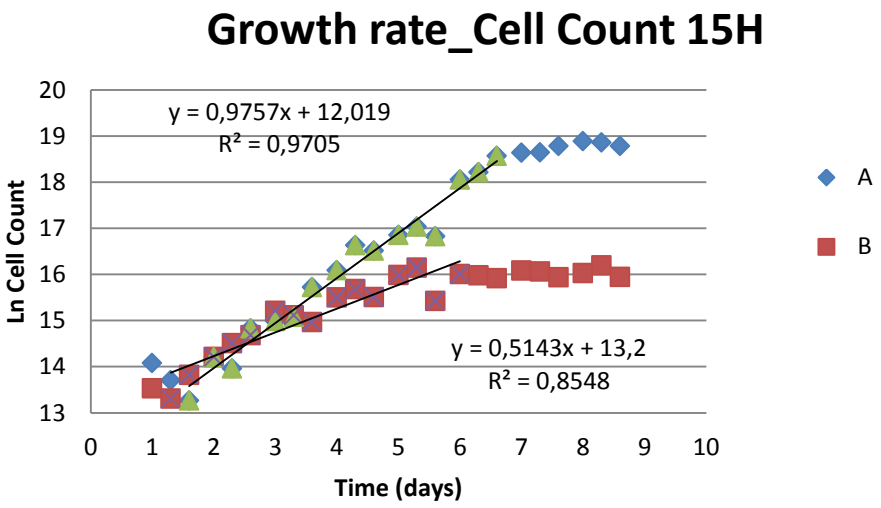

Figure 3.9. *Growth rate of Cellular concentration (Cells/ml) with 15 hours of photoperiod.*

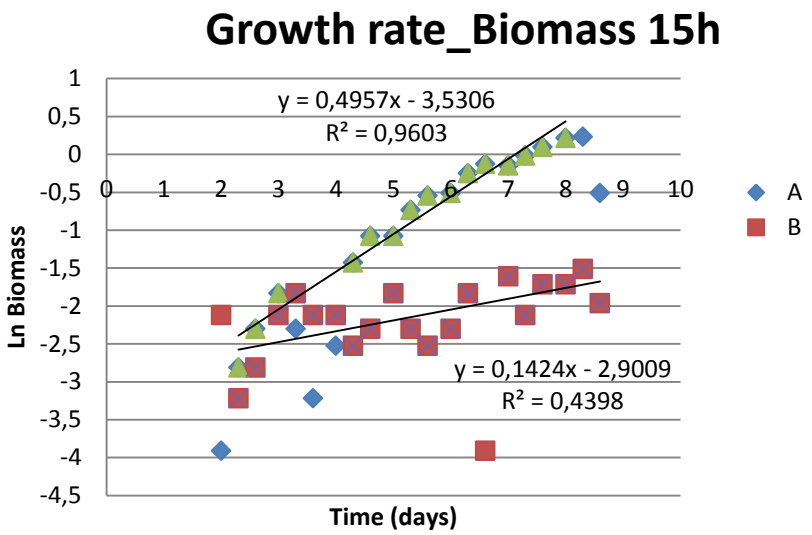

Figure 3.10. *Growth rate of Cellular concentration (g/l) with 15 hours of photoperiod.*

It is possible to observe from Figure 3.9 that even with 15 hours of illumination the difference in the growth rate, calculated in number of cells/ml, is nearly double between MCS-A (μ=0,9757) and MCS-B (μ=0,5143). In terms of dry weight, the growth rate of MCS-B (μ=0,1424) is 3,5 times lower than the one of MCS-A (μ=0,4957).

In Figure 3.11 the evolution of optical density is depicted, showing a remarkable difference in the values of the two systems starting from the 4th day.

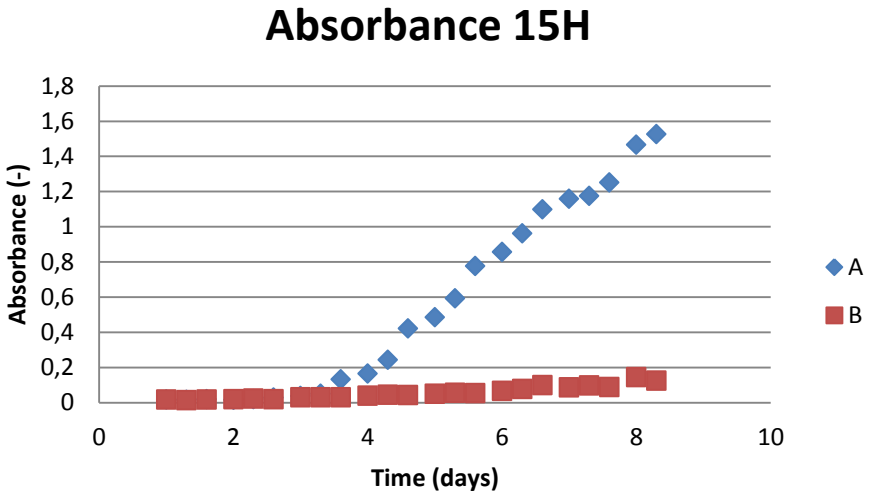

Figure 3.11. *Absorbance with 15 hours of photoperiod.*

Finally Figure 3.12 shows the cellular density index. In this case the data are quite scattered.

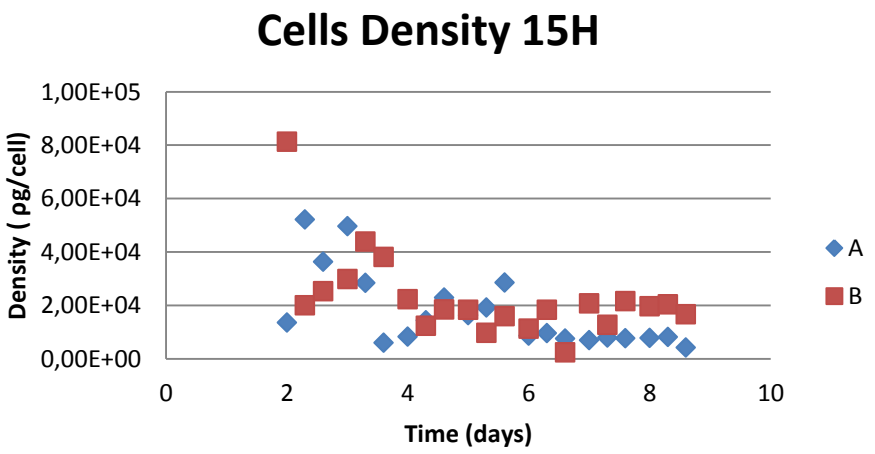

Figure 3.12. *Cells density (ρg/cell) with 15 hours photoperiod.*

3.3 Photoperiod of 10 hours

The third case analyzed is characterized by 10 hours of light and 14 hours of dark per day. The two MCSs were operated again for 8 days and both inoculated with an initial cellular concentration of 1 million cells/ml. The same average light intensity (128 µmol $m^{-2}s^{-1}$) and average temperature (23°C) were used.

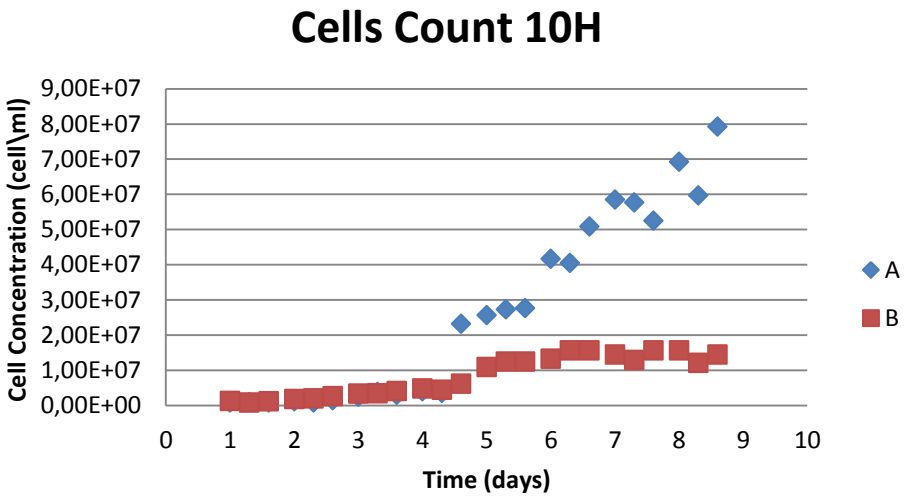

Figure 3.13. *Cellular concentration (Cells/ml) with 10 hours of photoperiod.*

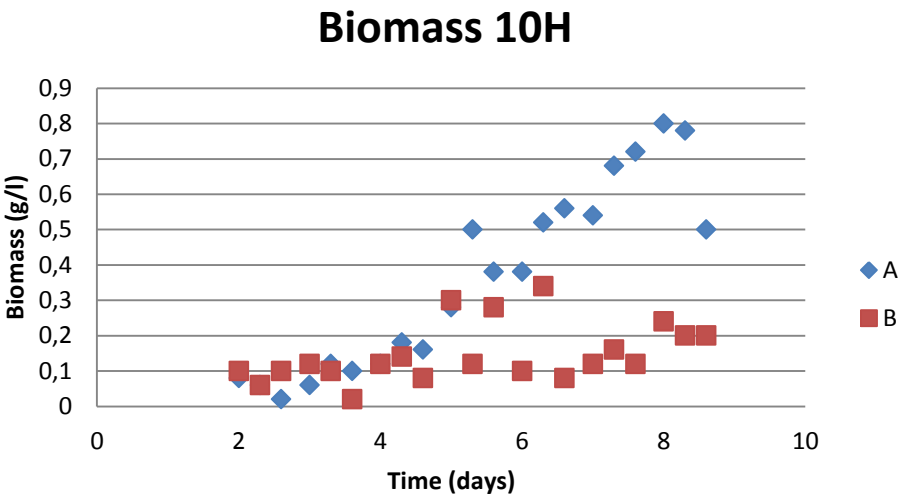

Figure 3.14. *Cellular concentration (g/l) with 10 hours of photoperiod.*

In Figure 3.13 it is confirmed that the exponential phase for the MCS-A starts on the 5th day and that the value of concentration reached in the MCS-A, supplied with additional CO_2, is higher than the one reached in the MCS-B. Nonetheless the difference in the concentration values is only of 65 million of cells/ml. It is noteworthy that this number is considerably lower than the previous ones, where the photoperiods had longer light time. Figure 3.14 shows a steady increase of concentration for the MCS-A but the measure becomes quite imprecise in the case of MCS-B.

This is related to the low cellular concentration reached into that system (MCS-B) that gives values of dry weight within the tolerance of the microbalance used to measure them. For this reason this result is not reliable. However the MCS-A reaches a value 0,64 times higher than the MCS-B.

The cellular concentration growth rates are illustrated in Figures 3.15 and 3.16.

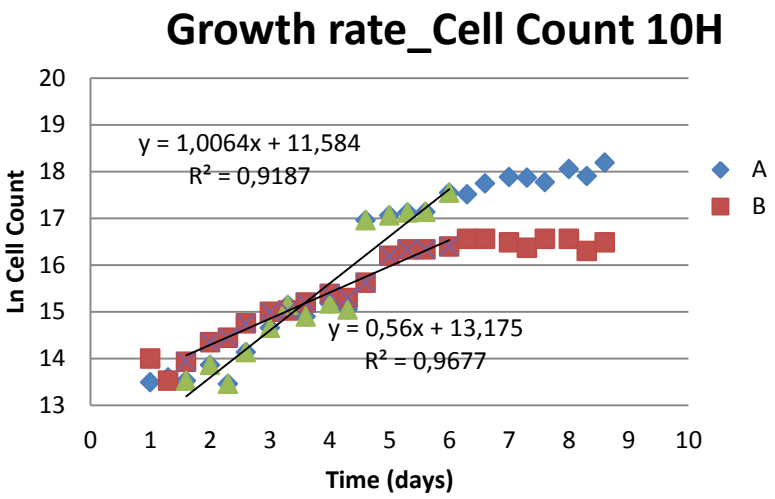

Figure 3.15. *Growth rate of Cellular concentration (Cells/ml) with 10 hours of photoperiod.*

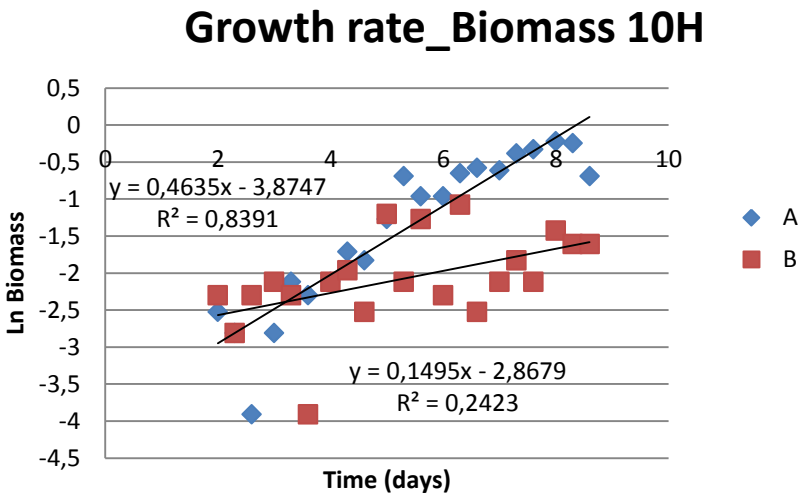

Figure 3.16. *Growth rate of Cellular concentration (g/l) with 10 hours of photoperiod.*

The trend expressed in Figure 3.15, related to the number of cells counted in one milliliter, is in agreement with previous data. The MCS-A has a growth rate μ=1,0064 [d-1] that is nearly double the value of the MCS-B, in which μ=0,56[d-1]. From Figure 3.16 it is confirmed that MCS-A is growing faster and that the values measured in case of the MCS-B are not reliable, being too dispersed.

In Figure 3.17 the absorbance for the two batches is illustrated, showing again a substantial difference in the values of the systems starting from the 4th day.

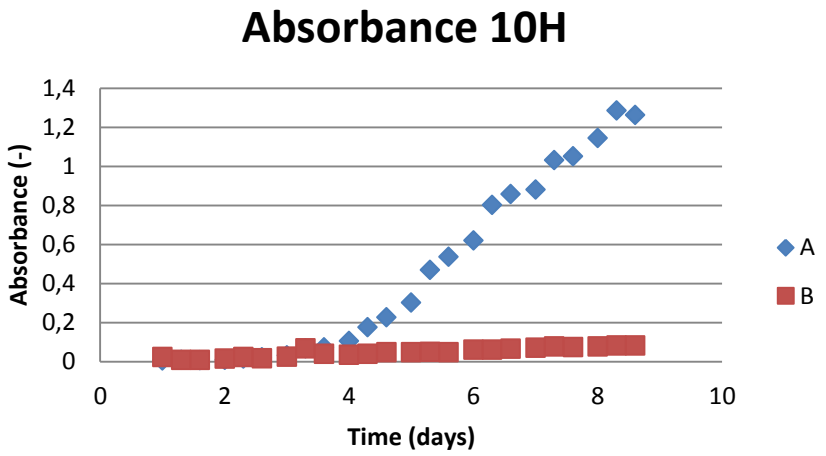

Figure 3.17. *Absorbance with 10 hours of photoperiod.*

The graph related to cells density, Figure 3.18, in this case is affected by the errors in the measures of dry weight for MCS-B. So the trend is not well definite and tends to a stabilization towards the last days of experiment, when the dry weight increase thus allowing also higher precisions of the measure.

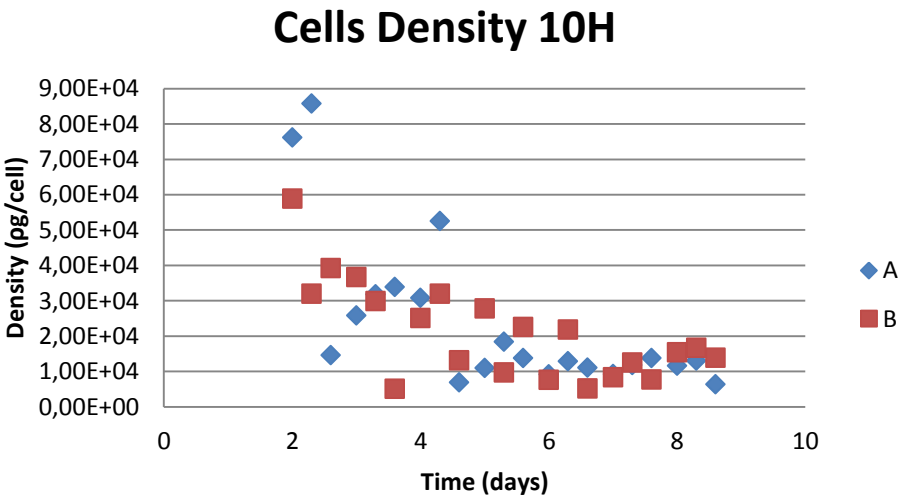

Figure 3.18. *Cells density (pg/cell) with 10 hours photoperiod.*

3.4 Photoperiod of 24 hours

During the fourth experiment the two MCSs were operated with a photoperiod of 24 hours for 8 days. The two systems were both inoculated with an initial cellular concentration of 1 million cells/ml. The same average light intensity (128 µmol $m^{-2}s^{-1}$) and average temperature (23°C) as in the previous experiments, were used.

In Figure 3.19 the cellular concentrations of both systems are presented. In this graph the MCS-A grow more than the MCS-B, in agreement with what observed until now. The value of concentrations reached in the system enriched with CO_2 is 194 million of cells/ml, the one for the system MCS-B (21 million of cells/ml) is nearly ten times lower.

The cellular concentrations calculated with regards to biomass show the typical behavior, with the MCS-A characterized by a growth higher of 11 times than the MCS-B, as presented in Figure 3.20.

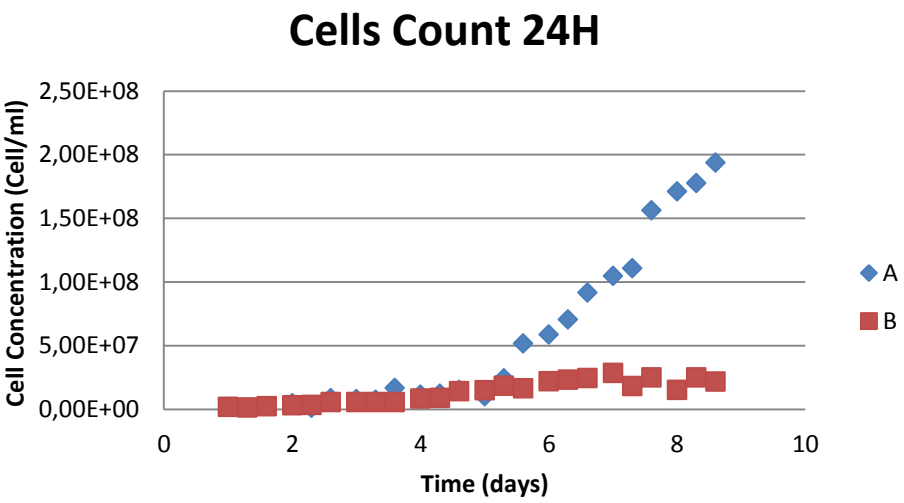

Figure 3.19. *Cellular concentration (Cells/ml) with 24 hours of photoperiod.*

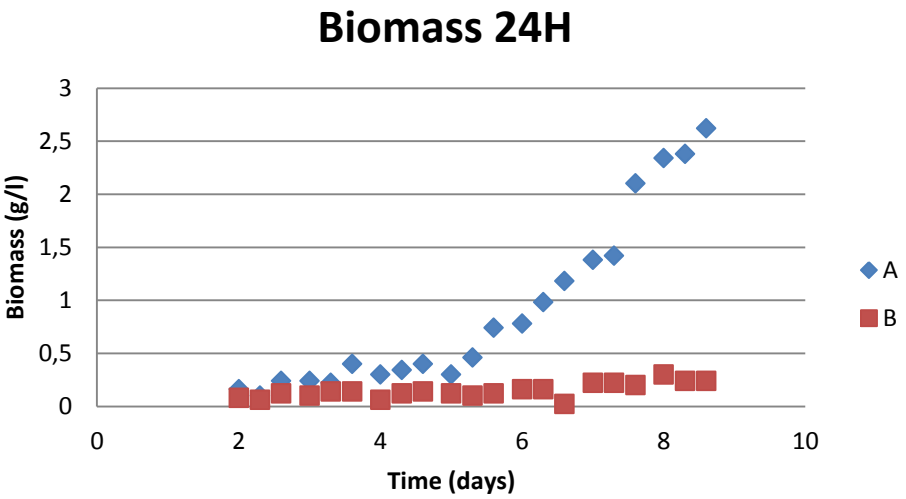

Figure 3.20. *Cellular concentration (g/l) with 24 hours of photoperiod.*

The growth rates referred to the numbers of cell/ml are calculated in Figure 3.21. It is evident that again the MCS-A, μ=0,6743 [d-1], is growing at double speed with respect to the MCS-B μ=0,3661 [d^{-1}].

Figure 3.22 instead shows that MCS-A has a growth rate referred to the dry weight μ=0,5209 [d^{-1}] that is nearly 3 times higher than the growth rate of the MCS-B, which is μ=0,1796 [d^{-1}].

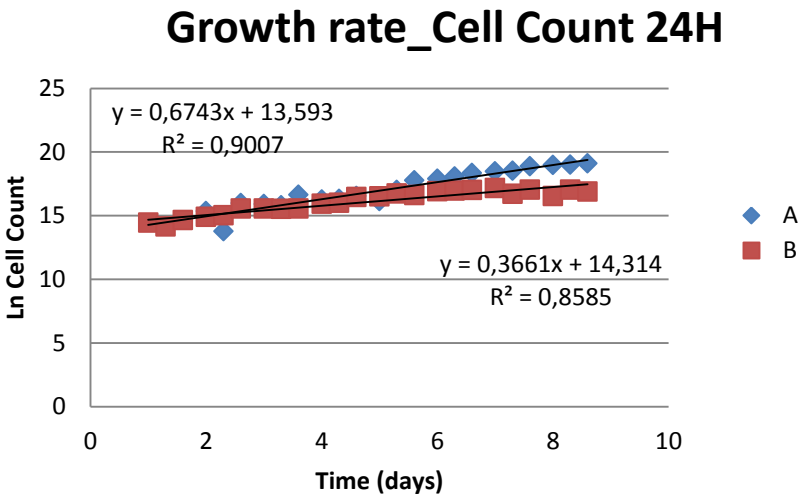

Figure 3.21. *Growth rate of Cellular concentration (Cells/ml) with 24 hours of photoperiod.*

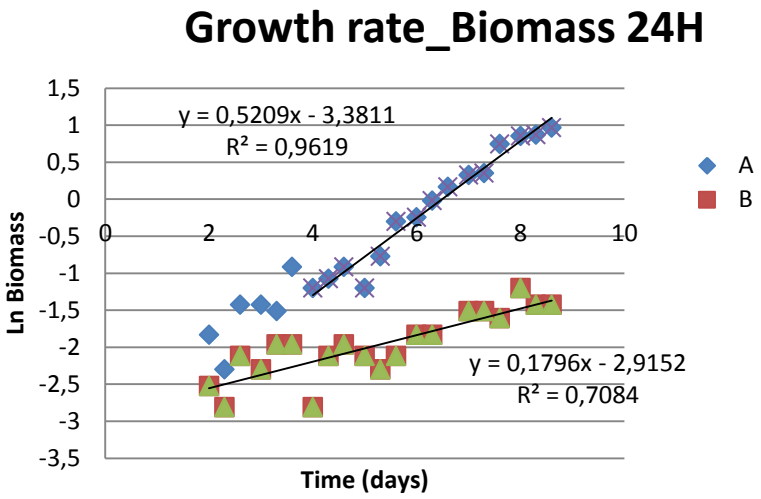

Figure 3.22. *Growth rate of Cellular concentration (g/l) with 24hours of photoperiod.*

In Figure 3.23 the optical density of the two systems operated with constant supply of light, is illustrated. These results confirm the ones obtained through the cells count procedure and biomass measurement. It is indeed clear that the MCS-A is growing more rapidly than the MCS-B. Moreover, the values of absorbance are comparable to the previous ones.

In closing, Figure 3.24 shows the evolution of the cellular density.

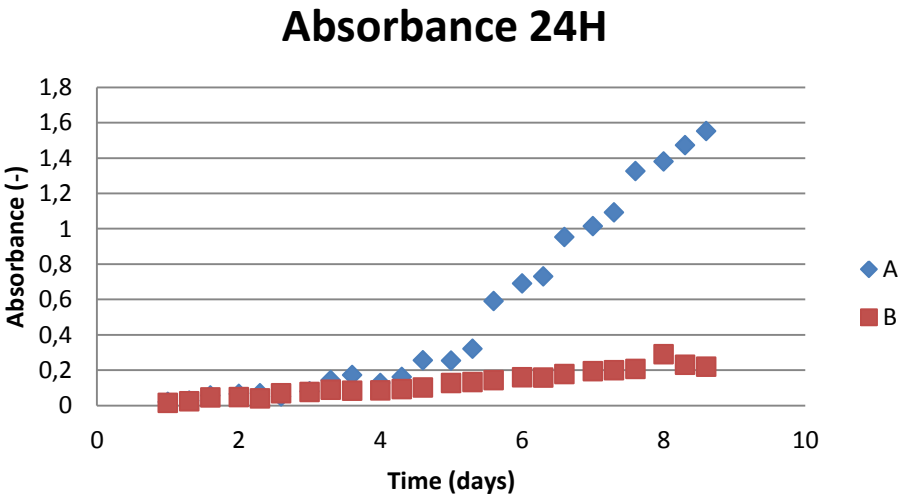

Figure 3.23. *Absorbance with 24 hours of photoperiod.*

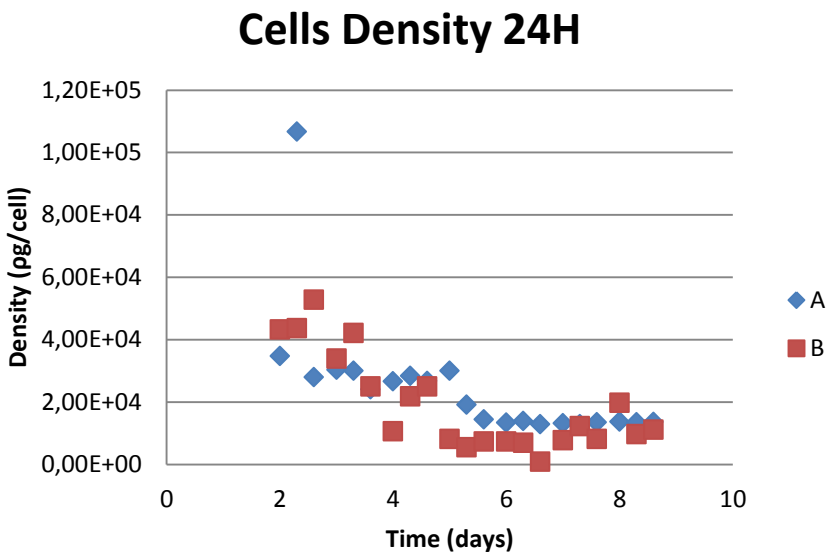

Figure 3.24. *Cells density (pg/cell) with 24 hours photoperiod.*

3.5 Different Light Intensity

In the last experiment a different light intensity was used. This experiment was aimed to address the difference in behavior of systems subject to higher or lower light intensity, to understand how this parameter affects the growing process.

In this case the two MCSs were operated with a photoperiod of 15 hours for 8 days. The two systems were both inoculated with an initial cellular concentration of 1 million cells/ml. The same average temperature (23°C) as in the previous experiments, was used. The average light intensity was instead different and set to 85 $\mu molm^{-2}s^{-1}$.

In Figure 3.25 the cellular concentrations of both systems are presented. As expected MCS-A grow more than the MCS-B. The value of concentrations reached in the system MCS-A is 72,4 million of cells/ml, the one reached into the system MCS-B is 7,28 million of cells/ml, which means it is nearly ten times lower, as already observed in § 3.4.

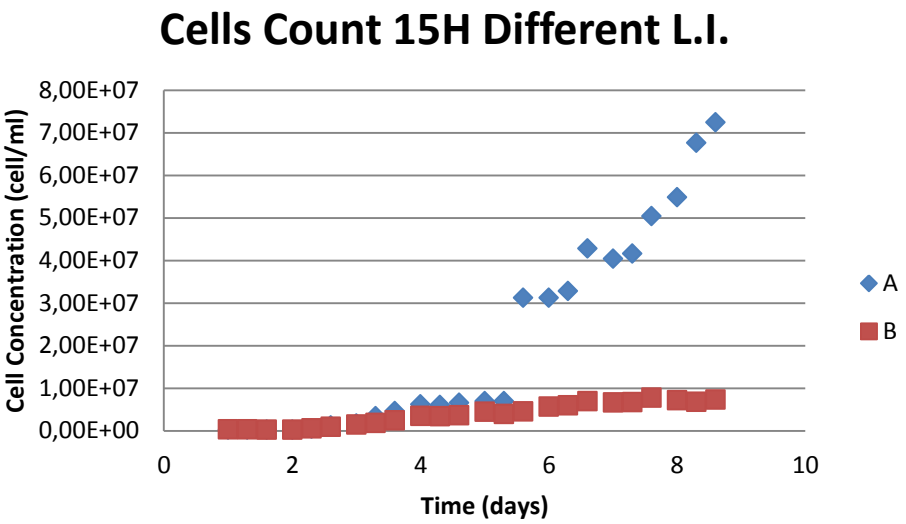

Figure 3.25. *Cells concentration (cell/ml) with 15 hours photoperiod and different Light Intensity.*

The cellular concentrations calculated with regards to biomass is a validation of the typical behavior, with the MCS-A characterized by a final dry weight of 0,76 g/l while the MCS-B shows a dry weight of 0,1 g/ as represented in Figure 3.26.

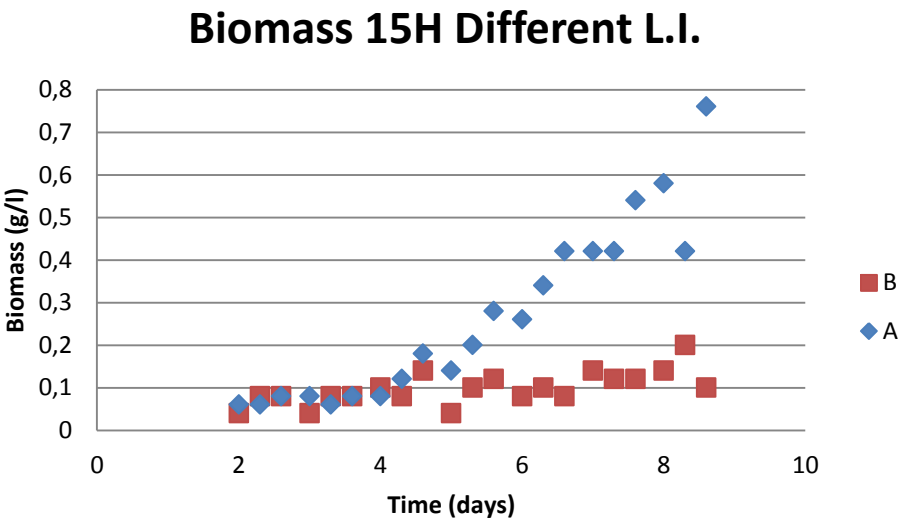

Figure 3.26. *Cells concentration (g/l) with 15 hours photoperiod and different Light Intensity.*

From Figure 3.27 it is possible to estimate the growth rate with regards to the number of cells counted. In the system MCS-A μ=0,8389 [d^{-1}] and MCS-B μ=0,483 [d^{-1}]. In Figure 3.28 the growth rate in terms of dry weight of MCS-B μ=0,2489 [d^{-1}] is as usually lower than the one of MCS-A μ=0,4027[d^{-1}].

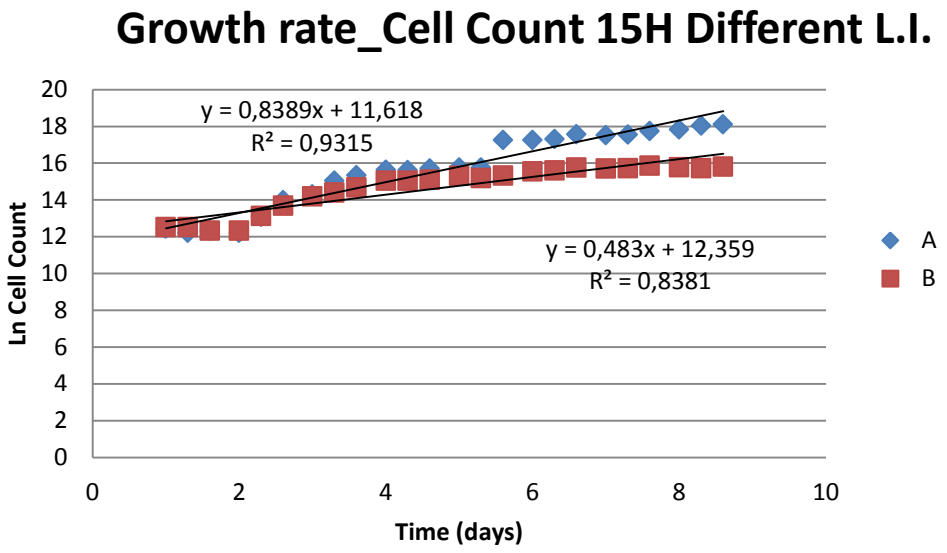

Figure 3.27. *Growth rate of Cellular Concentration (cell/ml) with 15 hours photoperiod and different Light Intensity.*

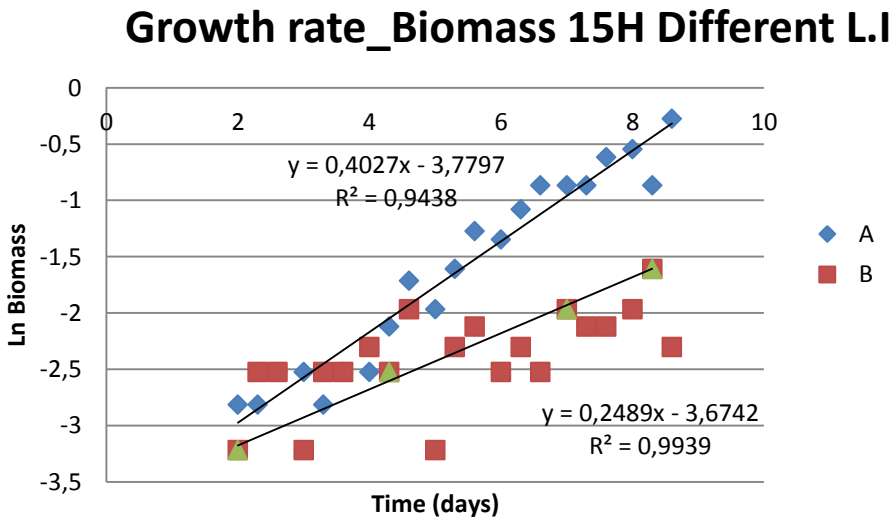

Figure 3.28. *Growth rate of Cellular Concentration (g/l)with 15 hours photoperiod and different Light Intensity.*

The optical density presented in Figure 3.29 shows a remarkable difference in the values of the two systems starting from the 4th day. This behavior is perfectly in agreement with the previous data.

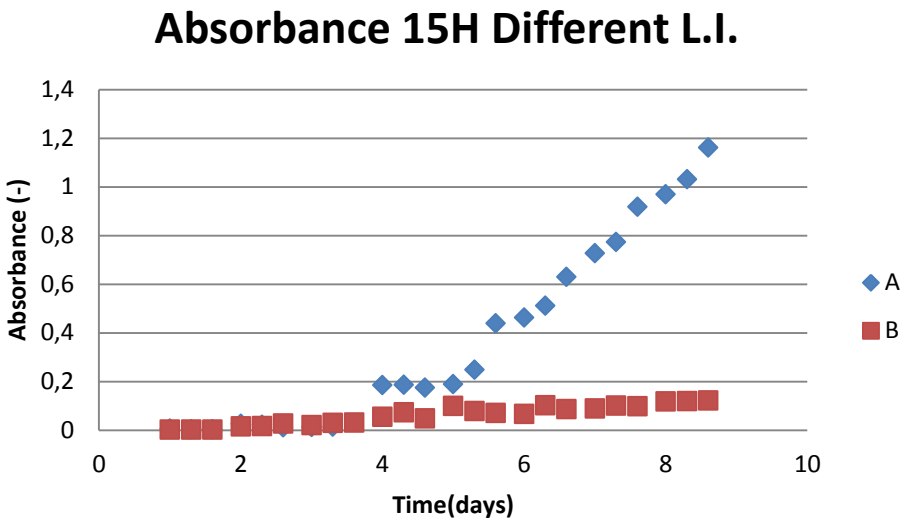

Figure 3.29. *Absorbance with 15 hours photoperiod and different Light Intensity.*

Finally Figure 3.30 shows the cellular density index. In this case this index is more definite than the case with the same photoperiod but higher Light Intensity.

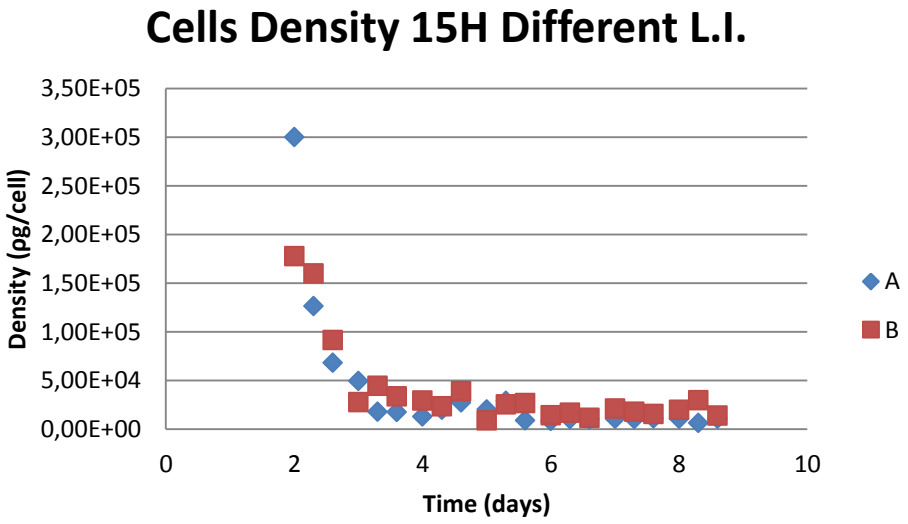

Figure 3.30. *Cells density (pg/cell) with 15 hours photoperiod and different Light Intensity.*

3.6 Comparison between performances of different photoperiods

The differences in the experimental conditions referred to the photoperiod and the gas supply. The investigation of the optimal photoperiod is linked to its fundamental role in the determination of the best possible performance for a photobioreactor (Jacob-Lopes et al., 2008). The advantage to compare two systems, one supplied with atmospheric air and one with air enriched by 5% of CO_2, lies in the possibility to quantify the performances of different metabolisms. The MCS-A is characterized by the use of both light and carbon as energy sources. The MCS-B instead, relies only on the energy supplied by the light. The results collected can be exploited to try to define how much these parameters affect the growth rate and to investigate the optimum growing conditions. In doing so it is important to highlight that each strain has specific optimal conditions (Costache et al., 2013) and the results obtained are related to the specific system illustrated here.

In Table 3.1 the final results and growth rates are summarized for each culture condition.

Table 3.1. *Final experimental results.*

	Cellular Growth Rate $\mu(d^{-1})$		**Biomass Growth Rate $\mu(d^{-1})$**		**Final Cellular Concentration (million Cell/ml)**		**Final Dry Weight (g/l)**		**Final Cellular Density (ρg/cell)**		**Final Absorbance (-)**	
	A	**B**	**A**	**B**	**A**	**B**	**A**	**B**	**A**	**B**	**A**	**B**
24 hours	0.674	0.366	0.52	0.179	194	21.6	2.62	0.24	13500	11100	1.552	0.22
20 hours	1.26	0.62	0.766	0.166	89.6	14.4	1.64	0.28	18303.57	19444.44	2.79	0.251
15 hours	0.976	0.514	0.495	0.142	144	8.40	0.6	0.22	4178.273	16666.67	1.526	0.124
10 hours	1.01	0.56	0.463	0.149	79.2	14.4	0.5	0.2	6313.131	13888.89	1.262	0.082

These results can be better represented graphically. Figure 3.31 shows the growth rate in terms of numbers of cells and Figure 3.32 in terms of dry weight. In both cases the growth rate tends to increase with the number of hours the systems are exposed to light. This result is in agreement with what stated by Jacob-Lopes et al. (2008).

However, this is not true for the last point of the graph, referring to the photoperiod of 24 hours for both systems. The growth rate seems to reach a maximum at 20hours of photoperiod instead of 24hours. The reasons of this behavior cannot be related to the phenomenon of photoinhibition. In fact it has been proven by Costache et al.(2013), that the threshold value of light intensity for the photoinhibition of *Chlorella vulgaris* is 1500μmol$m^{-2}s^{-1}$, which is considerably higher than the value used during the experiments (128 μmol $m^{-2}s^{-1}$). One possible explanation for the inconsistency of the results obtained and the conclusions of Jacob-Lopes et al. (2008), are the different culture conditions: different temperature, CO_2 enrichment and type of alga have been used. Furthermore the same work of Jacob-Lopes et al. (2008) asserts that different strains of algae could prefer different photoperiods with regards to the environmental conditions in which they were isolated in nature. Also Costache et al.(2013), report that between the parameters affecting the growth rate, the acclimation factor has to be taken into account.

In Figure 3.33 and Figure 3.34 the final values of cells per milliliter and dry weights, reached the 8^{th} day of cultivation, are displayed for each different photoperiod. It appears that the maximum is achieved with 24 hours of light, with a final value of 194 million cells/ml and 2,62 g/l for the MCS-A (supplied with additional CO_2) while the values reached in the system supplied with atmospheric air (MCS-B) are 21,6 million cells/ml and 0,29 g/l.

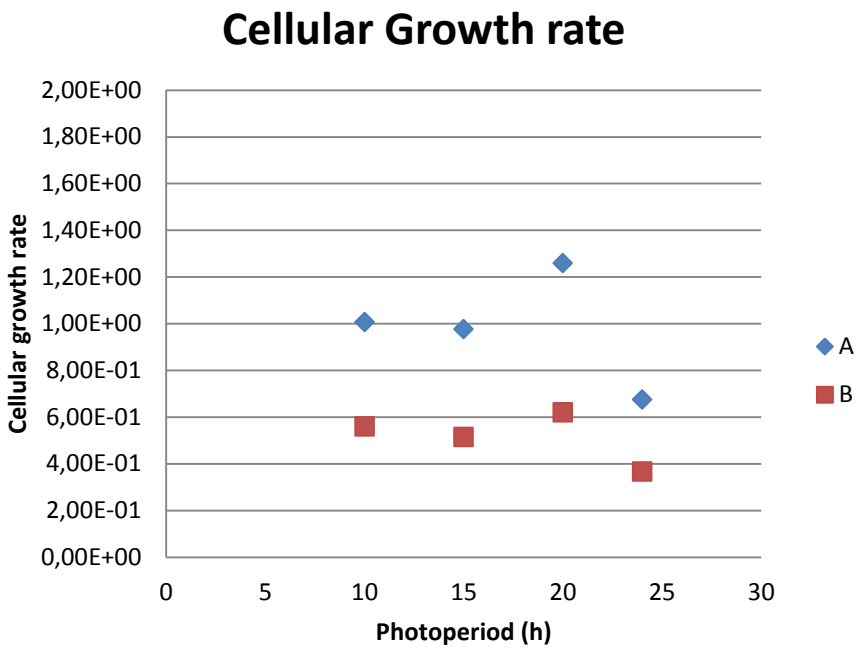

Figure 3.31. *Cellular growth rate for different photoperiods.*

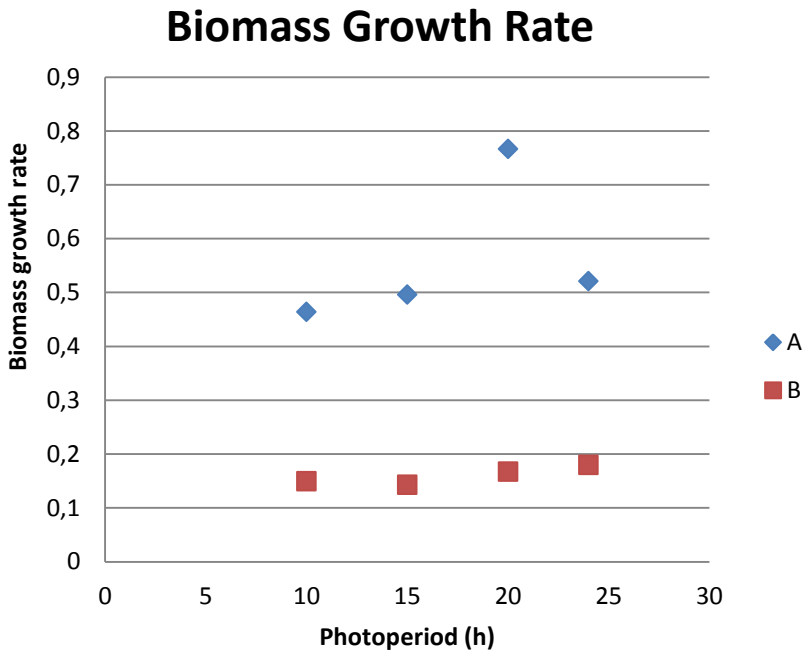

Figure 3.32. *Biomass growth rate for different photoperiods.*

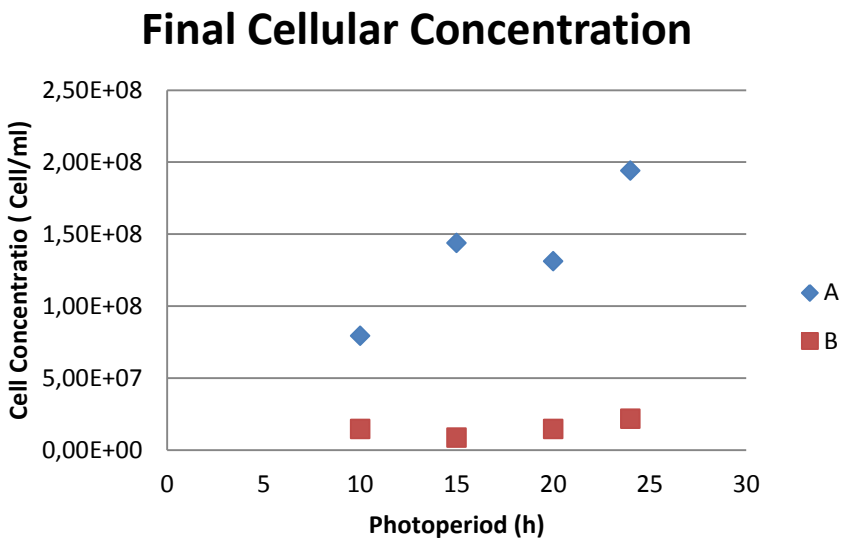

Figure 3.33. *Final value of cellular concentration for different photoperiods.*

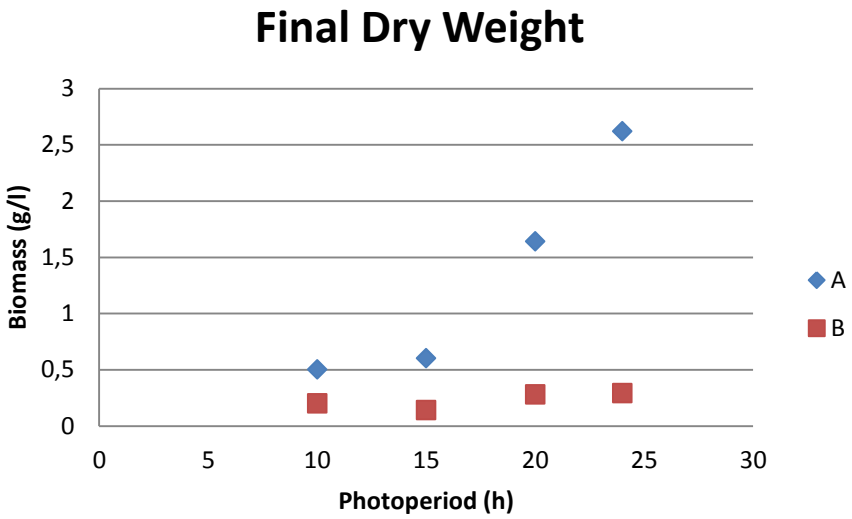

Figure 3.34. *Final value of dry weight for different photoperiods.*

The first observation is related to the results reached with the MCS-A.

These values correspond to what stated by Yeh and Chang (2011), that *Chlorella vulgaris* is able to reach a dry weight in the range of 2-5 g/l depending on numerous parameters like the medium composition and the light supply. Costache et al.(2013), report a maximum value of

biomass production of 5 g/l reached with a nitrogenous rich medium and additional CO_2 supply.

The second observation is about the MCS-B. It is evident that both growth rates are nearly constant. Even the final values of cells per milliliter and of dry weights are quite steady. It appears that the photoperiod is not having remarkable effect onto the system. This is probably linked to the fact that in the MCS-B the air supplied had not been enriched with CO_2, thus the limiting factor in this culture system is not light, but the carbon source. The availability of light is not altering the growing process of the algae, because it is being limited by the amount of carbon in the system.

The conclusions obtained from Figure 3.31 are confirmed by Figure 3.35, where it is possible to observe that the final value of absorbance reaches its maximum for a photoperiod of 20 hours.

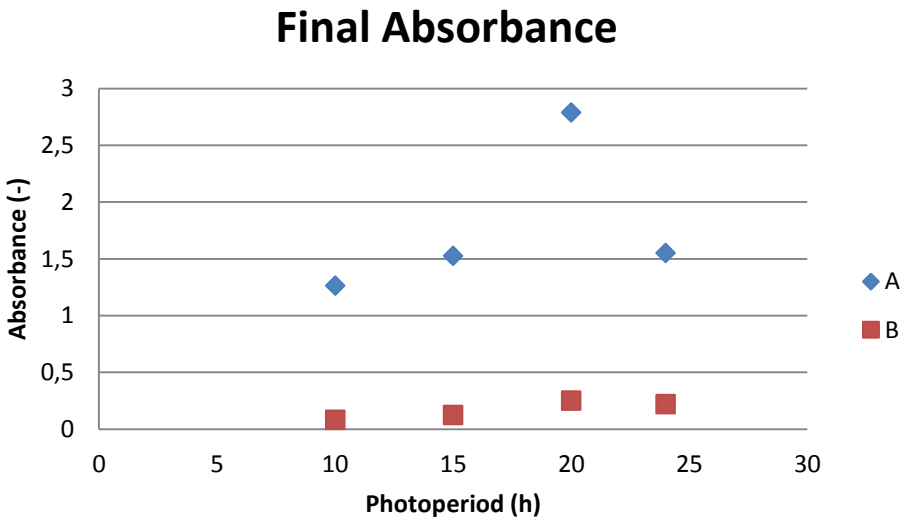

Figure 3.35. *Final value of absorbance for different photoperiods.*

Another factor to take into account in analyzing these data is that the cells in the external layer of the reactive system are exposed to higher light intensity than the ones in the internal layers. The growth of the internal cells is thus limited (Sforza et al., 2012). The cell concentration has an impact on light availability (Jacob-Lopes et al, 2008) for this reason it is possible to

explain the behavior in the case of 24 hours of photoperiod. With 24 hours of photoperiod the cell concentration reaches high values faster than with a lower number of light hours. In this case it becomes progressively more difficult for the light to reach the inner layers of the cell culture. This can lead to oxidative stress and damages for the external cells and to a low level of energy for the internal ones. To reduce this phenomenon as much as possible, the reactive systems were equipped with internal mixers. However it is possible that the mixing devices were not able to ensure an efficient mix of cells in the layers.

An important index to understand how much of the light supplied is effectively exploited by the growing process and not dispersed with thermal dissipation or metabolic functions is the Light Conversion Efficiency. It is represented in Figure 3.36. It is noteworthy that the maximum exploitation of the energy supplied by the light is in correspondence of the 24hours of photoperiod.

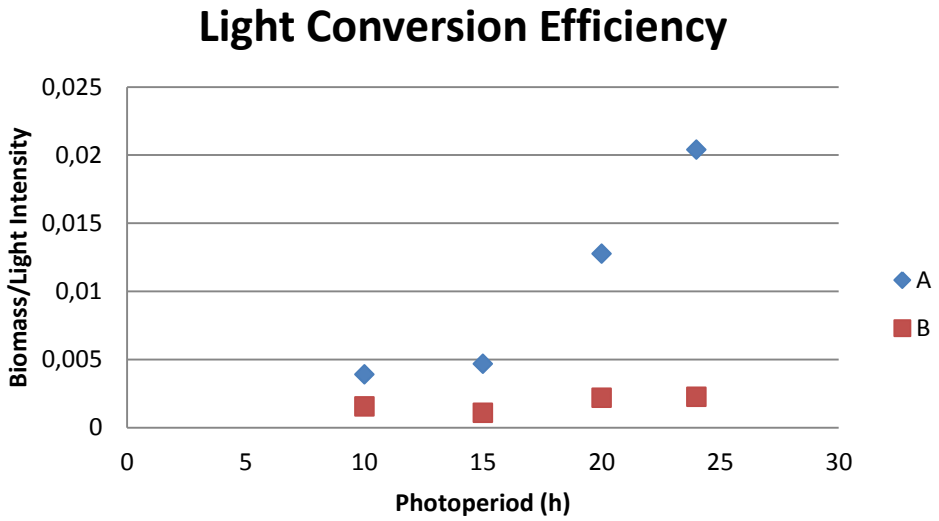

Figure 3.36. *Light Conversion Efficiency for different photoperiod.*

The performance of the reactive system is not only function of the duration of photoperiod, but also of the amount of energy conveyed to the system (Jacob-Lopes et al., 2008). To estimate the importance of this factor in the growing process of algae, the last experiment was run with a different light intensity. In particular the light intensity was reduced from 128 µmol $m^{-2}s^{-1}$ to 85 µmol $m^{-2}s^{-1}$, using 9 lamps out of 15. In table 3.2 the comparison between the two reactive systems operated with photoperiod of 15 hours are presented.

Table 3.2. *Comparison between the same system operated with different Light Intensity.*

	128 µmol $m^{-2}s^{-1}$	**85 µmol $m^{-2}s^{-1}$**
µA (cells/ml)	0.976	0.839
µB (cells/ml)	0.514	0.483
Final value A (cells/ml)	144000000	72400000
Final value B (cells/ml)	8400000	7280000
µA (g/l)	0.496	0.403
µB (g/l)	0.142	0.249
Final value dry weight A (g/l)	1.26	0.76
Final value dry weight B (g/l)	0.22	0.1
ρA (ρg/l)	4180	10500
ρB (ρg/l)	16700	12100
Final absorbance A	1.53	1.16
Final absorbance B	0.124	0.121

It is evident that the MCS-B is nearly unaffected by the difference in the light intensity. This result is in agreement with what stated before: the limiting factor to the growing process in this case is the amount of carbon available. For this reason the different light intensity has no great impact.

Observing the variation in the behavior of the MCS-A, it appears that the lower amount of energy supplied makes a remarkable difference. This difference is not very noticeable in the growth rate values, but it is blatant considering the final values of cells per milliliter. In this case the final value of cells reached in the system with higher light intensity is nearly double the one reached in the system with lower light intensity (from a value of 144 million of cells/ml to 72,4 million of cells/ml). The difference is obvious also in the final value of dry weight, which goes from 1,26 g/l with higher light intensity, to 0,76 g/l with the reduced one.

This experiment served to confirm that light is a dominant factor in the growing process of algae, both in terms of amount of energy supplied and in terms of period of supply.

Chapter 4

Photobioreactor simulation and modelling results

This chapter attempts to predict how a real photobioreactor for the production of microalgae would operate. Because the design of a cultivation system is fundamentally linked to the maximum production achievable, the aim of this part of the work is to simulate different type of reactors in order to find the design that assures the best performance. The production in photobioreactors of algae, which are photosynthetic microorganisms, is determined by the supply of light and nutrients. When the nutrients are not limited, the growing process is related only to the availability of light and its ability to penetrate the reactor depth. Two main cases will be studied: the case of constant light intensity and the case of variable light intensity, that simulates the night-day cycle. In this chapter the reactors and model used to describe the kinetic of microalgae production as a function of the irradiance profile inside the reactor will be presented. Subsequently, the simulation results obtained using this model, implemented with a Matlab® code, will be shown and the best design solution discussed.

4.1 Photobioreactors model

A schematic of the reactor considered for the simulations is provided in Figure 4.1. It is a flat-panel reactor, with the upper surface exposed to light and the gas inlet entering from the lower surface. It can be operated as a CSTR or PFR. In the latter case the use of recycle is considered.

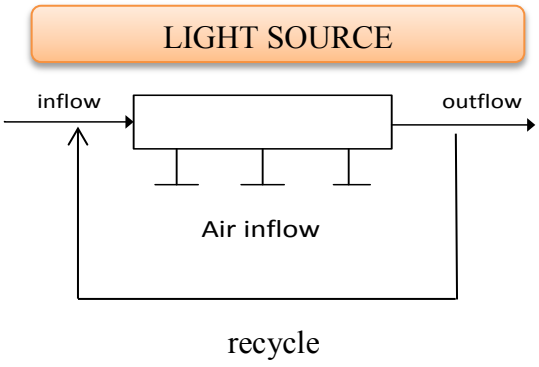

Figure 4.1. *Schematic of the reactor considered in the simulations.*

4.1.1 CSTR

The first reactor model is the CSTR one, which has been developed both at steady state and dynamically. The equation that represents the CSTR mass balance is:

$$\frac{dc_x}{dt} = \dot{V}c_{x,in} - \dot{V}c_{x,out} + r_x V \ , \tag{4.1}$$

Considering the steady state and that the entering biomass concentration equal to zero, the balance can be reduced to:

$$\dot{V}cx_{out} = r_x V \text{ or } cx_{out} = r_x \frac{V}{\dot{V}} = r_x \tau. \tag{4.2}$$

Where:

$c_{x,out}$= concentration inside the reactor, [g/L];

$\dot{V}$= volumetric flowrate, [L/h];

V= reactive volume, [L];

r_x= production rate, [g/(Lh)];

τ = residence time, [h].

It is possible to write a simplified energy balance considering the contribution of light:

$$\dot{W}_{out} \cdot LHV = I_{abs} \cdot A \ . \tag{4.3}$$

With: $\dot{W}_{out} = \dot{V} \cdot cx_{out}$,

$I_{abs} = ke(I_{in} - I_{out})$,

$\tau = \frac{A \cdot h}{\dot{V}}$ it , is possible to obtain:

$$c_{x,out} = k_e(I_{in} - I_{out}) \cdot \frac{\tau}{h} \cdot \frac{1}{LHV} \tag{4.4}$$

In this case:

LHV = lower heating value of algae, [W/kg];

I_{abs}= absorbed light intensity, [W/m^2];

I_{in}= light intensity entering the reactor, [W/m^2];

I_{out}= light intensity exiting the reactor, [W/m^2];

A= surface exposed to radiation,[m^2];

h = reactor depth, [m];

k_e = efficiency of light conversion, [adim].

4.1.2 PFR

The second reactor model is the PFR one, which has been developed both at steady state and dynamically.

The mass balance equation for the system without recycle is:

$$\frac{dcx}{dt} = -\frac{\dot{V}_{in}}{A}\frac{dcx}{dy} + r_x \quad . \tag{4.5}$$

Considering the steady state and introducing $\dot{y}$= y/L ($\dot{y}$ thus ranges between 0 and 1) it can be simplified into:

$$V \cdot r_x = \dot{V}_{in} \cdot \frac{dcx}{d\dot{y}} \rightarrow \frac{dcx}{d\dot{y}} = \tau \cdot r_x \quad . \tag{4.6}$$

Integrating between the values of the concentration entering and exiting the reactor, it can be obtained:

$$cx_{out} = cx_{in} + \tau \int_0^1 r_x \, d\dot{y} \quad . \tag{4.7}$$

Where:

y = reactor dimension parallel to the flow, [m];

L=length of the reactor, [m];

c_{xin} = inlet concentration, [g/L];

c_{xout} = outlet concentration, [g/L].

If the system is operated dynamically the balance becomes:

$$\frac{dcx}{dt} = r_x - \frac{1}{\tau}\frac{dcx}{d\dot{y}} \, . \tag{4.8}$$

If the scheme of the reactor operated with recycle is considered, the steady state balance con be expressed by Equation 4.9, while the dynamic balance is written by Equation 4.10:

$$cx_{out} = cx_{in} + \frac{\tau}{1+R}\int_0^1 r_x \, d\grave{y} \tag{4.9}$$

$$\frac{dcx}{dt} = r_x - \frac{R+1}{\tau}\frac{dcx}{d\grave{y}} \tag{4.10}$$

4.2 Cornet-Pruvost kinetic Model

As already stated, light is the main factor that affects algae growth in autotrophic systems. However, the radiation hitting the reactor surface is not entirely transmitted through the system. Optical properties of algae, distance from the surface and phenomena as absorption, self-shading and scattering need to be taken into account. To model the behavior of a photobioreactor three information have to be given:

- the value of the photosynthetic active radiation (PAR) hitting the surface of the reactor;
- the profile of the radiation available along the reactor depth;
- the algae growth rate as a function of light along the reactor depth.

The Cornet model, in the form generalized by Pruvost (Pruvost et al., 2011) is characterized by four steps. The first step is the determination of the irradiance at each point of the reactor's depth. The second step is the calculation of the growth rate for each point of the reactor's depth using the information about the irradiance at the correspondent point. The third step is the evaluation of the average growth rate along the reactor's depth. Finally this value is used to calculate the mass balance.

4.2.1 Light distribution

The Cornet model is based on two main assumption:

1) The radiative field is isotropic, omitting the angular distribution of both the radiation hitting the reactor's surface and the radiation deviated by the cells inside the reactor.
2) The scattered part of light is considered parallel to the main radiation direction.

This model is referred to constant light even though it can be used to describe the cyclical dynamic of solar radiation. In the latter case the radiation profile and the variation of the incident angle during the day and the different periods of the year must be considered. Moreover the difference between direct and diffuse light has to be addressed.

The irradiance value at each point along the reactor depth can be obtained knowing the irradiance reaching the surface and the optical properties of the microalgae species. It is calculated by the sum of the values of direct and diffused radiation :

$$I(z) = I_{dir}(z) + I_{dif}(z) \tag{4.11}$$

The expression for the extinction profile of direct and diffused radiation along the depth of the photobioreactor is, respectively:

$$\frac{I\ dir(z)}{I\ dir(0)} = \frac{2}{cos\theta}\frac{(1+\alpha)\exp[-\delta_{dir}(z-h)]-(1-\alpha)\exp[\delta_{dir}(z-h)]}{(1+\alpha)^2\exp[\delta_{dir}h]-(1-\alpha)^2\exp[-\delta_{dir}h]}\ , \tag{4.12}$$

$$\frac{I\ dif(z)}{I\ dif(0)} = 4\frac{(1+\alpha)\exp[-\delta_{dif}(z-h)]-(1-\alpha)\exp[\delta_{dif}(z-h)]}{(1+\alpha)^2\exp[\delta_{dif}h]-(1-\alpha)^2\exp[-\delta_{dif}h]}\ , \tag{4.13}$$

$$\delta_{dir} = \frac{\alpha c_x}{cos\theta}(Ea + 2bEs)\ , \tag{4.14}$$

$$\delta_{dif} = 2\alpha c_x(Ea + 2bEs)\ , \tag{4.15}$$

$$\alpha = \sqrt{\frac{Ea}{(Ea+2bEs)}}\ . \tag{4.16}$$

Where:

c_x = average concentration along the reactor depth, [kg/m^{2}s)

$I_{dir}(z)$ = direct PAR (photosynthetic active radiation) at depth z, [µmol/(m^{2}s)];

$I_{dir}(0)$ = direct PAR at depth 0, [µmol /(m^{2}s)];

$I_{dif}(z)$ = diffuse PAR at depth z, [µmol /(m^2s)];

$I_{dif}(0)$ = diffuse PAR at the reactor surface, [µmol /(m^2s)];

θ = incident radiation angle with respect to normal direction of reactor surface, [rad];

h = depth of PBR, [m];

z = reactor dimension along the depth, [m];

Ea = absorption mass coefficient, [m^2/kg];

Es = scattering mass coefficient, [m^2/kg];

b = backscattering fraction, [adim].

4.2.2 Kinetic growth

There are two different type of models able to correlate the photosynthesis rate and the light intensity (Luo and Al-Dahhan, 2003).

The first type of models are called Static models. These are gathered from fitting of experimental data of growth rate as a function of light. The main advantage of this type of models is that they are simple. For this reason the Static models are the most used ones in photobioreactor design and analysis. The principal drawback is the lack of generality and ability to describe the dynamic nature of the observed phenomena.

The second type of models are the Dynamic ones. These models are able to correlate the physiology of the photosynthetic process to the kinetic growth of the algae. Thus Dynamic models are able to describe phenomena such as photoinibition and photolimitation. The foremost disadvantage limiting the use of Dynamic models is related to their intrinsic complexity, and the use of suitable values for the model parameters.

The model used for the simulation in this work, the Cornet model, belongs to the first category, Static models, but it is considered one of the more accurate to describe the system of interest.

In order to solve the mass balance, the average biomass growth rate ($\overline{rx}$) as a function of the value of biomass concentration (c_x) has to be calculated. r_x is averaged because its value changes along the reactor. This is caused by the variable light distribution inside the reactor itself, due to phenomena like scattering and absorption. The hypothesis in the model analyzed here is that light undergoes a one-dimensional attenuation along the depth of the reactor. Thus the average biomass growth rate ($\overline{rx}$) can be calculated as the integral average:

$$\overline{rx} = \frac{1}{h}\int_0^h r_{x,z} * dz \ . \tag{4.17}$$

The value of $r_{x,z}$, which is the punctual growth rate at depth z, is determined by two factors: one expresses the biomass duplication rate, the other one takes into account the respiration and death kinetic and is called maintenance term. Thus $r_{x,z}$ can be written as:

$$r_{x,z} = r_{x,p,z} - r_{x,m,z} \ . \tag{4.18}$$

Where:

$r_{x,z}$= growth rate at depth z, [kg $m^{-3}s^{-1}$];

$r_{x,p,z}$=growth rate due to photosynthesis, [kg $m^{-3}s^{-1}$];

$r_{x,m,z}$=growth rate due to maintenance process, [kg $m^{-3}s^{-1}$].

The Cornet model allows to calculate the growth due to photosynthetic functions ($r_{x,p}$).
According to the model $r_{x,p,z}$ is calculated as:

$$r_{x,p,z} = \rho_m \frac{K}{K+I(z)} \Phi E_a I(z) c_x \ . \tag{4.19}$$

Where:

ρ_m = maximum energetic yield for photon conversion, [adim];

K = half saturation constant for photosynthesis, [μmol$m^{-2}s^{-1}$];

Φ = mass quantum yield for Z-scheme of photosynthesis, [kg/μmol];

The maintenance term consists of contributes from physiological functions of the cells and death kinetic. This limits the duplication rate because these phenomena use part of the energy conveyed by the light.

Examples of these functions are:

- shifts in metabolic pathways;
- cell motility;
- changes in stored polymeric carbon;
- osmoregulation;
- proofreading, synthesis and turnover of enzymes and other macromolecular compounds;
- defense against O_2 stress.

For the reasons stated above, the maintenance term generates a negative contribution that can be written as:

$$r_{x,m,z} = \mu_e c_x \ . \tag{4.20}$$

Where:

μ_e = maintenance coefficient, [time^{-1}].

In summery Equation 4.8 can be rewritten as:

$$r_{x,z} = \rho_{m\frac{K}{K+I(z)}} \Phi E_a I(z) c_x - \mu_e c_x = \mu c_x - \mu_e c_x \ . \tag{4.21}$$

4.3 Model Parameters

The Cornet-Pruvost model described in §4.2 contains many parameters that are specific for the considered system. Their values depend on the type of algae used, the operating conditions and the reactor's geometry. In this section the parameters definition for the species considered, *Scenedesmus obliquus*, will be given and the values used in the Matlab® simulations discussed.

4.3.1 Absorption, scattering and backscattering coefficient

The reactive system is made of three different phases. The liquid phase is the aqueous medium, the solid one is represented by the algae, while the air and CO_2 form the gas phase. In such system the entering light is partially absorbed and partially scattered.

These phenomena are caused by the presence of chlorophyll and carotenoids inside the algae cells and by the volume of the cells itself. Thus it becomes important to know the optical properties of the specific alga, which can be determined once three basic information are given (Pottier et al., 2005):

- type and amount of each pigment contained in the solution;
- microalgae dimensions distribution;
- microalgae shape.

If the information needed is not available, an efficient alternative can be the fitting of the parameters on experimental data. The values used in the Matlab® code that simulates the behavior of the reactive system in the present work obtained from literature are:

Ea (absorption mass coefficient) = 220 [m^2/kg],

bEs (backscattering fraction*scattering mass coefficient) = 5 [m^2/kg].

4.3.2 Half saturation constant for photosynthesis

This term (K) represents the value of irradiance at which half of the maximum exponential growth rate is reached. In agreement with values found in the literature for other species, K was set to 150 μmol/m^2s.

4.3.3 Maximum energetic yield for photon conversion and Mass quantum yield for Z-scheme of photosynthesis

The maximum energetic yield for photon conversion and the mass quantum yield for Z-scheme of photosynthesis are here considered together as a unique term. The value of their

product was taken from the thesis of Urbani, 2014. For a constant light intensity of 150 [μmol/(m^2s)] the value is equal to 2,52*10^{-9} [kg/μmol].

When simulating the solar radiation as source of light for the modelling of the summer period, the value of ρφ , is changed to 1,32*10^{-6}[kg/μmol].

4.3.4 Maintenance term

As stated in § 4.2.2, the maintenance term represents a limitation to cell duplication. It is indicated by the letter μ_e and its value depends on the species considered and other factors, most of all the light intensity. According to the literature (Urbani, 2014) the value of μ_e for *Scenedesmus obliquus* at 150 [μmol/(m^2s)] was taken equal to 1,7361*10^{-6} [s^{-1}]. However, when simulating the solar radiation during the modelling of the summer period, the maintenance term depends on the residence time (τ) through the following equation (Urbani, 2014):

$$\mu_e=(Y_{app})\, m_e\,, \tag{4.22}$$

$$Y_{app}=a/\tau+\beta\,. \tag{4.23}$$

Where:

a = 0.00049 [g*d/μmol];

β = 0.00025 [g/μmol];

m_e = maintenance coefficient: 543,143 [mmol /(g*d)].

4.3.5 Other parameters

Other parameters are needed to implement the Matlab® code that simulates the photobioreactor.

Namely:

- θ = incident radiation angle with respect to normal direction of reactor surface, that is fixed to 0 [rad] when simulating the constant light intensity. When simulating the solar radiation, the daily profile was calculated from Enzo, (2012) depending on the different hour of the day for the summer season;
- I_in = light intensity at depth 0. For constant light intensity was fixed to 133,5 [μmol/m^2s]. It is calculated considering the light intensity hitting the reactor's surface (I=150 [μmol/m^2s]) and the absorption of the polycarbonate (11% of the hitting light

intensity). While simulating the solar radiation during summer season the value of the light intensity is time-dependent and its value will be discussed in § 4.6.1;

- h = depth of PBR, that is taken equal to 0.012 [m];
- LHV = lower heating value, assumed from literature equal to 20 [MJ/kg].

4.4 Maximum and real productivity

The maximum productivity represents the upper limit of biomass production, defined as the annual productivity per unit of area. It is important to evaluate its value because it can be used to measure the performance of the photobioreactors, confronting their effective productivity with the maximum thermodynamically possible.

4.4.1 Maximum productivity

Two fundamental hypothesis need to be considered in order to evaluate the theoretical limit:

1. each photon hitting the surface is converted into chemical energy;
2. the energy is fully exploited to produce biomass.

The first law of thermodynamics fixes the upper limit to the productivity of a natural system. In the examined case it can be expressed by the following relation:

$$\dot{E}_{in} \geq \dot{E}_{stored} \quad , \tag{4.24}$$

where:

$\dot{E}_{in}$= incident solar radiation per unit area, [MJ $m^{-2}y^{-1}$];

$\dot{E}_{stored}$= energy stored as biomass per unit area, [MJ $m^{-2}y^{-1}$].

This means that the energy stored as biomass is limited by the amount of solar energy available. The mechanism that transforms solar energy into chemical energy is the photosynthesis. It can be approximately considered that the basic molecular form in which the chemical energy is stored is the one of the simplest carbohydrate, the formaldehyde CH_2O. Thus the photosynthetic process can be formulated as:

$$CO_2 + H_2O + 8photons = CH_2O + O_2 \, . \tag{4.25}$$

As a consequence, the maximum biomass productivity can be calculated from Equation 4.26:

$$P_{max} = \frac{M_{co2,red} \cdot E_{carb}}{E_{bio}} \quad . \tag{4.26}$$

Where:

P_{max}= maximum productivity per unit area per year, [kg m^{-2} y^{-1}];

M_{CO2red}= moles of CO_2 reduced to carbohydrate per unit area per year, [mol/(m^2y)];

E_{carb}= carbohydrate heat of combustion, [J/mol];

E_{bio}= biomass heat of combustion, [J/kg].

The number of moles of CO_2 reduced to carbohydrate per unit area per year (M_{CO2red}) are function of:

- the total solar energy reaching the system per unit area per year,
- the percentage of photosynthetic active radiation (PAR), which is the portion of the total solar radiation that can be absorbed by the algae and used for the photosynthesis (approximately 43% of the entire spectrum),
- the average energy per mole of photons and the quantum requirement (QR), which is the number of photons needed to reduce one mole of CO_2 to one of CH_2O.

A realistic value of maximum biomass productivity is equal to 12% of the total solar energy reaching the system.

4.4.2 Real productivity

The real value of biomass productivity is much lower than the theoretical maximum. This is caused by the non-ideality of the phenomena considered. The photons hitting the reactor's surface are not entirely transformed into chemical energy. Indeed reflection and dissipation are always present. Moreover part of the energy stored is used by the algal cells for biological functions, like respiration, rather than to increase the biomass. Thus the real productivity can be written as:

$$P_{real} = P_{max} \cdot K_e \ . \tag{4.27}$$

Where k_e is an efficiency term that considers the efficiency in photons transmission, photons utilization and biomass accumulation. It can be evaluated from the following:

$$k_e = \frac{\dot{E}_{out}}{\dot{E}_{in}} = \frac{c_{out} \cdot \dot{V} \cdot LHV}{(I_{in} - I_{out}) \cdot A} \quad . \tag{4.28}$$

Where:

$\dot{E}_{in}$= energetic flux entering the system, [W];

$\dot{E}_{out}$=energetic output in the form of biomass, [W];

c_{out}= final concentration, [kg/m^3];

LHV = lower heating value, [W/kg];

I_{in}= inlet light intensity, [W/m^2];

I_{out}= outlet light intensity, [W/m^2];

A= reactor's surface exposed to light, [m^2].

4.5 Results: Constant light intensity simulations

To predict the growth rate of microalgae inside a PBR, different Matlab® codes were implemented. Firstly the simulations were realized considering a constant light intensity of 150 μmol/(m^{2}s), thus simulating the use of artificial lamps as source of illumination. This section is divided in two parts: the first one refers to the simulation of steady state systems; the second one contains the results of dynamic simulations.

4.5.1 Steady State simulations

The first case analyzed refers to a photobioreactor behaving as a CSTR. The description of the plant and the balances equations, are reported in § 4.1.1.

The Matlab® code used is *prgCSTR.m.* The input given to the code are the biomass concentration (which ranges between 0 to 6 g/L) and the parameters used in the equation of

the Cornet-Pruvost model. The parameters used are listed in Table 4.1., according to what discussed in §4.3. The code enables to calculate the extinction profile of the radiation hitting the surface along the depth of the reactor with Equation(4.12). Only the direct component of radiation is considered. The second step consists in the calculation of the corresponding values of the growth rate. After that, the average growth rate inside the reactor is evaluated and used in the mass balance (Equation .4.2) to obtain the value of the residence time (τ) corresponding to the value of c_x initially selected. Moreover it is possible to use this code to estimate the radiation coming out of the reactor to calculate the efficiency factor (k_e) that represents a measure of the efficiency of light absorption, according to Equation 4.28.

Table 4.1. *Parameters of the Matlab code prgCSTR.m.*

Name	Value	Unit of measure
bEs	5	m^2/kg
Ea	220	m^2/kg
θ	0	rad
h	0.012	m
K	150	µmol/m^2s
ρ φ	$2.52*10^{-9}$	kg/ µmol
µe	$1.7361*10^{-6}$	1/s
I	150	µmol/m^2s
I_in	0.89*I=133.5	µmol/m^2s
LHV	20	MJ/kg

The results obtained with *prgCSTR.m* are presented in the following figures. Figure 4.2 shows how the growth rate changes with the concentration.

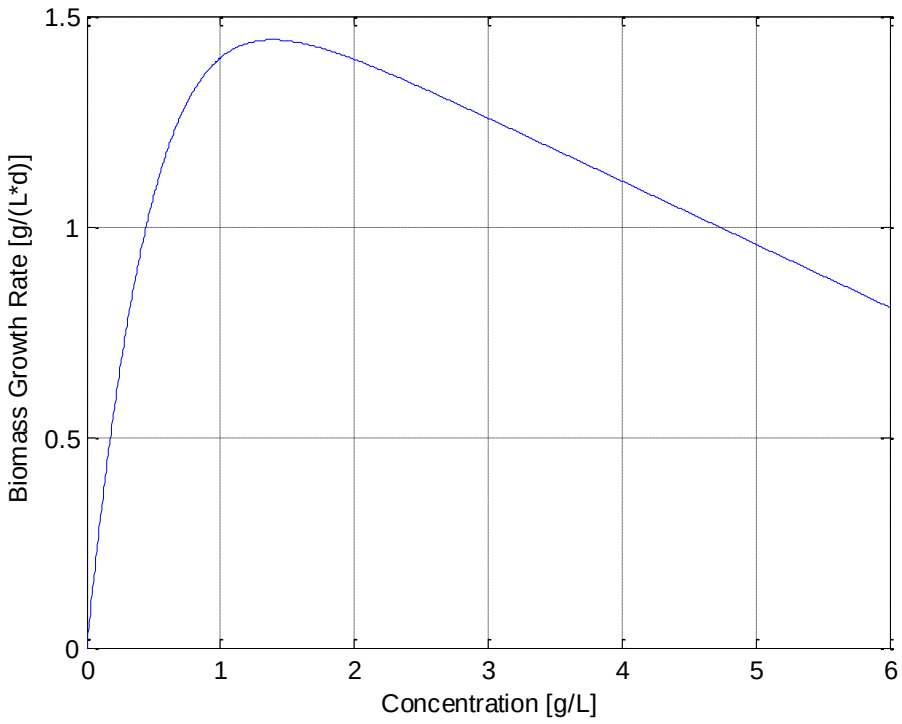

Figure 4.2. *Biomass growth rate evolution as a function of the concentration. Steady state CSTR.*

It is noteworthy that there is a concentration at which growth rate reaches a maximum. With the selected set of parameters values the maximum productivity (equal to 1,4437 $gL^{-1}d^{-1}$), appears at a concentration of 1.4 g/L that corresponds to a residence time (τ) of 0,9697 [d]. For a given reactor volume it is possible to calculate the volumetric flow rate ($\dot{V}$) that assures the best performance. Since:

$$\tau = \frac{Vr}{\dot{V}} = \frac{A*h}{\dot{V}} = 0{,}9697 \text{ [d]} . \tag{4.29}$$

With : A= 10000, [m^2];

h= 0.012, [m].

The optimal volumetric flow rate results $\dot{V}$= 123,75 m^3/d.

This observation is confirmed by Figure 4.3 that represents how the growth rate changes according to the residence time. Indeed it shows that the maximum production reaches a peak for a value of τ close to 1[d].

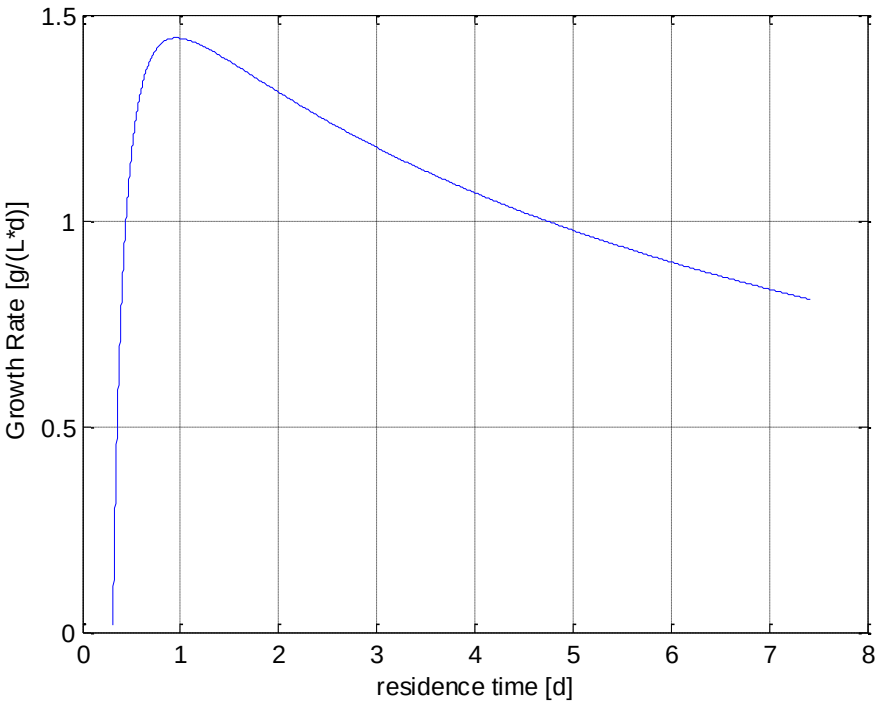

Figure 4.3. *Biomass growth rate evolution as a function of the residence time. Steady state CSTR.*

Figure 4.4 depicts the concentration increasing trend as function of the residence time. Reasonably, the value of the concentration inside the reactor increases with increasing residence times, but this increase is less than linear.

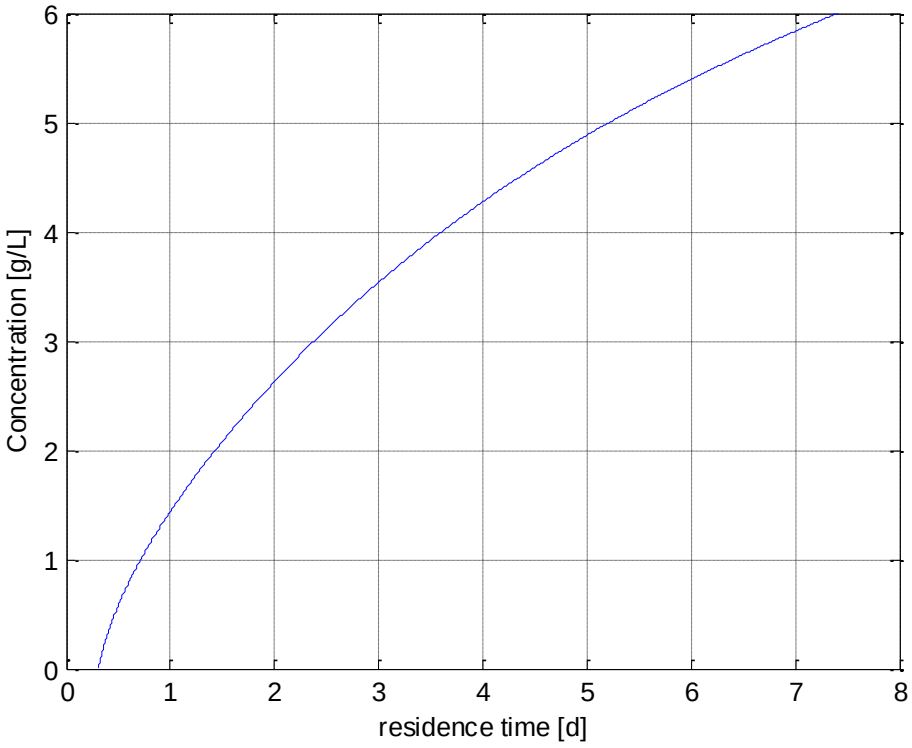

Figure 4.4. *Concentration evolution as a function of the residence time. Steady state CSTR.*

Both Figures 4.3 and 4.4 evidences the values of the washout residence time. With the selected parameters τ_{wo}=0.3 [d].

Alternatively, Equation 4.29 gives the optimum reactor depth for a given value of the ratio $\dot{V}$/A, or the optimal $\dot{V}$/A for a given reactor depth.

The volumetric productivity in the CSTR is defined as in Equation 4.30:

$$P_x = \frac{C}{\tau} \text{ [g/Ld]} . \tag{4.30}$$

Thus, in this case it is equal to the value of the growth rate r_x and is plotted in previous Figure 4.3.

Finally it is possible to calculate the efficiency factor (k_e) that represent a measure of the efficiency of the light absorption trough Equation 4.28. Figure 4.5 shows that there is a maximum value of efficiency approximately equal to 0.138. This value is in correspondence

of a residence time lower than 0.9697 [d] which was the residence time for the maximum production.

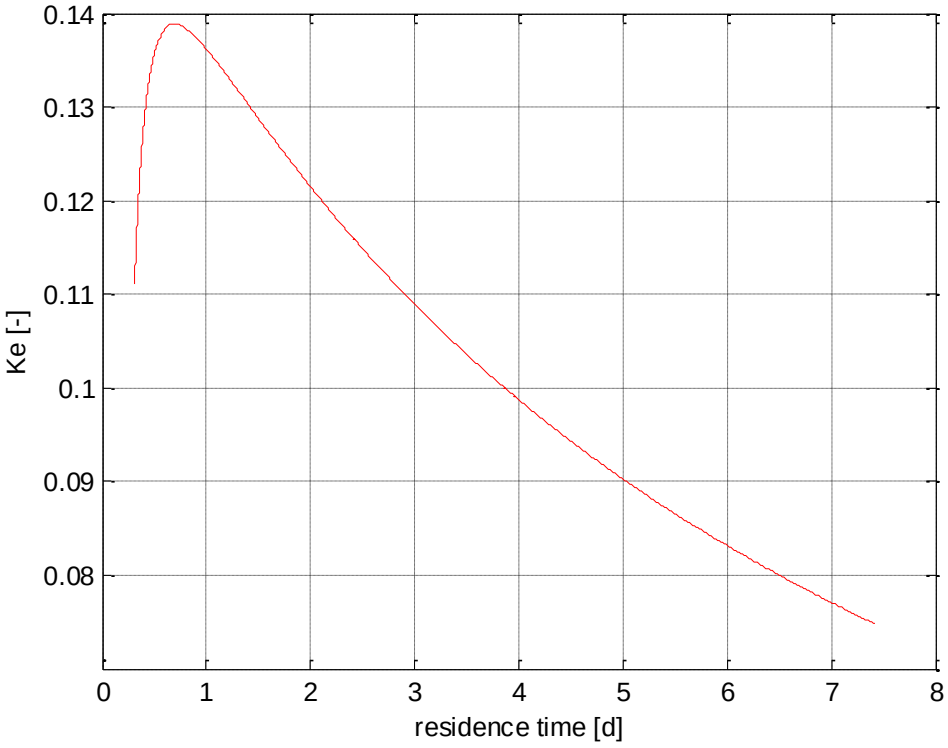

Figure 4.5. *Efficiency factor evolution as a function of the residence time. Steady state CSTR.*

The second case analyzed refers to a photobioreactor behaving as a PFR. The simulation was performed both with and without the recycle. In the latter case an inlet constant biomass concentration of 0.3 g/L was considered, to avoid washout. The description of the plant and the balances equations, are exposed in §4.1.2.

The Matlab® code used to simulate the PFR system without recycle is *prgPFR.m.* The information given to the code are the parameters used in the equation of the Cornet-Pruvost model (listed in Table 4.1), the value of the residence time and the inlet concentration. The program calculates, at every *y* (length) the extinction profile of the radiation hitting the surface along the depth of the reactor with Equations 4.12. Then it calculates the corresponding values of the growth rate and the average growth rate at position y, which is used in the mass balance (Equation 4.7) to obtain the concentration profile along the PFR length. Equation 4.7 was solved using ode45 function.

The result obtained with a residence time of 1[d] and inlet concentration of 0.3 g/L is shown in Figure 4.6. It can be observed that the outlet concentration is 1.56 g/L.

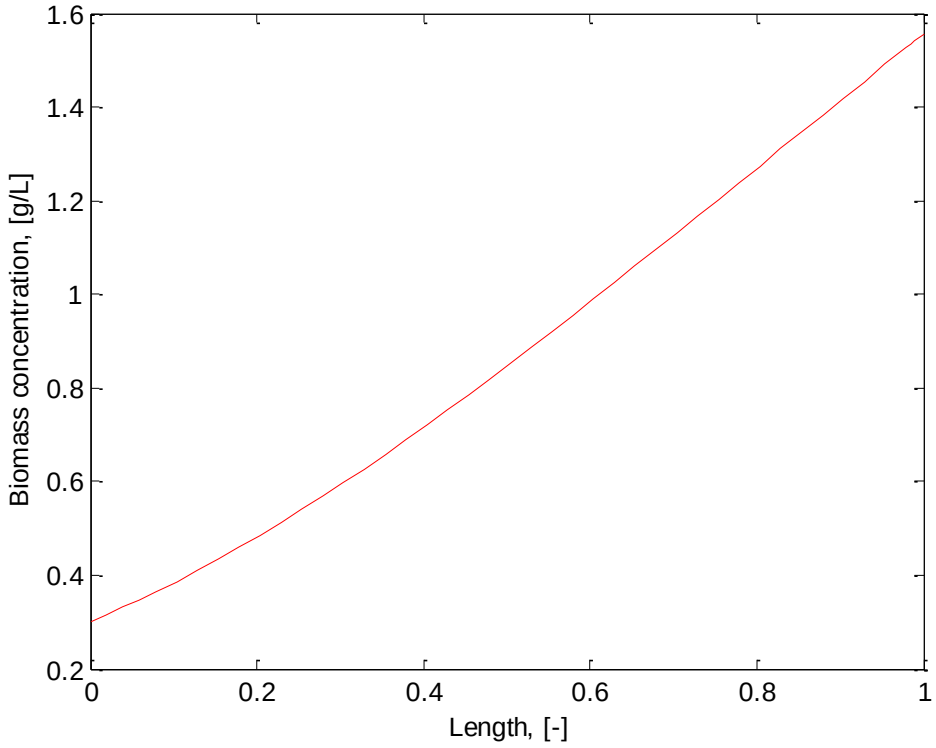

Figure 4.6. *Biomass concentration evolution as a function of the reactor length. Steady state PFR without recycle.*

The PFR system with recycle is simulated by the Matlab® code *prgceiter2.m* in which, compared to the previous one, the mass balance is adjusted on the recycle ratio (Equation 4.9). In this case the inlet concentration is determined iteratively to satisfy the material balances, with a tolerance of 10^{-6}.

The information given in this case are again the parameters listed in Table 4.1, the residence time and the first attempt inlet concentration.

Figure 4.7 shows the evolution of the concentration along the reactor's length with a residence time (τ) of 1[d] a first attempt concentration entering the system of 0.3 g/L is then adjusted iteratively with the value of the concentration exiting the reactor, considering the recycle. Three different values of recycle are compared. It is noteworthy that the outlet concentration increases according to the increasing value of the recycle.

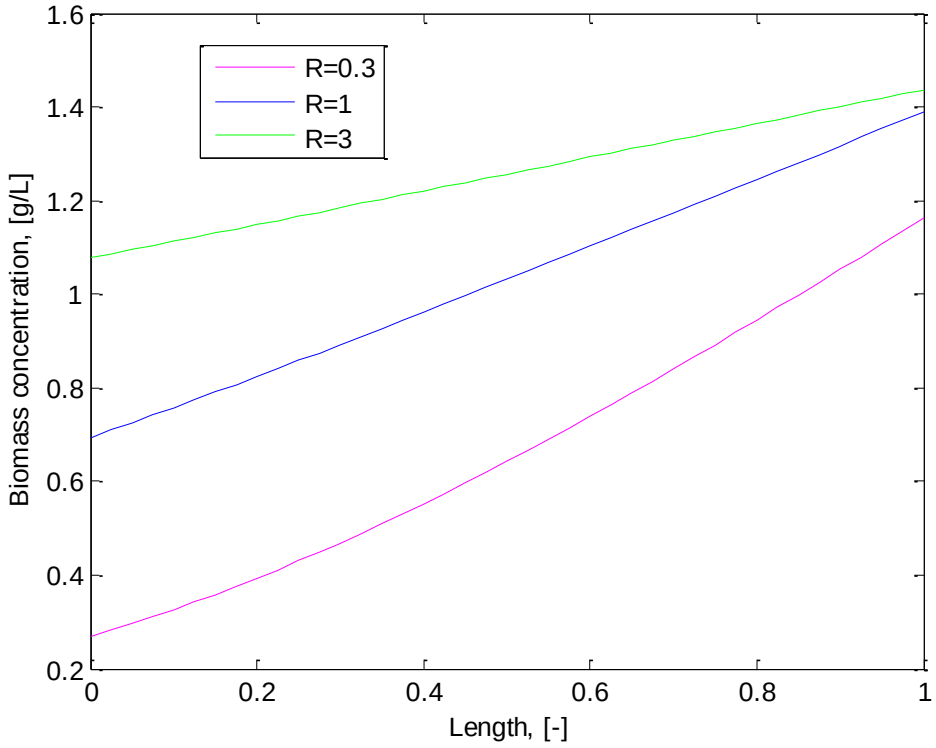

Figure 4.7. *Biomass concentration evolution as a function of the reactor length and recycle value. Steady state PFR with recycle.*

In the case of PFR with recycle it is possible to study how different values of the recycle ratio can affect the performance of the reactor. A first comparison can be done about the outlet concentration reached at the end of the reactor's length. Figure 4.8 represents the results obtained with the code *prgceiter2.m* with equal residence time for values of the recycle of 0.1, 0.3, 1, 3. It seems to suggest that, especially for high value of τ, lower recycle values are able to give higher outlet concentration.

In Figure 4.9 it is possible to study how the productivity changes with respect to the outlet concentration. In this case the higher recycle ratio (R=3) seems to achieve a better performance, in terms of maximum productivity.

Finally in Figure 4.10 the performances of a PFR with different recycle ratio and those of a CSTR are compared from the productivity point of view as a function of the residence time. The graph clearly demonstrates that for small value of residence time, i.e. until τ is around 1 day, the CSTR assures the best performance. When the residence time increases the best productivity becomes progressively the one related to the PFR with lower recycle ratio.

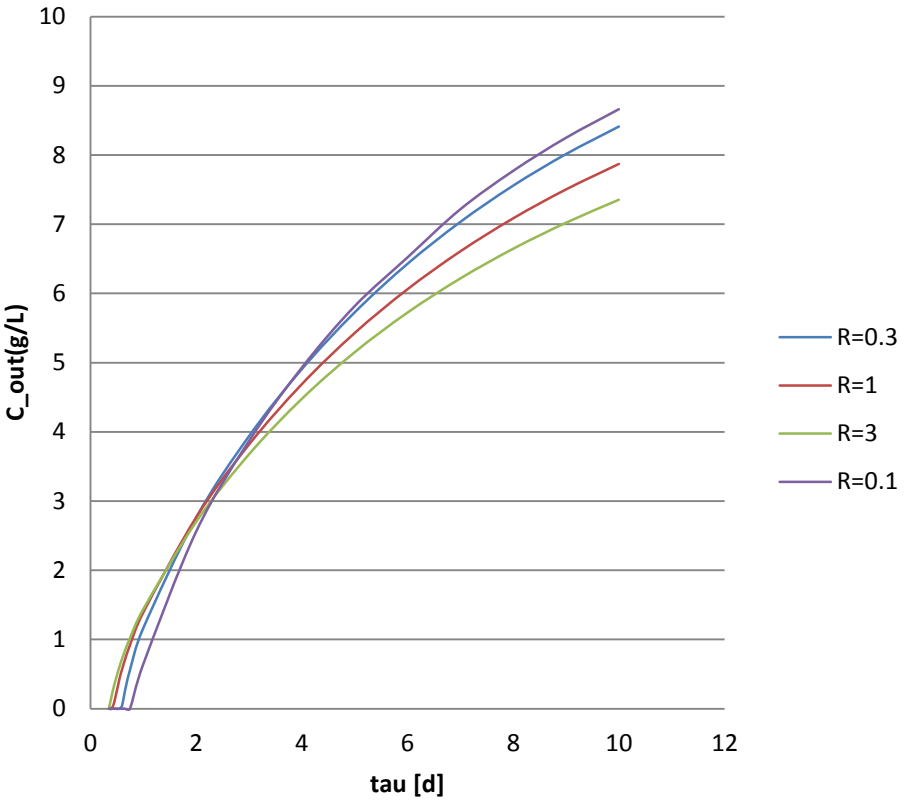

Figure 4.8. *Cells concentration evolution as a function of the residence time and recycle value. Steady state PFR with recycle.*

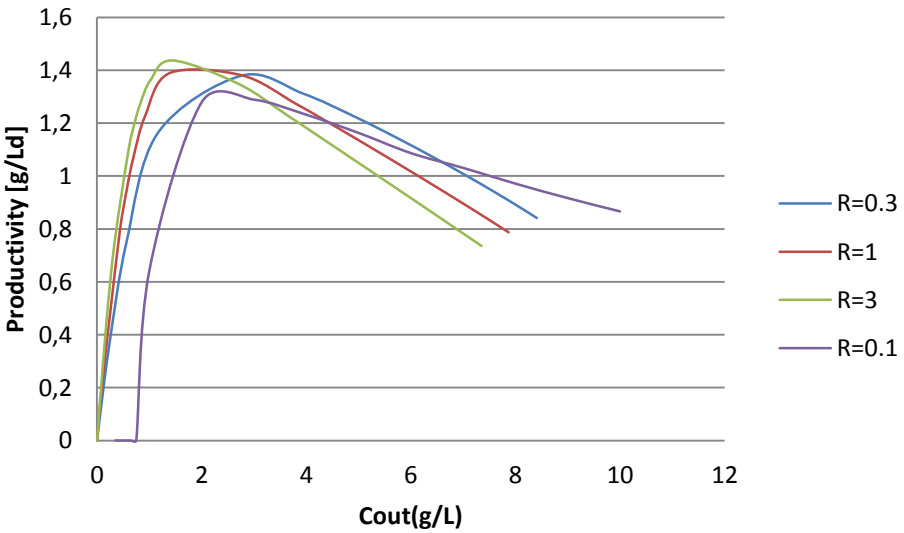

Figure 4.9. *Productivity as a function of final concentration for different values of recycle ratio. Steady state PFR with recycle.*

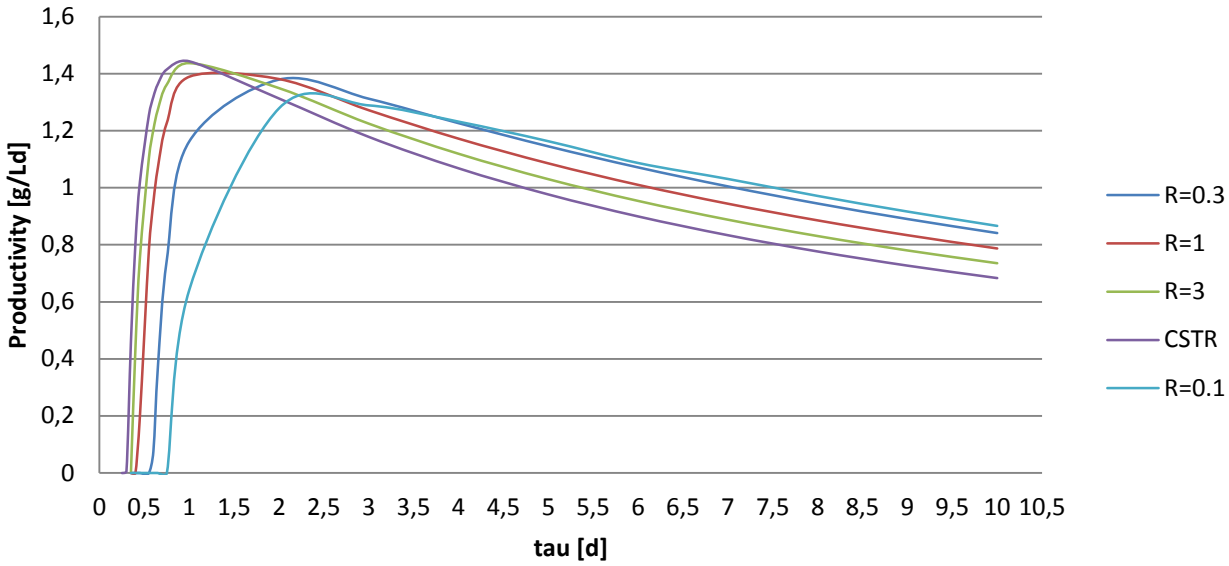

Figure 4.10. *Productivity as a function of residence time. Steady state PFR with different recycle ratio and CSTR.*

One last conclusion can be done with regards to the washout conditions. It is clear that the CSTR assures safer operating condition because the washout occurs at lower residence time compared to the PFR. In Table 4.2 it is possible to compare the washout conditions for the CSTR and the PFR with different recycle ratios.

Table 4.2. *Washout conditions in the reactors simulated.*

CSTR	**τ = 0.25 [d]**
PFR R=0.1	τ = 0.75 [d]
PFR R=0.3	τ = 0.55 [d]
PFR R=1	τ = 0.4 [d]
PFR R=3	τ = 0.35 [d]

4.5.2 Dynamic simulations

Again, the first case considered is a photobioreactor behaving as a CSTR. Balance equations are reported in §4.1.1.

The Matlab® code developed is *prgCSTRdinamico.m*. It operates differently from the code *prgCSTR.m*. It calculates the extinction profile of the radiation hitting the surface, along the depth of the reactor then it calculates the corresponding values of the growth rate and their average. Finally it determines the mass balance (Equation 4.1). The differences introduced here are that the system is time-dependent and that the value of the residence time (τ) is given, while the concentration is the result of calculation at convergence. The information given to the code are the parameters used in the equation of the Cornet-Pruvost model (presented in Table 4.1), the residence time (τ) and the initial value of the concentration.

In Figure 4.11 it is presented how the biomass concentration inside the reactor changes during the evolution of time. The system is operated with a residence time equal to 1 [d]. The concentration starts from the arbitrarily assumed value of 0.3 g/L and it reaches 1.4432 g/L after a transient time of almost 5 [d]. Subsequently the system is at stationary state where the value of the concentration does not change anymore. As expected, the steady state concentration value is equal to the one calculated with *prgCSTR.m* at the corresponding residence time.

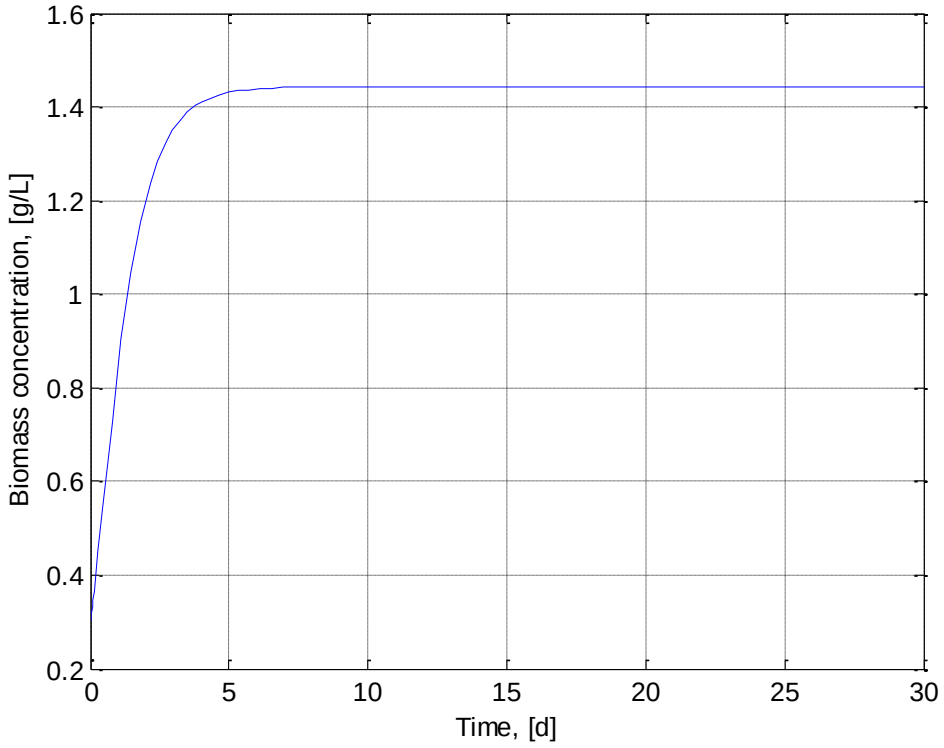

Figure 4.11. *Biomass concentration evolution as a function of the time. Dynamic state CSTR.*

Afterwards, the PFR photobioreactor dynamic evolution was examined. A description of the balances equations is presented in § 4.1.2.

The Matlab® code used in this case is called *pfrdinnoR.m*. It reproduces the behavior of a PFR dynamic system operating without recycle. This code operates like the previous ones and gives the evolution of the concentration inside the reactor as function of both time and space. The input information required by the code are the usual parameters listed in Table 4.1, the value of the residence time plus the initial and boundary concentration conditions.

The results presented in Figure 4.12, 4.13 and 4.14 are obtained with a residence time of 1[d], a boundary condition that is a constant inlet concentration of 0.3 g/L and an initial condition that is the flat profile of concentration equal to 0.3 g/L inside the reactor. It is noteworthy that the final concentration profile in Figure 4.12, is equal to that obtained with the equivalent steady state simulation (Figure 4.6) with an outlet concentration of 1.5474 g/L.

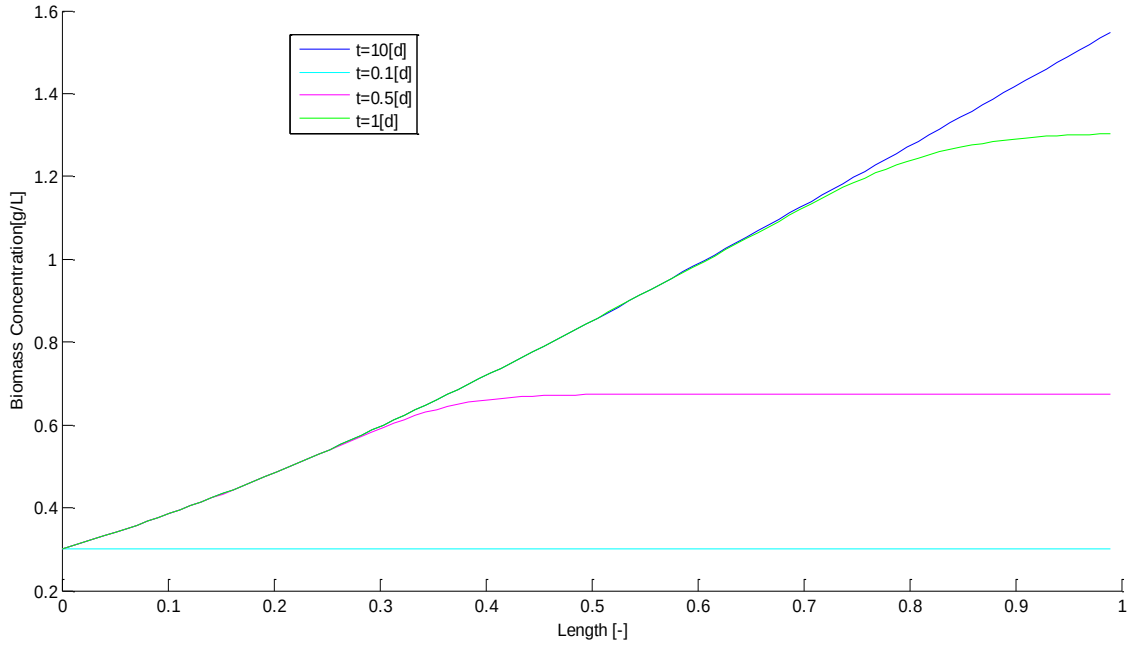

Figure 4.12. *Biomass concentration evolution as a function of the space. Dynamic state PFR without recycle.*

Figure 4.13 shows the time evolution of biomass concentration at the outlet. The final steady state value of 1.5474 g/L is reached after less than 2 days.

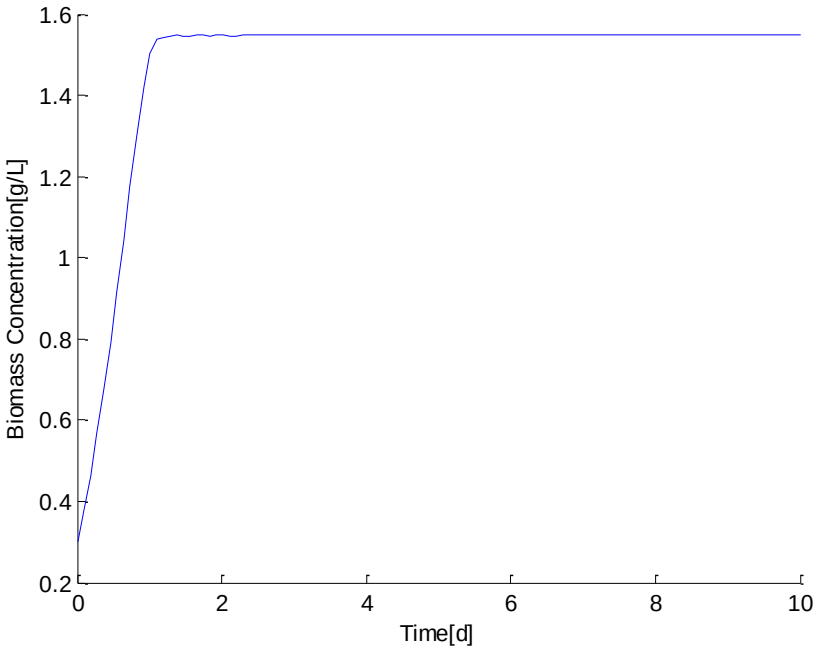

Figure 4.13. *Outlet biomass concentration evolution as a function of time. Dynamic state PFR without recycle.*

Finally, Figure 4.14 represents how the concentration evolves along the reactor as function of time and space.

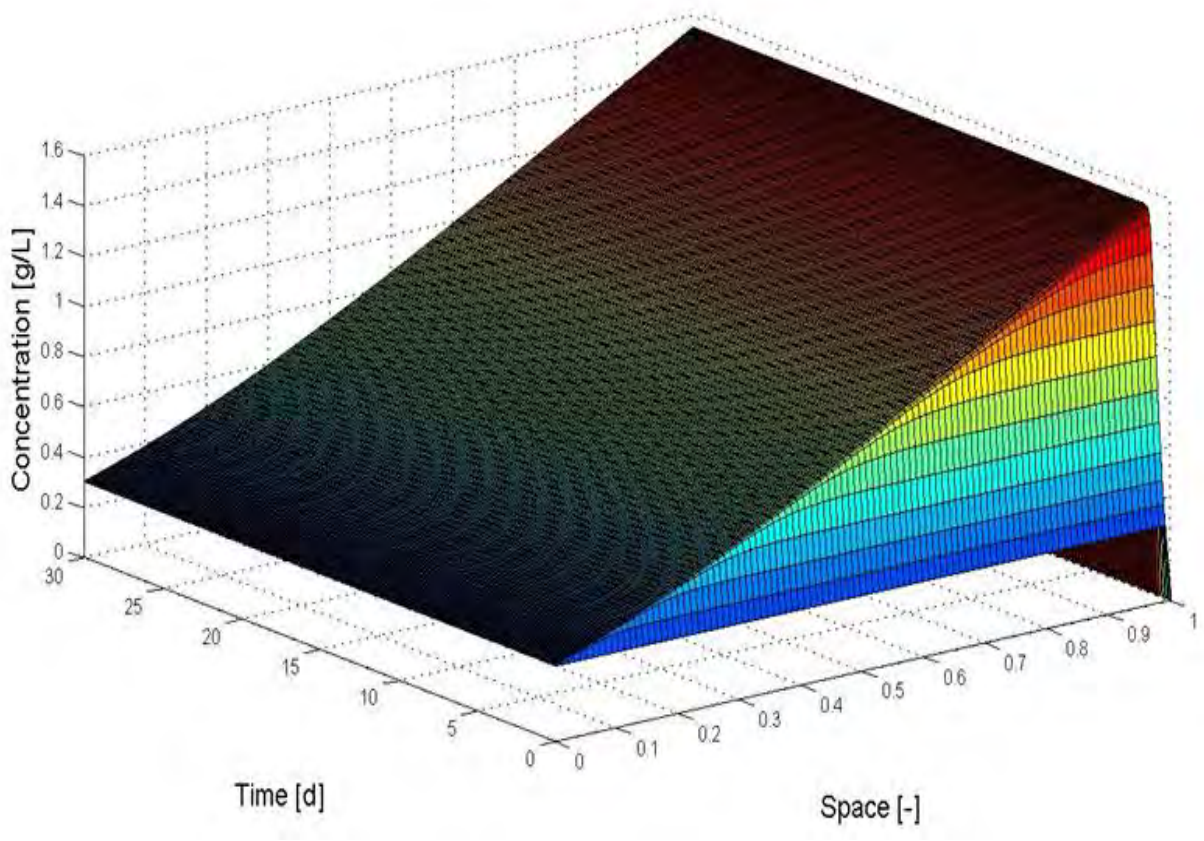

Figure 4.14. *Biomass concentration evolution as a function of time and space. Dynamic state PFR without recycle.*

The PFR dynamic system with recycle is simulated by the Matlab® code *conR.m*, in which the dynamic mass balance equation is adjusted on the recycle ratio R, according to Equation 4.10. The information given in this case are the usual parameters listed in Table 4.1, the residence time and the initial and boundary conditions.

Figure 4.15 shows the results obtained with a residence time of 1[d], a boundary condition that is the inlet concentration of 0.3 g/L and an initial condition that is the flat profile of concentration equal to 0.3 g/L inside the reactor at the beginning. The inlet concentration changes in time depending on the outlet concentration. The value of the recycle ratio is 3,1 or 0.3 respectively.

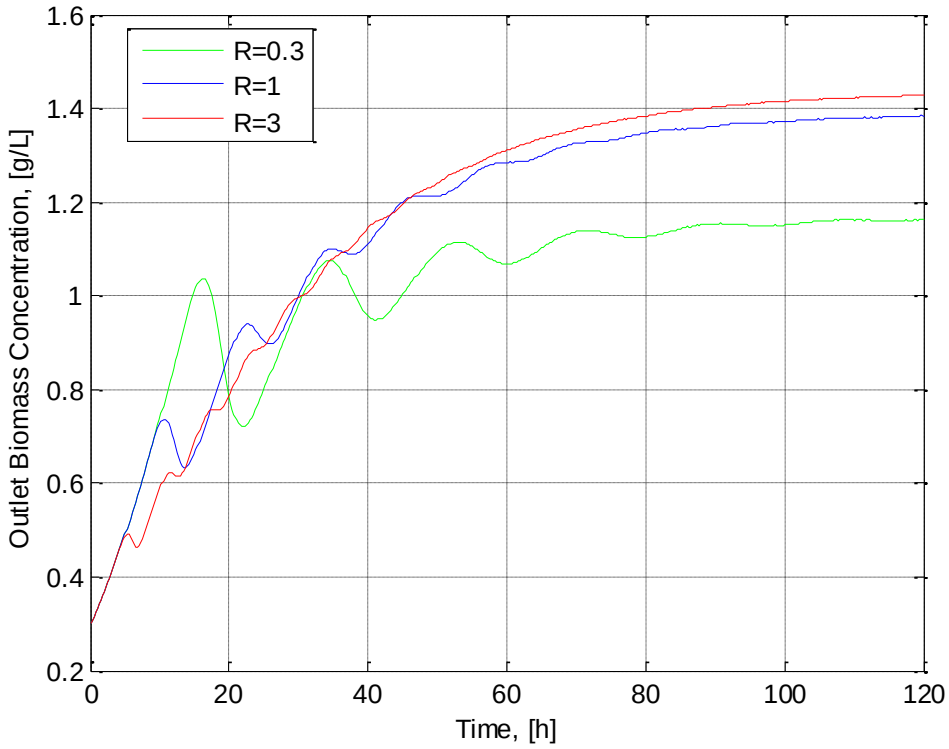

Figure 4.15. *Biomass concentration evolution as a function of time. Dynamic state PFR with recycle.*

It can be noticed that the final value of outlet concentration increases with the recycle ratio even though it remains lower than the value obtained operating the system without recycle (Figure 4.13). Again the final outlet concentration values, obtained with the simulation of the dynamic PFR are, for the three different values of the recycle, the same as those obtained simulating the steady state system (Figure 4.7).

4.6 Results: Variable light intensity simulations

In this section with the Matlab® codes implemented the microalgae growth considering a cyclical pattern of light intensity was simulated. The illumination corresponds to the solar radiation. In this situation the PBRs performances are strongly affected by the night-day alternation and by the different season of the year considered. In fact, the sun rises at different times in different seasons and during the day the radiation changes: it increases from dawn to

midday and then decreases until the sunset. This simulation allows to analyze how a real photobioreactor would operate in natural conditions, i.e. without artificial sources of light.

The study in particular is referred to the summer season.

4.6.1 Summer simulations

To implement the Matlab® code able to simulate the cyclical light pattern, it is necessary to define how the light intensity changes during the day. The data of irradiance are collected online from the Photovoltaic Geographical Information System (PVGIS Solar Irradiation Data, 2014). These data are interpolated for the month of July as shown in Figure 4.16. The direct radiation is obtained from the difference between the total radiation and the diffuse one, represented in Figure 4.17.

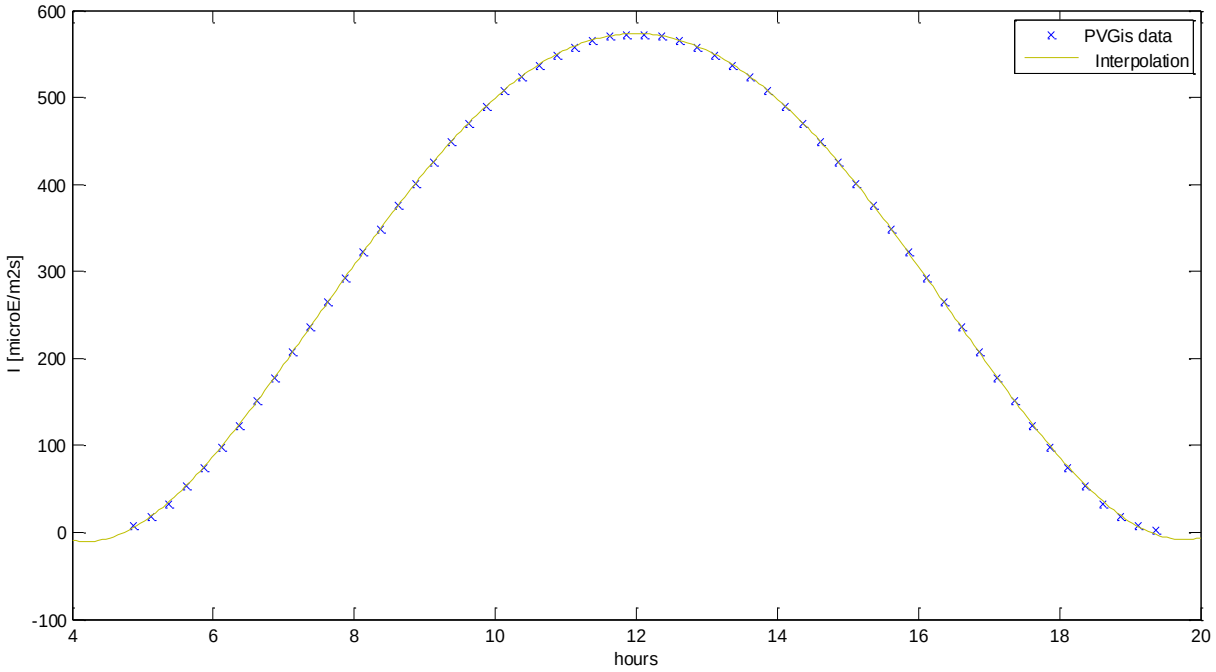

Figure 4.16. *Direct radiation as a function of hours during the day. July.*

$$y = 0.16x^4 - 7.6x^3 + 120x^2 - 630x + 1100.$$

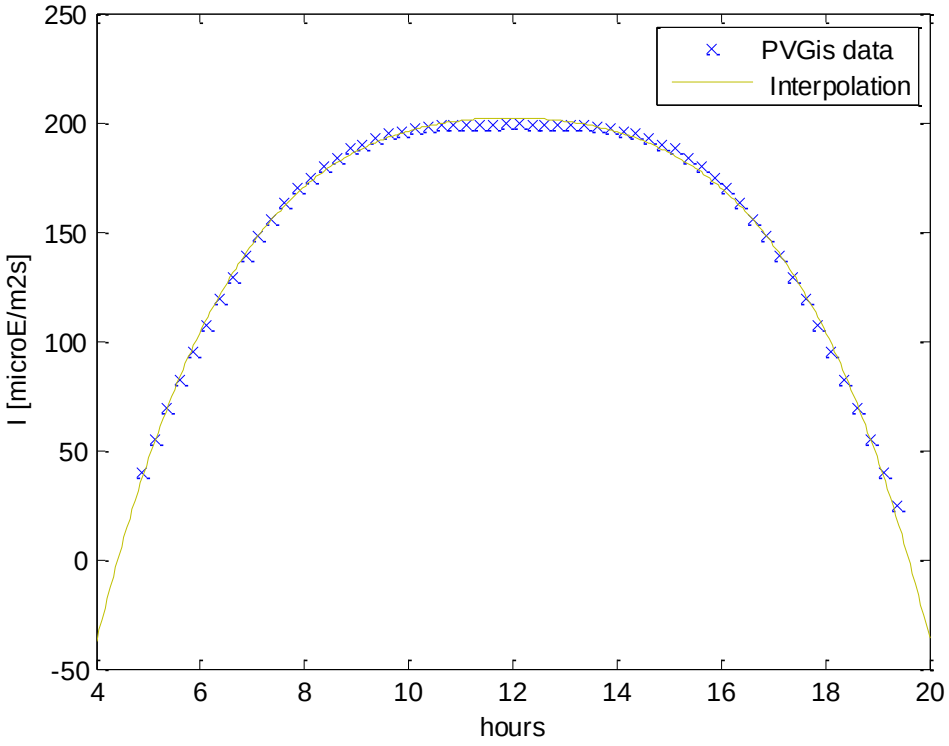

Figure 4.17. *Diffuse radiation as a function of hours during the day. July.*

$$y = -0.036x^4 - 1.7x^3 - 33x^2 + 290x - 760.$$

Again the Matlab® code *prgCSTRdinINT.m* was used to analyze the behavior of a CSTR photobioreactor. The direct and the diffuse radiation depends on the different time of the day. The program calculates the value of the radiation along the depth of the reactor and the value of the incident radiation angle (θ). After that, it evaluates the corresponding values of the growth rate. Finally the average growth rate inside the reactor is calculated to be used in the mass balance (Equation 4.1). Before the dawn and after the dusk the program considers only the maintenance term in the production rate, thus the growth rate will assume negative values and the concentration decreases. The input data given to the code are the hours of the day and their corresponding value of radiation (collected online from the Photovoltaic Geographical Information System). The parameters used in the Cornet-Pruvost model are different from those discussed in §4.3. They are resumed in Table 4.3. In addition the values of the entering concentration and the residence time must be specified.

Table 4.3. *Parameters of the Matlab code prgCSTRdinINT.m and prgPFRdinINT.m for summer conditions.*

Name	**Value**	**Unit of measure**
bEs	5	m^2/kg
Ea	220	m^2/kg
θ	0	rad
h	0.012	m
K	150	$\mu mol/m^2s$
ρ φ	$1.32*10^{-6}$	kg/ µmol
a	0.0005	(gd)/ µmol
β	0.0003	g/ µmol
me	543.143	µmol/(gd)
τ	48	h
y_app	$5.5*10^{-7}$	kg/ µmol
µe	0.0124	1/h

Figure 4.18 represents how the biomass concentration varies as a function of time. Obviously the peaks represent the maximum production during the day, the lowest points represent the decreasing production during the night. The system is simulated with initial concentration of 0.3 g/L and a residence time of 48 hours. The steady state is reached after nearly 4 days. This corresponds to what was found with constant light intensity (Figures 4.11).

In this case it is possible to calculate the value of the average efficiency factor, k_e, as in §4.5.1 through Equation 4.28. For a given residence time of 1 [d] k_e = 7,12% of PAR (which means k_e=7,12*0,43=3,06% of the total solar energy). It is noteworthy that this value is nearly half the one obtained with the same residence time but constant illumination (13,8% of PAR).

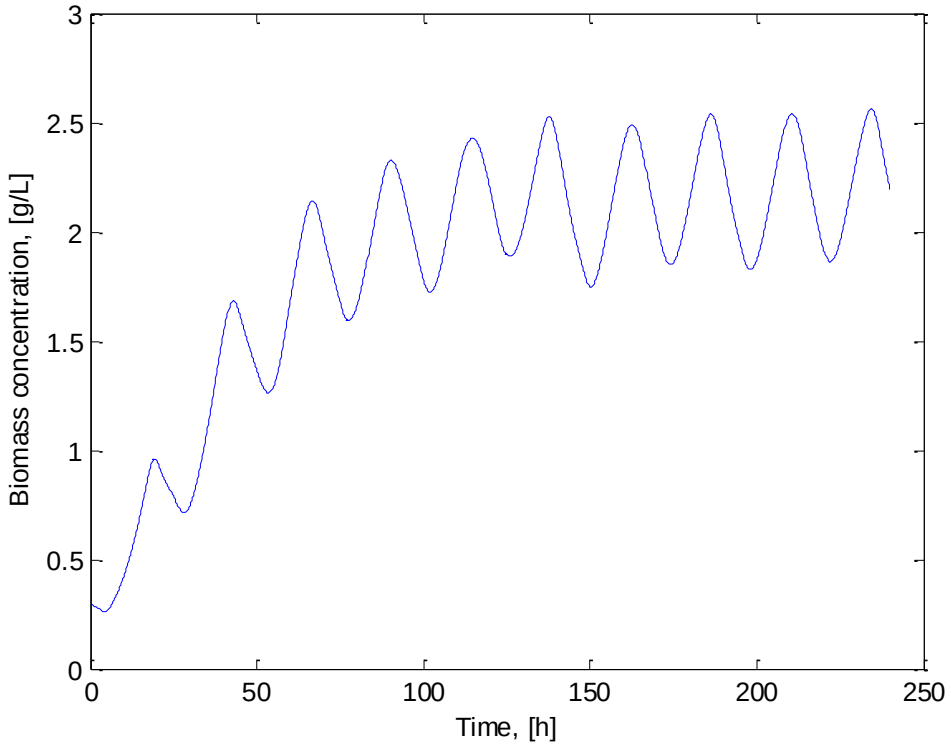

Figure 4.18. *Biomass concentration evolution as a function of time. Dynamic CSTR in summer conditions. Tau=48hours.*

Through the Matlab® code *prgPFRdinINT.m* a dynamic PFR system with recycle, was simulated under variable light intensity in summer condition.

Taking into account the different hour of the day, the program calculates the value of the diffuse and direct radiation through the depth of the reactor, the incident radiation angle (θ), the punctual values of the growth rate, the average growth rate and the mass balances as written in the Equation 4.10. The input information are the parameters for the summer period as listed in Table 4.3, plus the residence time and the recycle ratio. Moreover the boundary and initial conditions are required.

In Figure 4.19 the results for a system operated with a residence time of 48 hours are shown, with a value of the recycle equal to 3, a boundary condition that is the entering concentration equal to 0.3 g/L and an initial condition that is the flat profile of concentration equal to 0.3 g/L inside the reactor. The cells concentration inside the reactor is predictably fluctuating, following the night/day cycle. It is noteworthy that it takes nearly 5 days to the system to reach the steady state.

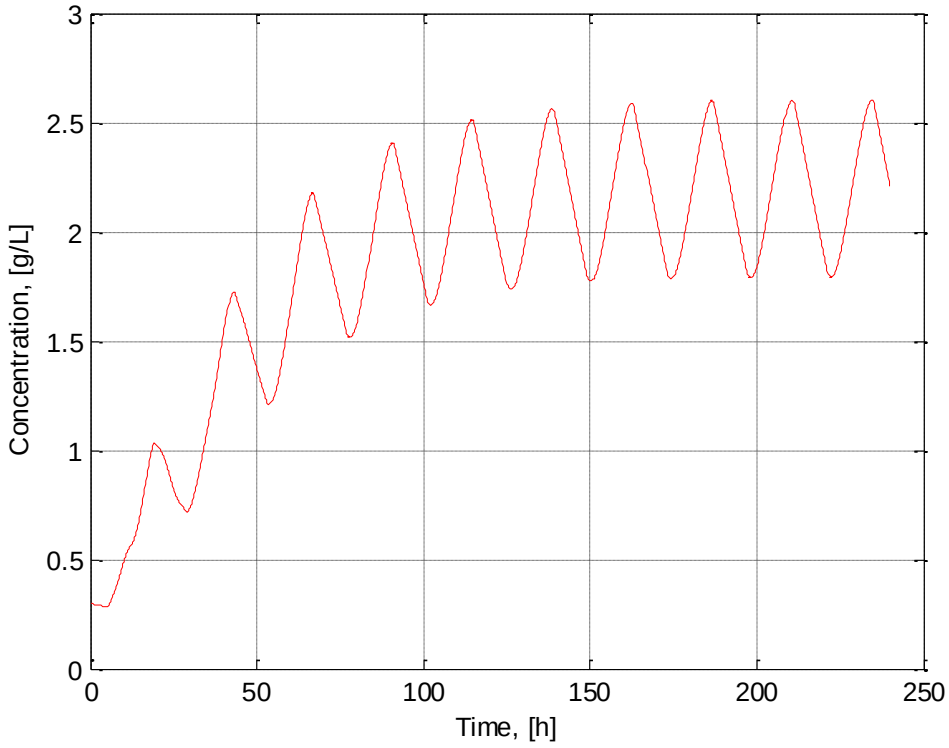

Figure 4.19. *Biomass concentration evolution as a function of time. Dynamic PFR in summer conditions. R=3. Tau=48hours.*

In Figure 4.20 a comparison in the performances of the system with different recycle ratios is presented.

It seems that the washout conditions are not reached, even with a recycle ratio equal to 0.1. Indeed it appears that a higher value of the recycle gives higher concentrations in the beginning, even though the difference between the curves obtained with R=3 and R=0.3 are not relevant after a period of 100 [h].

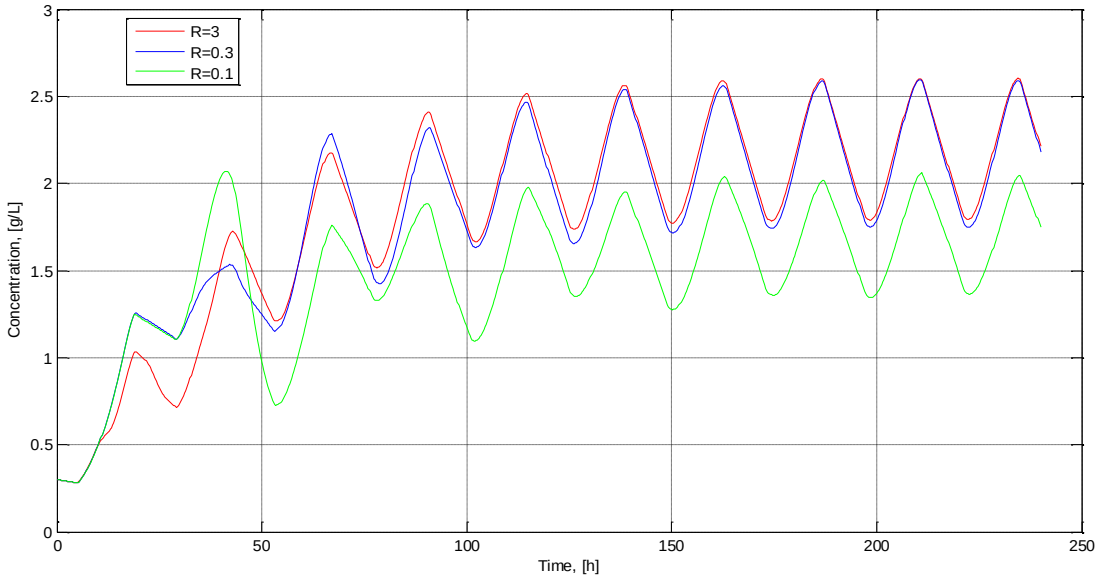

Figure 4.20. *Biomass concentration evolution as a function of time. Dynamic PFR in summer conditions. Tau=48h.*

Finally a comparison between the performances of two types of reactors, PFR and CSTR, is presented in the following figure. In Figure 4.21 the systems are compared under Summer condition, with a recycle ratio of the PFR equal to 3 and a residence time for both the reactors of 48 hours. It appears that the performance of the PFR is very similar to those of the CSTR.

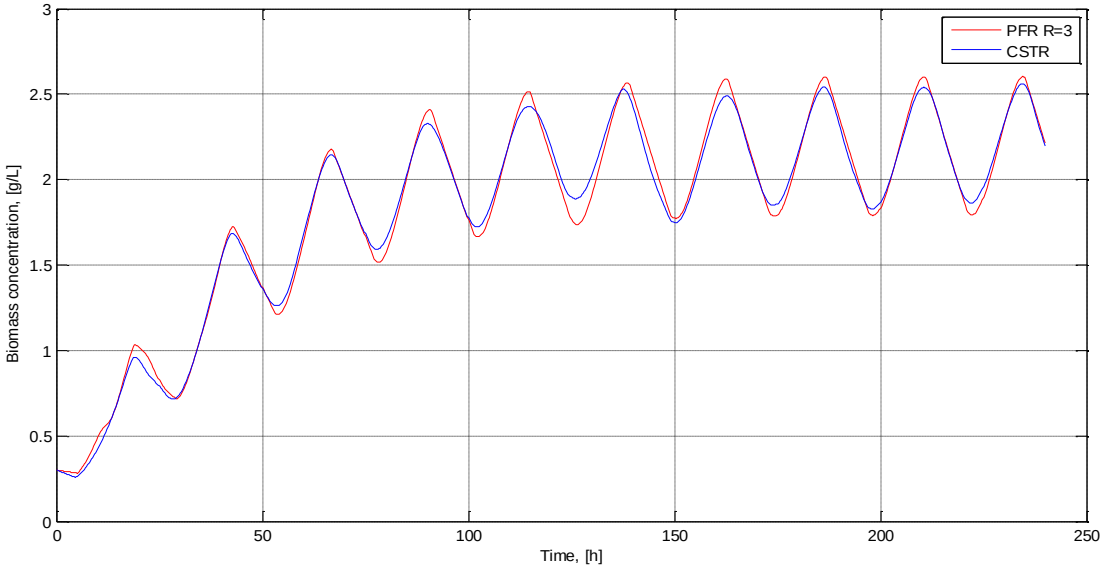

Figure 4.21. *Biomass concentration evolution as a function of time. Comparison PFR-CSTR in summer conditions. Tau=48h.*

From Figure 4.22 To 4.24 it is possible to observe that increasing the residence time the performances of the PFR model are increasing and passing those of the CSTR, as observed with constant light intensity in § 4.5.1.

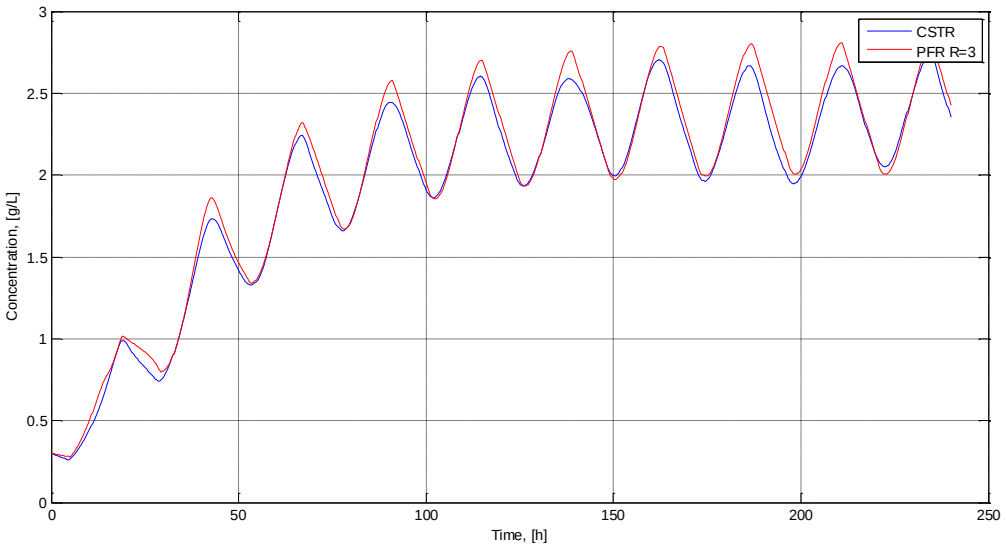

Figure 4.22. *Biomass concentration evolution as a function of time. Comparison PFR-CSTR in summer conditions. Tau=60h.*

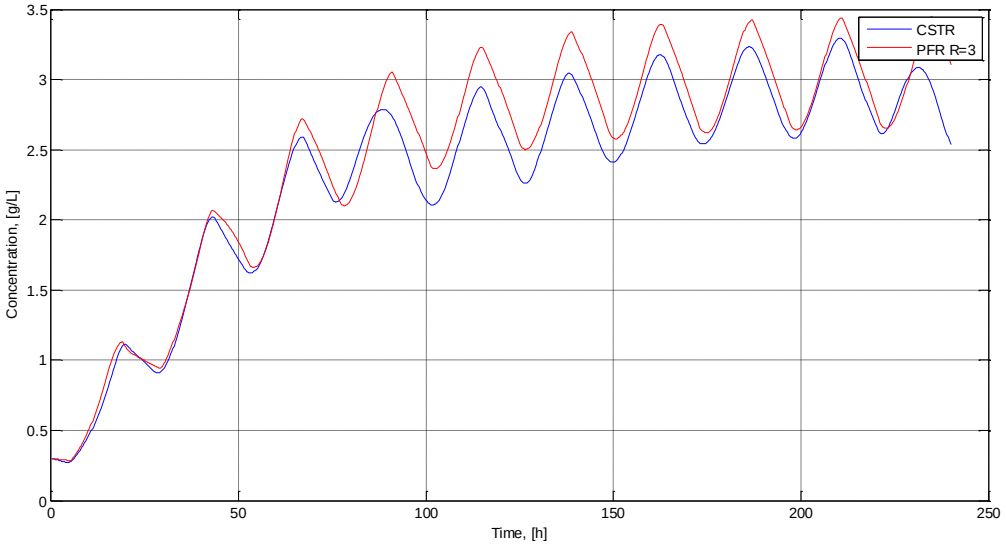

Figure 4.23. *Biomass concentration evolution as a function of time. Comparison PFR-CSTR in summer conditions. Tau=72h.*

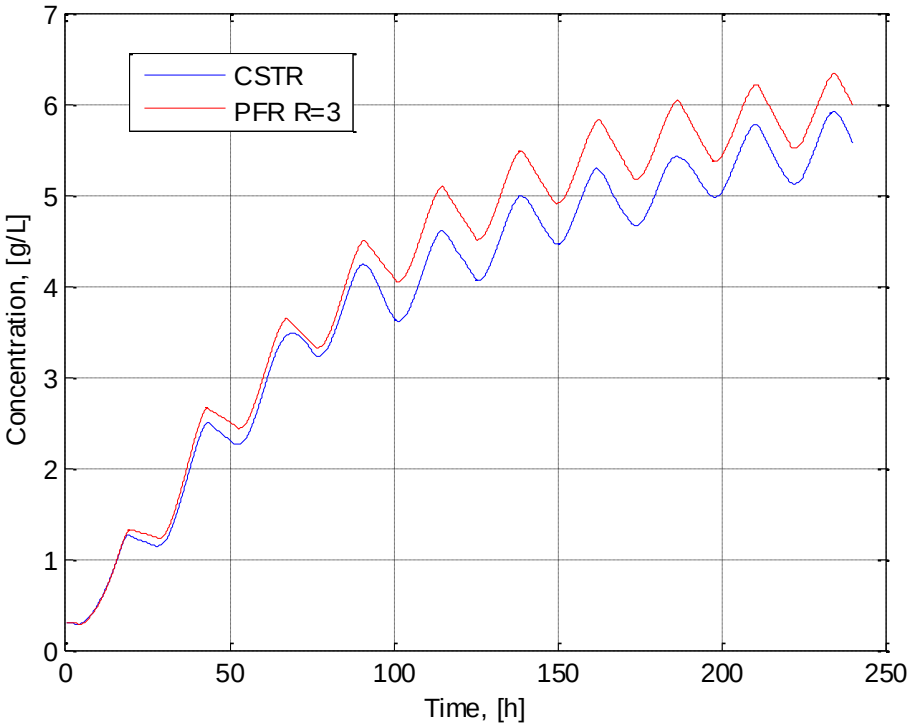

Figure 4.24. *Biomass concentration evolution as a function of time. Comparison PFR-CSTR in summer conditions. Tau=240h.*

Conclusions

The ultimate purpose of the thesis was to investigate the optimum growing conditions for the cultivation of microalgae. In particular the analysis was focused on *Chlorella vulgaris* ans *Scenedesmus obliquus* species, because of their adaptability and fast growth rate.

The first part was performed by different experiments. The reactive system was made of two batch photobioreactors manufactured specifically for the purpose. The only difference between the two was the gas supply. In the Manufactured Control System indicated with the letter A (MCS-A) the air supplied was enriched by 5% CO_2; while the MCS-B was fed with atmospheric air. Through these reactors different photoperiods (24, 20, 15, 10 hours of light per day) and light intensities (128 μmol $m^{-2}s^{-1}$ and 85 $\mu molm^{-2}s^{-1}$) were investigated for a fixed time frame of 8 days, in order to assess the significance of the illumination and the carbon source in the productivity of the systems. The performances of the photobioreactors were evaluated by measuring the cells concentration [n°cells/mL], the dry weight [g/L], the cells density [n°cells/g] and the absorbance values. The results obtained clearly demonstrate that the carbon source is preeminent in the growth of *Chlorella vulgaris*. Indeed the MCS-B operated without the air enriched with CO_2 is nearly unaffected by the variations in the period of exposure to the light or its intensity. Nonetheless, when carbon is not the limiting factor, the significance of light is proved. The higher light intensity is responsible for higher growth. The same trend is observed increasing the photoperiod. It is noteworthy that the case of 24 hours presents the highest final values of concentration (196 million cell/ml) and dry weight (2,62 g/L), even though the biomass growth rate, equal to 0.52 d^{-1} is the lowest. The one measured with 20 hours of photoperiod is the maximum growth rate observed and its value is 0.766 d^{-1}, thus evidencing oxidative stress phenomena.

The second part of the thesis was aimed to the implementation of a model that connects the light reaching the reactor's surface to the biomass production rate into the reactor. This analysis is realized through the simulation of different types of reactor (CSTR, PFR with and without recycle), using the Cornet model generalized by Pruvost into a Matlab® code. The aim remains the investigation of the optimal growing conditions, focusing on the type of reactive system that would ensure the maximum productivity. The simulations were performed with respect to *Scenedesmus obliquus*, for which the relevant parameter values are known, considering two lightening conditions. Initially the performances of the different

reactors were analyzed with constant light intensity (fixed to 150 [μmol/m^2s]) both at steady state and from a dynamic point of view. Considering the CSTR, a maximum in the productivity as function of the cells concentration, is obtained. Thus it is possible to calculate the corresponding optimal residence time and, for a fixed volume, the flow rate assuring the maximum production. The optimum conditions were verified for τ = 0.9697 d, with a volumetric flow rate of 123,75 m^3/d. The PFR system operated with recycle shows an increasing value of outlet concentration, according to the increasing recycle ratio. Comparing the two systems it is evident that for small values of the residence time (until τ =1÷2 d) the performance of the CSTR is better than the one of the PFR, while the situation is reversed for longer residence time. Furthermore, it was possible to estimate the washout conditions for both systems. The CSTR is the system that assures the safest operating condition, avoiding the washout with residence times higher than 0.25 d. For the PFR it is observed that increasing the value of the recycle ratio the washout limit decreases.

The analysis was carried out also considering a variable light intensity, in order to simulate the behavior of reactors exposed to the solar radiation, that changes during the day and with the period of the year. The conditions investigated were referred to the summer period. As about the PFR it was observed that in these lightening condition the washout is avoided (at τ=48h) and increasing the recycle ratio generally improves the performance, up to R=0.3. From a comparison of the two types of reactors in the same conditions it appears that the PFR is able to pass the biomass concentration reached with the CSTR model, for residence times higher than 48 hours, confirming the results obtained with constant light intensity.

The simulated results allow to direct the next steps towards the design of a real plant for the production of biodiesel from microalgae. Exploiting the data obtained in this thesis it is possible to choose the direction for future developments in the study of the viability and opportune conditions to cultivate *Chlorella vulgaris* and *Scenedesmus obliquus*.

Nomenclature

A= surface exposed to radiation, [m^2].

a = constant of the maintenance term , [g*d/µmol].

b = backscattering fraction, [adim].

c_{out}= outlet concentration, [g/L].

c_x= concentration inside the reactor, [g/L].

c_{xin} = concentration entering the reactor, [g/L].

c_{xout} = concentration exiting the reactor, [g/L].

Ea = absorption mass coefficient, [m^2/kg].

$\dot{E}_{in}$= incident solar radiation per unit area, [MJ $m^{-2}y^{-1}$].

$\dot{E}_{stored}$= energy stored as biomass per unit area, [MJ $m^{-2}y^{-1}$].

Es = scattering mass coefficient, [m^2/kg].

h = reactor's depth, [m].

I_{abs}= absorbed light intensity, [µmol/(m^2s)].

Idir(z) = direct PAR at depth z, [mol/(m^2s)].

Idir(0) = direct PAR at depth 0, [mol/(m^2s)].

Idif(z) = diffuse PAR at depth z, [mol/(m^2s)].

Idif(0) = diffuse PAR at depth 0, [mol/(m^2s)].

I_{in}= light intensity entering the reactor, [µmol/(m^2s)].

I_{out}= light intensity exiting the reactor, [µmol/(m^2s)].

K = half saturation constant for photosynthesis, [µmol $m^{-2}s^{-1}$].

k_e = efficiency of light conversion, [adim].

L= length of the reactor, [m].

m_e = maintenance coefficient, [µmol /(g*d)].

Pr = productivity, [g/(L*d)].

r_x= production rate, [g/(Lh)].

$r_{(x,z)}$ = growth rate at point z, [kg $m^{-3}s^{-1}$].

$r_{(x,p)}$ = growth rate due to photosynthesis, [kg $m^{-3}s^{-1}$].

$r_{(x,m)}$ = growth rate due to maintenance process, [kg $m^{-3}s^{-1}$].

$r_{x,p\,(z)}$ = biomass growth rate at depth z, [kg $m^{-3}s^{-1}$].

r_x,m = maintenance term, [kg $m^{-3}s^{-1}$].

$\dot{V}$= volumetric flowrate, [L/h].

V= reactive volume, [L].

y = dimension parallel to the flow, [m].

z = reactor dimension along the depth, [m].

Greek letters

β = Constant term in the maintenance term [g/µmol].

θ= Incident radiation angle with respect to normal direction of reactor surface, [rad].

λ = Wavelength, [m].

µe = Maintenance term, [$time^{-1}$].

μ = Growth rate, [d^{-1}].

ρm = Maximum energetic yield for photon conversion, [adim].

τ = Residence time, [d].

Φ = Mass quantum yield for Z-scheme of photosynthesis, [kg/mol].

Acronym

CCAP = Culture Collection of Algae and Protozoa.

CSTR = Continuous streaming reactor.

Ebio= Biomass heat of combustion, [J/g].

Ecarb= Carbohydrate heat of combustion, [J/mol].

L.I. = Light Intensity, [$\mu mol/m^2s$].

LHV = Lower Heating Value, [MJ/kg].

MCO_{2red}= moles of CO2 reduced to carbohydrate per unit area per year, [$mol/(m^2y)$].

MCS = Manufactured Culture System.

MCS-A = Manufactured Culture System supplied with air enriched with 5% CO_2.

MCS-B = Manufactured Culture System supplied with atmospheric air.

PBR = Photobioreactor.

PFR = Plug Flow Reactor.

PAR = Photosynthetic Active Radiation.

Pmax = Maximum Productivity per unit area per year, [$kg\ m^{-2}\ y^{-1}$].

PVGis = Photovoltaic Geographical Information System.

QR = Quantum Requirement, [photons].

Bibliography

Beraldi, M. (2012). Effetto dei cicli giorno-notte sul funzionamento di fotobioreattori per la produzione industriale di microalghe: sperimentazione e simulazione. Thesis in Chemical Engineering, DII, University of Padova (Italy).

Brennan, L., P. Owende (2010). Biofuels from microalgae-A review of technologies for production, processing, and extractions of biofuels and co-products. *Renewable and Sustainable Energy Reviews*, **14**, 557–577.

Chisti, Y. (2007). Biodiesel from microalgae. *Biotechnology Advances*, **25**, 294–306.

Costache, T. A., F. Gabriel Acién Fernández, M. M. Morales, J. M. Fernández-Sevilla, I. Stamatin and E. Molina (2013). Comprehensive model of microalgae photosynthesis rate as a function of culture conditions in photobioreactors. Appl. *Microbiol. Biotechnol.*, **97**, 7627-7637.

Domenicali, G. (2013). Analisi economica di un impianto industriale per la produzione autotrofa di olio da microalghe. Thesis in Chemical Engineering, DII, University of Padova (Italy).

Enzo, M. (2012). Sviluppo di un impianto pilota per la produzione di microalghe: misure di laboratorio e progetto di impianto. Thesis in Chemical Engineering, DII, University of Padova (Italy).

Fon Sing, S., A. Isdepsky, M. A. Borowitzka and N. R. Moheimani (2013). Production of biofuels from microalgae. *Mitig. Adapt. Strateg. Glob. Change*, **18**, 47–72.

Ghasemi, Y., S. R. Amini, A. T. Naseri, N. M. Najafabady, M. A. Mobasher and F. Dabbagh (2011). Microalgae Biofuel Potentials (Review). *Applied Biochemistry and Microbiology*, **48**(2), 126-144.

Gonçalves, A. L., J. C. M. Pires, M. Simo (2013). Green fuel production: processes applied to microalgae. *Environ. Chem. Lett.*, **11**, 315–324.

Jacob-Lopes, E., C. H. Gimenes Scoparo, L. M. Cacia Ferreira Lacerda, T. Teixeira Franco (2008). Effect of light cycles (night/day) on CO_2 fixation and biomass production by microalgae in photobioreactors. *Chemical Engineering and Processing*, **48**, 306-310.

Lam, M. K., K. T. Lee (2011). Microalgae biofuels: A critical review of issues, problems and the way forward. *Biotechnology Advances*, **30**, 673–690.

Lin, C.S., J.T. Wu (2014). Tolerance of soil algae and cyanobacteria to drought stress. *Journal of phycology*, **50**(1),131-139.

Luo, H.P., M.H. Al-Dahhan (2003). Analyzing and Modeling of Photobioreactors by Combining First Principles of Physiology and Hydrodynamics. *Biotechnology and Bioengineering*, **85**, 382–393.

Mata, T. M., A. A. Martins and N. S. Caetano (2010). Microalgae for biodiesel production and other applications: A review. *Renewable and Sustainable Energy Reviews*, **14**, 217–232.

Oncel, S. S. (2013). Microalgae for a macroenergy world. *Renewable and Sustainable Energy Reviews*, **26**, 241–264.

Palma, G. (2011). Produzione di microalghe in fotobioreattori: influenza della luce e sfruttamento della biomassa esausta. Thesis in Chemical Engineering, DII, University of Padova (Italy).

Perez-Garcia, O., L.E. Bashan, J.-P. Hernandez, Y. Bashan (2010). Efficiency of growth and nutrient uptake from wastewater by heterotrophic, autotrophic, and mixotrophic cultivation of Chlorella vulgaris immobilized with Azospirillum brasilense. *Journal of Phycology*, **46**(4), 800-812.

Pottier, L., J. Pruvost, J. Deremetz, J-F. Cornet, J. Legrand and C. G. Dussap (2005). A fully predictive model for one-dimensional light attenuation by Chlamydomonas reinhardtii in a torus photobioreactor. *Biotechnology and Bioengineering*, **91**(5), 569–582.

Pruvost, J., J. F. Cornet, V. Goetz and J. Legrand (2010). Modeling Dynamic Functioning of Rectangular Photobioreactors in Solar Conditions. *AIChE Journal*, **57**(7), 1947–1960.

Schenk, P.M., S. R. Thomas-Hall, E. Stephens, U. C. Marx, J. H. Mussgnug, C. Posten, O. Kruse and B. Hankamer (2008). Second Generation Biofuels: High-Efficiency Microalgae for Biodiesel Production. *Bioenerg. Res*., **1**, 20–43.

Sforza, E., D. Simionato, G. M. Giacometti, A. Bertucco and T. Morosinotto (2012). Adjusted Light and Dark Cycles Can Optimize Photosynthetic Efficiency in Algae Growing in Photobioreactors. *PLoS ONE*, 7, e38975.

Suali, E., R. Sarbatly (2012). Conversion of microalgae to biofuel. *Renewable and Sustainable Energy Reviews*, **16**, 4316–4342.

Urbani, S. (2014). Microalgal culture in PBRs: experimental measurement of maintenance energy requirement as a function of light energy. Thesis in Chemical Engineering, DII, University of Padova (Italy).

Wiley, P. E., J. E. Campbell and B. McKuin (2011). Production of Biodiesel and Biogas from Algae: A Review of Process Train Options. *Water Environment Research*, **83**(4), 326-338.

Yanfeng, O., X. Wang, M. K. Lim, (2012). Food, Energy, and Environment Trilemma: Sustainable Farmland Use and Biofuel Industry Development. Available at SSRN: http://ssrn.com/abstract=2268688.

Yeh, K. L., J-S. Chang (2011). Effects of cultivation conditions and media composition on cell growth and lipid productivity of indigenous microalga *Chlorella vulgaris* ESP-31. *Bioresource Technology*, **105**, 120-127

Web sites

http: //algaebase.com/ (last seen 2/07/14)

http: //algaeenergy.co.uk/ (last seen 26/06/14)

http: //bae.uky.edu/ (last seen 27/07/14)

http: //ccap.ac.uk/ (last seen 13/07/14)

http: //marienfeld-superior.com/ (last seen 23/07/14)

http: //oilgae.com/ (last seen 10/08/14)

http: // photovoltaic-software.com/pvgis.php / (last seen 15/9/14).